Temperature Mould Maintenance during Automatic Welding

by

Luz Gabriela Vazquez Pasqualli

A thesis
presented to the University of Waterloo
in fulfillment of the
thesis requirement for the degree of
Master of Applied Science
in
Mechanical Engineering

Waterloo, Ontario, Canada, 2011

AUTHOR'S DECLARATION

I hereby declare that I am the sole author of this thesis. This is a true copy of the thesis, including any required final revisions, as accepted by my examiners.

I understand that my thesis may be made electronically available to the public.

Abstract

An automatic system to weld multiple layers using Tungsten Arc (TIG) welding was in the process of being developed by Tool-Tec Welding Inc, prior to the company's recent bankruptcy and subsequent closure. One of the project's main concerns was the thermal expansion experienced by the part to be welded. To avoid having to install expensive sensors, it is necessary to predict the temperature and the dilatation of the mould during the welding process.

The mould to be welded is preheated to prevent excessive stress due to extreme temperature differences in the material. As well, it is necessary to maintain the temperature of the mould during the welding process in order to avoid distortions or changes in size larger than 1 mm.

Two models have been developed to predict the size of the preheat temperature of the mould and prevent mould size changes. One model uses the results of several simulations made with finite element analysis (FEA), while the other one takes advantage of Tool-Tec expert knowledge using the Fuzzy Logic method.

Validation of both theories was done at the University of Waterloo, as Tool-Tec had at that point closed down. For the experiment, an MIG (Metal Arc Welding) robot was used, together with a medium-sized mould and an infrared camera.

Using an IR camera is preferable to using sensors because a camera gives the whole temperature of the mould while the sensors provide information only about some points, and these may not necessarily be representative ones. However, an IR camera can record hundreds of pictures in a single experiment and analyzing them one by one to sort the useful from the useless is tedious work. Therefore, an automatic selection of the useful pictures and recognition of the mould was the best way to review the data.

In the end, successful results were obtained since it was possible to maintain the preheat temperature of the mould within the required limits in order to avoid changes in size larger than 0.05mm. Nevertheless, future tests should involve larger and smaller moulds in order to tune the models presented in this thesis.

Acknowledgements

I would like to thank my supervisor, Dr. J.P. Huissoon, for his guidance and continued support through the duration of this research. His suggestions and encouragements were key parts to the fulfillment of this thesis project.

I wish to thank Tool Tec Welding Inc. for their innovative project which helped me to develop my own research. As well as my readers Dr. HJ Kwon and Dr. Behrad Khamesee. Moreover, Shesha Jayaram for borrow me the IR camera I used to do my experiments.

Vlad and Steven were very nice with me, they help me in my firts days in Canada and I want to thank them because of that.

Dedication

To Julieta

who helped me at all times

and

to my parents

who have always been with me.

Table of Contents

List of Figures

List of Tables

Chapter 1
Introduction

The introductory chapter provides an overview of the entire project on which this thesis is based, followed, in the second section, by the specific research problem investigated in this study. The chapter's third section outlines the objectives of this thesis, while the fourth and final part of this chapter explains the structure of this thesis in order to help the reader understand this proposal.

1.1 Background

Tool-Tec Welding Inc., the OMEGA group and the University of Waterloo developed an automated robotic system to weld multiple Tungsten Arc Welding (TIG) layers to build a 3-D Class 'A' surface on a contour shape using a six-axis robot. TIG welding is used to achieve a class "A" surface, as this type of welding is a clean process that does not have metal across the arc and does not spatter if the process is free of contaminants. Figure 1-1 shows an example of the kind of work this system can perform.

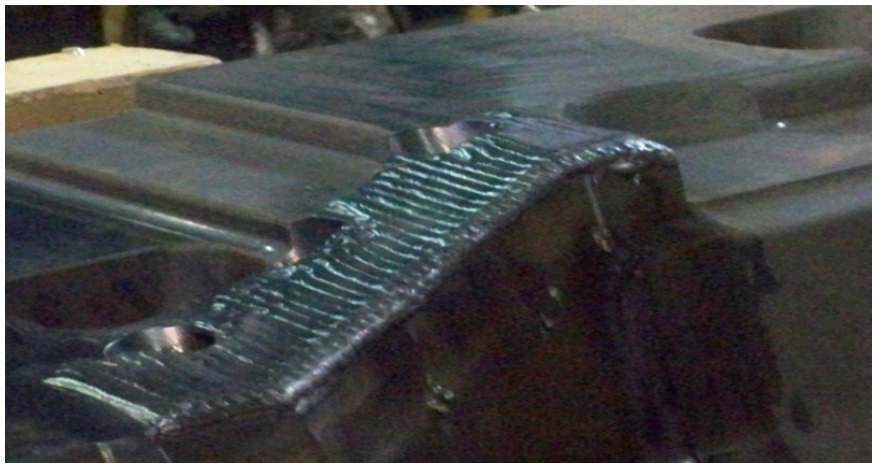

Figure 1-1: Example of a class "A" surface

The idea for the system arose due to a real-life scenario. Tool-Tec used to build up layers of welding material to modify moulds of plastic injection frequently used in the automotive industry. Thus, if a part needed to be changed, the mould would not have to be thrown out but could be modified by welding. Modifications had to be performed manually, which can be very exhausting for the person doing the work and may also last several days.

The process consists of the following steps:

1. *Preheat the mould*. The mould to be welded is preheated to avoid excessive stress due to extreme differences in temperature in the material. The preheat temperature can range from 200 to 400 degrees Celsius. If the mould is not large, it can be preheated in a preheat table where the welding also takes place. Two preheat tables are shown in Figure 1-2. These tables have burners that can be turned on separately depending on the size of the mould. If the mould is very large (e.g., a bumper mould), it has to be preheated in an industrial oven and then moved by a bridge crane, as the mould has to be at least 300 degrees C and could weigh more than 1 ton.

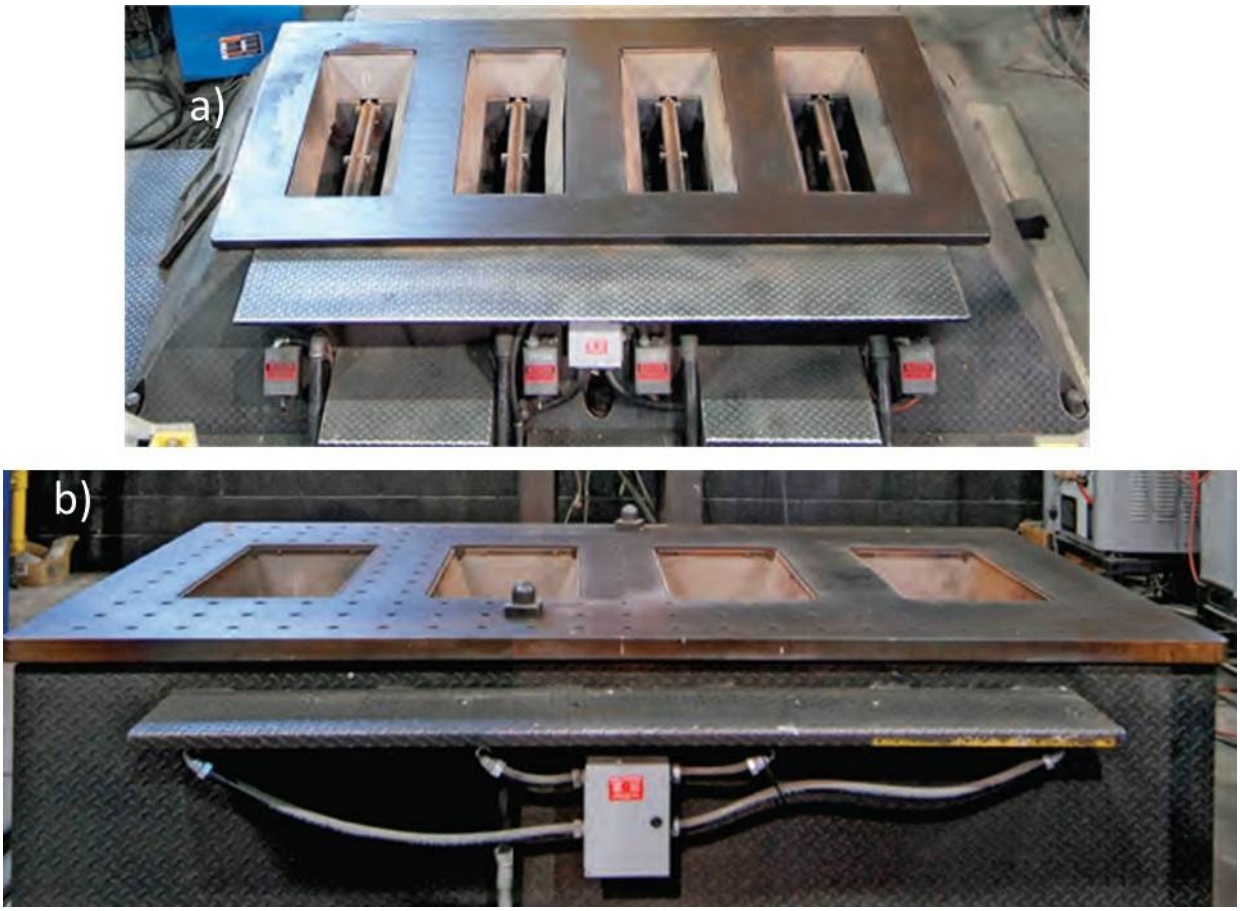

Figure 1-2: Preheat tables for welding system

2. *Maintain the preheat temperature*. If the mould has been preheated on a preheat table, it has to be covered with thermal cloths until the temperature of the mould reaches a uniform temperature. If the mould has been preheated in an industrial oven, it also has to be covered in order to maintain the preheat temperature after it is moved to the welding place.

3. *Correct the size*. One of the main concerns during the preheat process is thermal expansion. This dilatation depends on the material, material temperature, ambient temperature, size and shape of the mould. The robot then must detect a key point of the mould (called tooling balls) to determine the new size of the mould as well as its orientation.
4. *Welding work*. Finally, the welding process starts and, to obtain the best results, the robot should already know the path it has to follow, the new size of the mould, the orientation of the mould the welding parameters, and so on. However, as any of these parameters can change, the temperature of the mould must remain at the preheat temperature at all times. Therefore, it is necessary to know the temperature of the mould during the welding process in order to avoid distortions or changes in size larger than 1 mm.
5. *Rectify quality of mould*. Quality verification has to be done in order to return the mould within the customer's specifications.

The automatic system is divided in two parts: an Engineering Station and a Welding Station.

The Engineering Station is composed of:

Engineering PC & Software

〉 High-End PC with

- ✓ Access to network/internet
- ✓ 8GB Ram min
- ✓ High-End Video card
- ✓ High-End Processers (duo)

〉 Software

- ✓ Tool-Tec Software
- ✓ SolidWorks
- ✓ PowerMill
- ✓ Robot Studio

The PC description is the minimum required to support the Tool-Tec software which interacts with Solid-Works to extract the CAD data of the mould to be modified. An example of a mould that is

reproduced with CAD data in Solid Works is presented in Figure 1-3. This software also acts together with Power-Mill to create layers and paths that the robot will follow. Robot Studio performs the weld simulation to validate the paths. Once the simulation is done, information about the paths and layers is sent to the Welding Station via the network or internet.

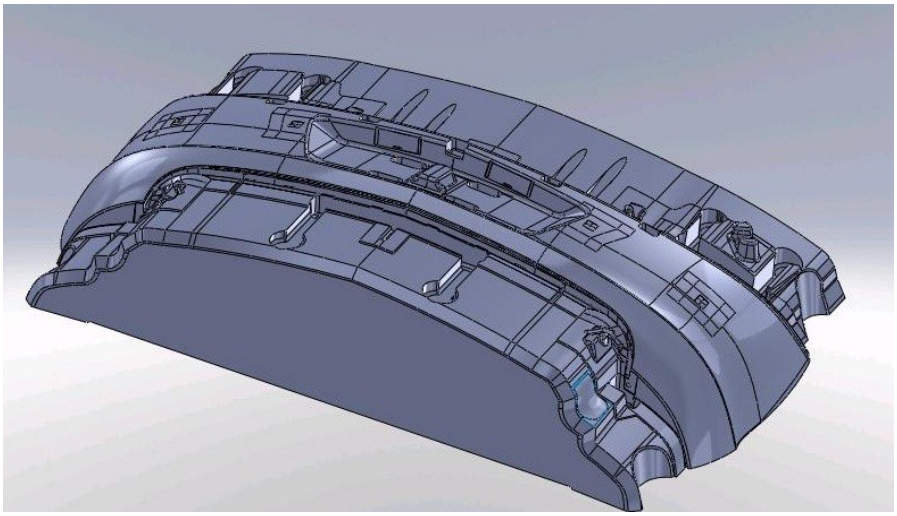

Figure 1-3: Example of mould reproduced with CAD data in Solid Works

The welding station is composed of:

- Robotic Welding Station:
  - ✓ ABB Robot/Controller (specific robot based on need)
  - ✓ Liburdi Welding Controller/Wire Feeder
  - ✓ Tool-Tec Welding Torch
  - ✓ Tool-Tec Heating Table with Heat Controller/Monitors
  - ✓ Welding Cage and Safety Controls
  - ✓ Air, Gas and Electrical Hook-Ups
- Weld Station PC & Software
  - ✓ Mid+ Range PC with access to network/internet
  - ✓ Tool-Tec, and supporting Software (ABB)
  - ✓ Tool-Tec Flex-pendant Controller

Figure 1-4 and Figure 1-5 show the welding station built by Tool-Tec, following all safety requirements, in order to develop a complete automatic system. These figures are labelled to identify some of the components of the welding station. Note that even though a TIG welding process normally does not have a wire feeder, the Tool-Tec process does. Tool-Tec designed its own torch in order to make an automatic wire feed. Moreover, the Tool-Tec table is very important since it helps maintain the preheat temperature of the mould. The computer here does not have to be as powerful as the one in the engineering station because this computer receives the instruction to weld, creates and adjusts weld parameters, controls and monitors welding operations, and could easily validate the welding through simulation. It does not work with CAD data.

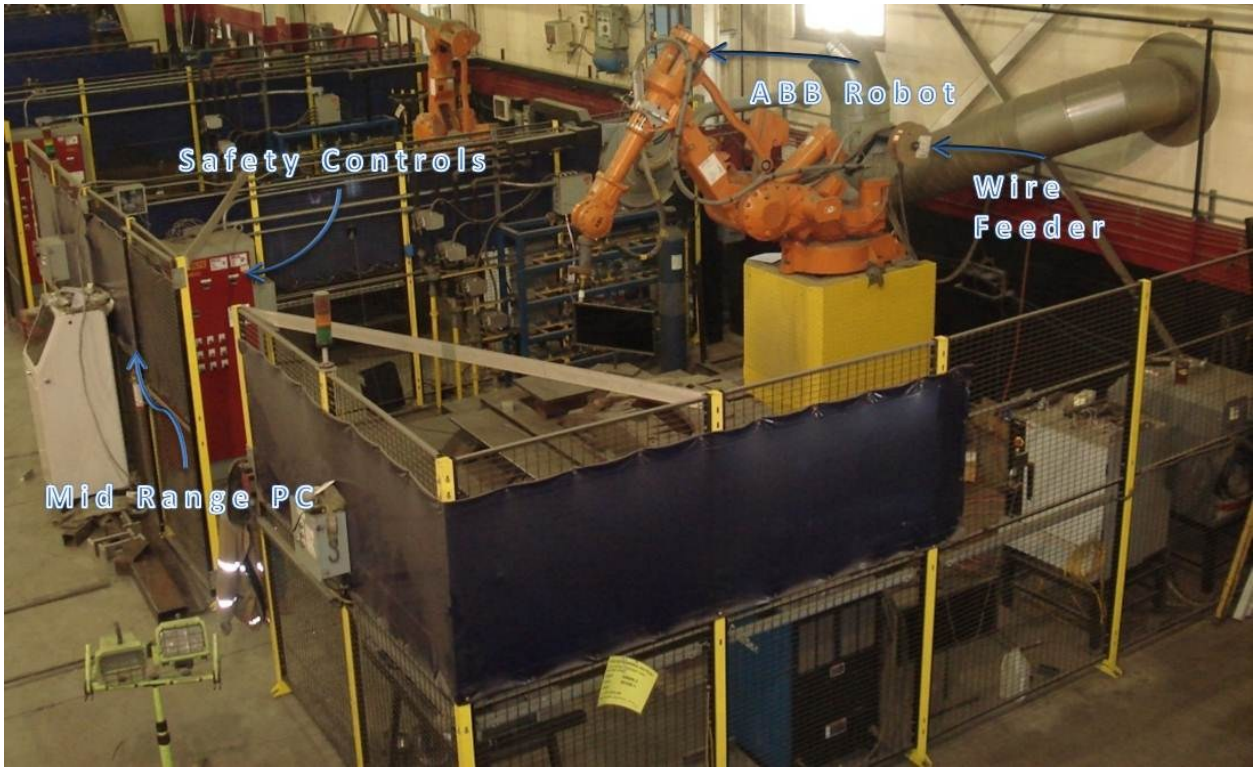

Figure 1-4: Welding Station

Figure 1-5: Welding Station: a closer look

The first purpose of this system was to modify automotive plastic moulds. However, the automotive industry is not the only one that can use this technology; it can be used for any object that requires welding. Figure 1-6 demonstrates an example of a potential high-volume production that can be done according to the system described above.

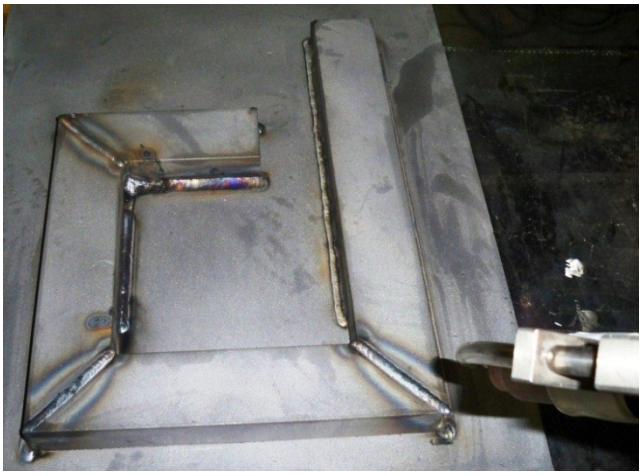

Figure 1-6: This robot could be used in high-volume production

1.2 Description of the Problem

In general, metals tend to expand or contract due to the energy in them. This means that if a steel object is modified by adding energy and mass, the molecules will react and the size of this part will change. Thus, if P-20[1] steel mould is preheated and welded, some distortions can be expected. This process can be divided into two parts: the first part is the initial temperature of the mould, and the second part is the temperature of the mould when mass and energy are added.

When a piece of the steel is preheated, it is a steady-state problem from the thermal point of view, because there is no change in time. It can thus be said that the element has uniform temperature, especially if it was preheated in an oven.

However, the accumulation of mass and energy while welding is time-dependent, since it is a continuous process. Moreover, the temperature of the mould will no longer be uniform, as the energy is concentrated in a single point in order to melt the material already in the mould as well as the added material which is going to be part of the element.

1.3 Objectives

The purpose of this thesis is to present a simple explanation for the preheated thermal expansion problem and provide two alternative solutions to predict the temperature of the mould while the mould is being

[1] In this report, P-20 steel means AISI P-20, DIN 1.2330, ASTM A681 or UNS T51620, which accords with the various systems and designations of this steel.

welded to avoid the use of expensive sensors. The experimental data confirms the efficiency of these resolutions.

1.4 Structure

Figure 1-7 shows schematically the body of this thesis. There are five blocks, each representing a group of sections with the same purpose. The Opening provides information about the project that took place at Tool-Tec Welding Inc. It also gives details of the research problem, the main purpose of this thesis, and the structure of this writing. The next block presents four sections that describe a robotic system for welding multiple TIG layers to build a 3-D Class 'A' surface on a contour shape using a six-axis robot. Included in this section are two temperature problems that may affect the quality of the final shape after the welding process. This section also details the objective of this study, which involves helping to solve the heat problems.

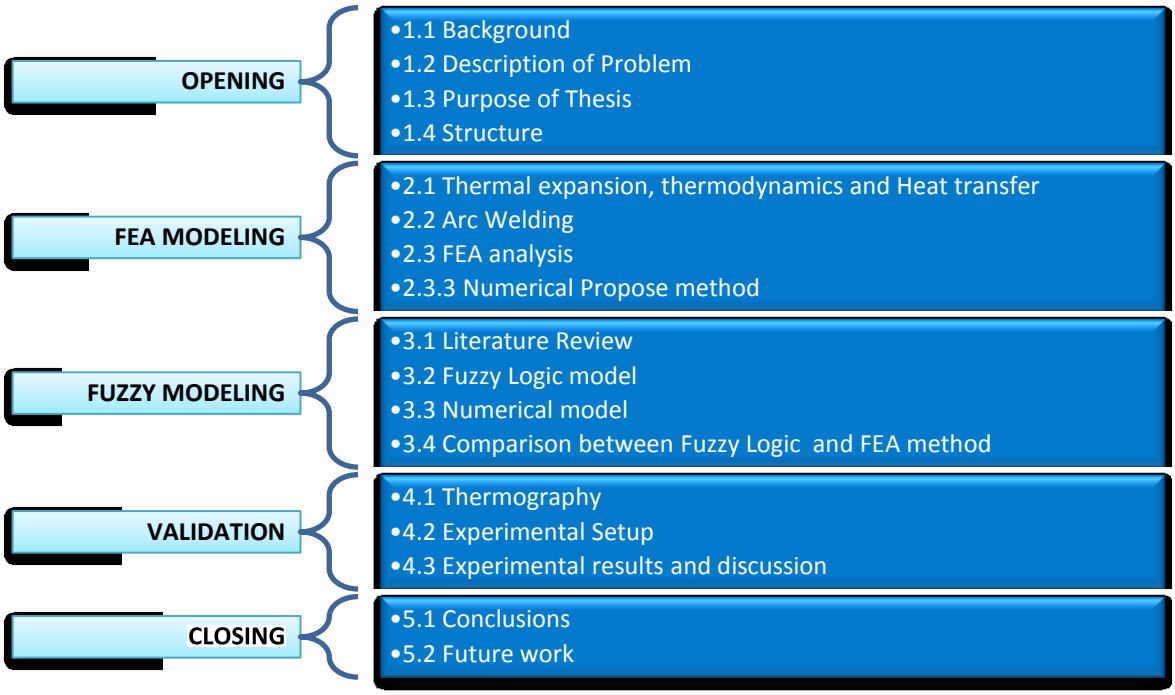

Figure 1-7: Structure of thesis

Chapter 2 and Chapter 3 contain explanations of both models suggested here. One of the models applies fuzzy logic and the other numerical method. The finite element analysis model is explained at the end of the second chapter, in section 2.3.3., while sections 2.1 to 2.3.2 provide information concerning the principles followed to develop this model. This theory gives an overview of thermal expansion, arc welding, thermodynamics and heat transfer, and numerical methods, providing sufficient information for the reader to understand the foundations on which the two resolutions are constructed. For example, the arc welding (AW) subject does not describe all processes that use AW but only Tungsten Arc Welding (TIG) and Metal Arc Welding (MIG). This is because Tool-Tec uses TIG welding in its system and the experimental validation uses MIG process. Describing other processes would be beyond the scope of this research.

The third block explains the fuzzy logic method, starting with a literature review of how Fuzzy Logic has been used to solve welding automatic problems, and continuing with the fundamentals of this method. This is followed by a presentation of the proposed model to solve the dynamic temperature problem this thesis is addressing. The block concludes with a comparison between the proposed methods, the FEA model and the Fuzzy Logic model.

The validation part consists of three sections: Thermography, Experimental Set Up and Experimental Results and Discussion. The first part of this block is included because the test was performed with an infrared camera that uses thermography principals.

Chapter 5 provides concluding remarks and proposes future work to continue investigations into this important research field.

Chapter 2
Preheat Moulds and Thermal Modeling

In order to change the shape of a mould using TIG Welding, Tool-Tec Welding Inc. used to preheat the working piece at a temperatures range from 200 to 400 degrees Celsius (depending on the size of the mould) to prevent cracks due to temperature shocks. This preheating process can be done in an oven (if the mould is very large) or by using burners (if the mould is small). During this practice, the mould undergoes thermal expansion, which changes its size, sometimes significantly. This is the steady state process that the mould experiences, which is explained in section 2.1.1.

The second part of the process is continuously changing. From the time the work piece is taken out of the oven it starts cooling down, but once the arc welding process starts, a continuous rate of heat mass is added to the mould to transform the its shape. From a thermal point of view, the piece of steel loses heat on one side while gaining heat and mass on the other. The problem with this scenario is that it is necessary to determine the temperature of the mould in order to know its size. Thus, it is important to understand how convection (section 2.1.3.2) and conduction heat transfer (section 2.1.3.1) as well as the first law of thermodynamics (section 2.1.2) work together in a complex and dynamic situation.

As mentioned previously, Tool-Tec used TIG welding to create a class “A” surface. However, as the company shut down before experimental validation of the models were made, tests were done using a Metal Arc Welding (MIG) welding robot instead of a TIG robot. (For an explanation of TIG and MIG welding, see section 2.2.3)

The purpose of this research is to determine the temperature of the work piece during the welding process and to make the necessary changes. These changes include turning on the burners to compensate for heat loss, pausing the procedure in order to dissipate excessive heat, and maintaining the temperature of the mould as close as possible to the preheat temperature to avoid thermal expansion of the mould. Thus far, the physics fundamentals of the problem have been presented. Now, a simulation using Finite Element Analysis (FEA) tools such as ANSYS Workbench will be used to put in place all the parameters at the same time and analyse the results with the intention of predicting the behaviour of the mould’s temperature. Section 2.3 offers an overview of FEA, explains how ANSYS works, and proposes a model that uses ANSYS results to solve the thesis problem.

2.1 Thermal Expansion, Thermodynamics and Heat Transfer

2.1.1 Thermal Expansion

The goal in the first part of the process is to determine the size of the mould when it is already preheated so that the robot can be programmed with the correct information. To do that, it is necessary to know the behaviour of the material when heat is added to it. Thermal expansion is the physical effect on any metal when it is heated up. In this section, the dilatation effect is explained as well as the specific reaction for P-20 steel, which is used in the automatic welding system of Tool-Tec Inc.

Thermal expansion occurs when the regular separation between atoms increases. At ambient temperature, solid atoms have a separation of roughly 10-^{10}m and move at a rate of 10^{13}Hz. If more heat is applied to a solid, its atoms move at increased amplitudes and the object expands. Figure 2-1 a) shows a typical example of dilatation in metals, which is what happened when the first train rails were built. Nowadays, civil engineers know that thermal expansion is a very important consideration in construction, and plan accordingly. Figure 2-1 b) presents the solution for this problem.

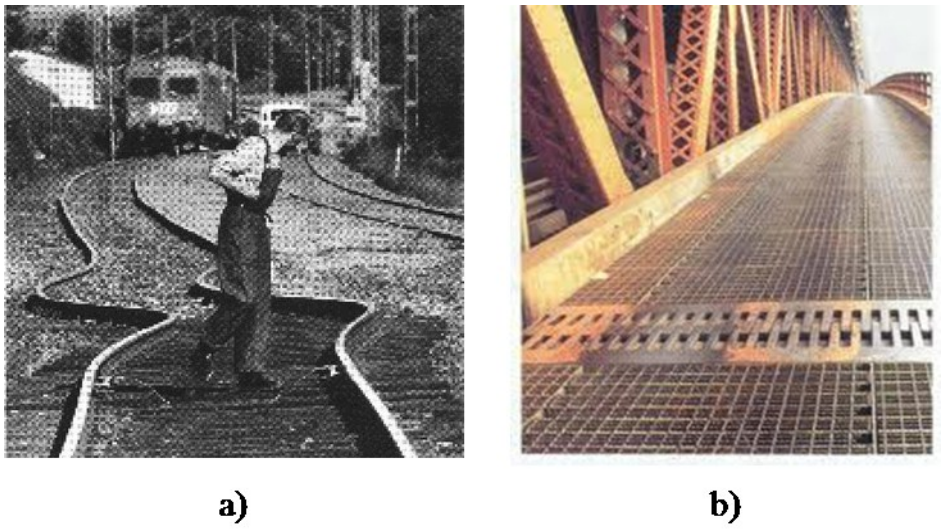

Figure 2-1: a) Thermal expansion problem with early train rails b) Resolving the problem paved the way for larger construction projects

Thermal expansion can be quantified with the following formula:

Equation 2-1

$\Delta L = Li * e * (Tf-Ti)$,

where:

ΔL = difference in length (mm)

Li = initial length (mm)

e = coefficient of thermal expansion (C^{-1})

Tf = final Temperature (C)

Ti = initial Temperature (C)

From Equation 2-1, we can see that the difference in length is proportional to the difference in temperature, and if the original size is large, the gradient of the final dimension is also large. If a mould is small, the difference in length in all directions will be insignificant, but if a mould is huge, the difference in measurement will likewise be huge. As well, the final size depends on the e constant, which is different for each material. It is important to mention here that the value of e is constant only if the gradient of the temperature is not large, and that thermal expansion is proportional in all directions of an object, including holes. Thus, the volume of an object will change uniformly as it expands.

2.1.1.1 Preheat thermal expansion for P-20 steel

The Table below shows the coefficient of thermal expansion for P-20 steel at different temperatures, taking as a reference temperature 20 degrees C.

Coefficient of Thermal Expansion C^-1	Temperature C
1.27e-005	200
1.36e-005	400

Coefficient of Thermal Expansion C^-1	Temperature C
1.37e-005	540
Reference Temperature C	
20	

Table I: Coefficient of thermal expansion for P-20 steel

For TIG welding, it is necessary to preheat the material to be welded to avoid cold cracking in the HAZ (heat affected zone). In the case of P-20 steel, the temperature of the object must be between 200 and 400 degrees C, depending on the size of the part to be welded. The chart below presents the material's differences in length. It can be seen that if the size of the mould is less than 250 mm in total length, the width and height of the dilatation will not be more than 1 mm when the difference in temperature is 300 degrees C. On the other hand, if the difference in temperature is 200 degrees C, the initial dimension of the mould can be 400 mm and linear expansion will not exceed 1 mm.

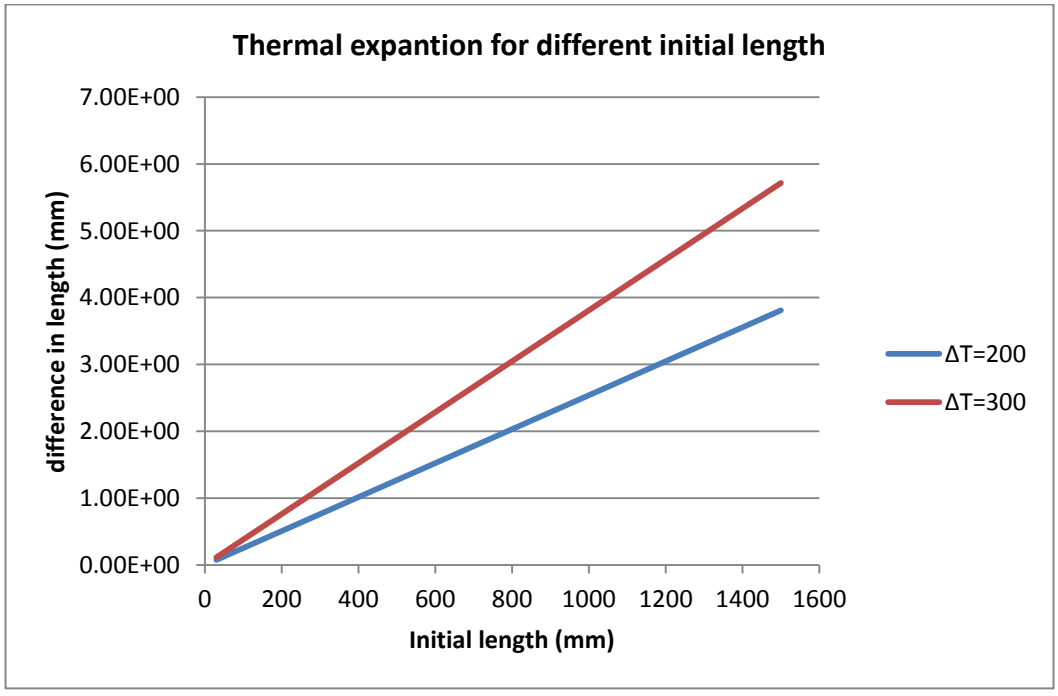

Figure 2-2: Thermal expansion for different initial lengths

2.1.2 First Law of Thermodynamics

Thermodynamics is a science that studies transformation, power generation, refrigeration and relationships between energy and matter. During the welding process, energy is used to melt a fraction of material in seconds, an action, however small, that will affect the entire object. In order to understand the welding process, we have to understand the first law of thermodynamics, as all bodies in nature are in a constant state of flux, obeying thermodynamics laws.

The first law of thermodynamics concerns the conservation of energy. It states: "Energy cannot be created or destroyed, only transformed". Further, the energy inside a system is equal to the difference between the energy input and the energy output. The formula for this is:

Equation 2-2

$$E_{in} - E_{out} = \Delta E_{system}$$

where E is energy. Figure 2-3 gives an example of this law. In the picture, the total energy of the pot is equal to the difference between the energy gained and the heat lost. Energy can also be transformed into work. For example, the heat inside a mould is converted into work when thermal expansion occurs.

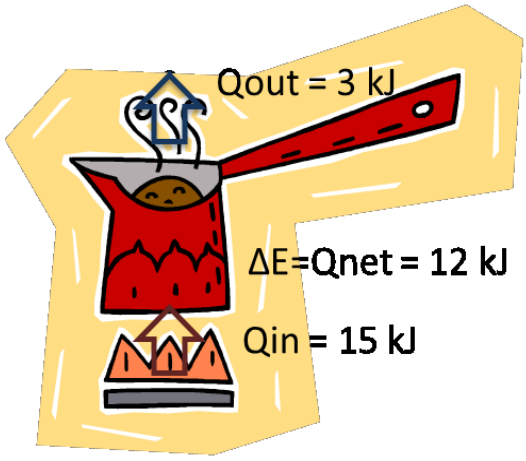

Figure 2-3: The energy of the pot is equal to the net heat transfer, assuming absence of work in the system

2.1.3 Heat Transfer

When there is a difference in temperature between two bodies or systems, the object with a higher temperature will transfer some of its energy to the object with a lower temperature. This transfer can be done by conduction, convection, radiation or a combination of these.

Conduction happens when the particles of a substance are in contact with the particles of another substance and they have more or less energy. These substances can be solid, liquid or gases.

Convection arises when a solid is in contact with a gas or liquid in motion. The faster the motion, the larger the heat transfer rate, as the solid is in contact with new particles with the same temperature at all times.

Radiation is the transmission of energy by any kind of matter which is above absolute zero in a form of electromagnetic waves of photos. (For more information about thermal radiation, see section 4.1.2 of this thesis.)

2.1.3.1 Fourier's Law of heat conduction

The rate of heat conduction is proportional to the difference in temperature between two systems. It also depends on the materials in contact, that is, not all materials will have the same conduction at the same temperature gradient, as some elements have better conductivity than others. Fourier's Law states:

Equation 2-3

$$\dot{Q} = k\Delta T$$

where Q is the local heat flux which can be given in W/m^2, k is the material's conductivity (W/m.C), and ΔT (C) is the temperature gradient.

The thermal conductivity for P-20 steel is given in Table II below. The conductivity is given in mm, since the analysis of the problem of this thesis is in mm. Note that conductivity depends on the temperature of the object (i.e., a higher temperature leads to faster conductivity).

Table II: Thermal conductivity of P-20 steel

Thermal Conductivity [W/mm.C]	Temperature [C]
2.90E-02	20
2.95E-02	200
3.10E-02	400

2.1.3.2 Newton's Law of cooling

The rate of heat transfer due to convection is governed by Newton's Law:

Equation 2-4

$$\dot{Q} = hA_s(T_s - T_\infty)$$

where h is the convection heat transfer coefficient in W/m^2, As is the surface area through which the convection heat transfer takes place in m^2, Ts is the surface temperature in C, and T∞ is the ambient temperature in C.

The coefficient of convection is not an easy value. It depends on the temperature of the fluid among the hot material, the shape of the surface, the velocity of the fluid, etc. In most cases, this value is experimentally found, but there are some formulas that can be used to find this number. If we consider a thin plate, insulated on one side and in contact with gas on the other, its rate of heat transfer will be different if the position of the plate changes.

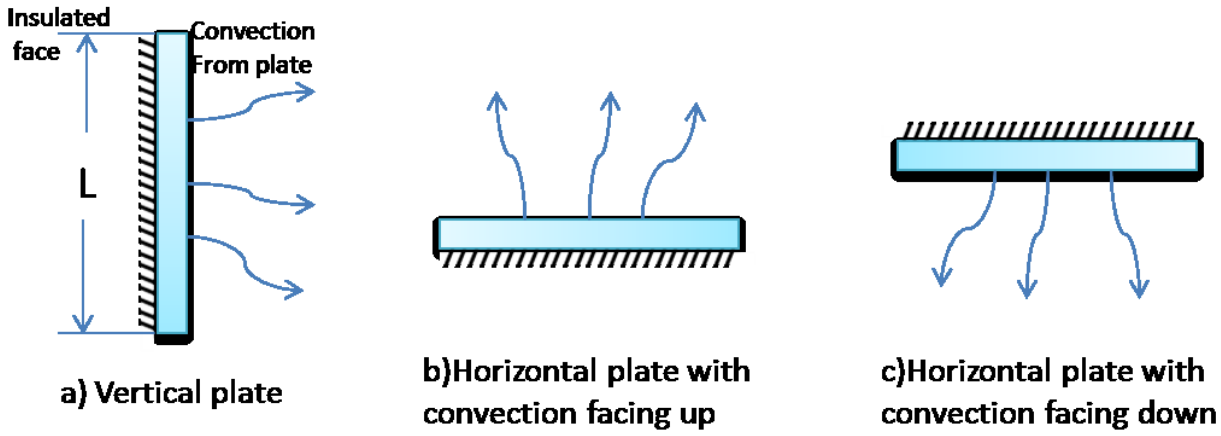

Figure 2-4: Thin hot plate in different positions

Figure 2-4 a) shows a plate with the convective face in a vertical position. We can find the value of the coefficient of convective heat transfer with the following formula:

Equation 2-5

$$h = \frac{k}{L}Nu$$

where k is the thermal conductivity in W/m.K, L is the length of the plate, and Nu is the Nusselt number[2]. This number represents the improvement of heat transfer through a fluid layer as a result of convection relative to conduction across the same fluid layer. The larger the Nusselt number, the more effective the convection. Thus:

Equation 2-6

$$Nu = \frac{\dot{q}_{conv}}{\dot{q}_{cond}} = \frac{h\Delta T}{k\frac{\Delta T}{L}} = \frac{hL}{k}$$

This brings us to a dilemma: we are trying to find the value of h, but it depends on the Nu number, and the Nusselt number also depends on the coefficient of convection. However, there are other ways to find the value of Nu. Some formulas have been developed in relation to the geometry of a hot surface. So, for a plane vertical plate:

Equation 2-7

$$Nu = \left\{ .0825 + \frac{0.387Ra_L^{1/6}}{\left[1 + (\frac{0.492}{\mathrm{Pr}})^{9/16}\right]^{8/27}} \right\}^2$$

where Pr is the Prandtl number of the fluid. This number is dimensionless and is equal to the ratio of momentum diffusivity or kinematic viscosity to thermal diffusivity. For liquid metals such as mercury, the kinematic viscosity is very low in comparison with the heat diffusion. The value of Pr for mercury is less than 0.01. On the other hand, the value of Pr for heavy oil can be more than 100e[3], with very low diffusivity. For air, Pr is nearly 1, but this value changes depending on pressure and ambient temperature. Thus,

Equation 2-8

$$Pr = \frac{v}{\alpha} = \frac{viscous\ diffusion\ rate}{thermal\ diffuson\ rate} = \frac{c_p\mu}{k}$$

where:

- ν : kinematic viscosity, ν = μ / ρ, (SI units : m^2/s)

[2] This is a dimensionless convection heat transfer coefficient that Wilhelm Nusselt found in the first half of the twentieth century

- α : thermal diffusivity, α = k / (ρcp), (SI units : m^2/s)
- μ : dynamic viscosity, (SI units : Pa s = (N s)/m^2)
- k : thermal conductivity, (SI units : W/(m K))
- cp : specific heat, (SI units : J/(kg K))
- ρ : density, (SI units : kg/m^3).

Pr is considered a property of a fluid and can be found in thermal property tables.

The other variable that appears in Equation 2-7 is the Rayleigh number, which is also a dimensionless number. Its formula for a vertical flat face is:

Equation 2-9

$$Ra_L = \frac{g\beta(T_s - T_\infty)L^3}{v^2} Pr$$

where:

- Pr = Prandtl number
- g = acceleration due to gravity
- Ts = Surface temperature
- T∞ = ambient temperature
- ν = Kinematic viscosity
- α = Thermal diffusivity
- β = 1/Tf (K)
- Tf = film temperature = (Ts-T∞)/2

We can now find the value of h for vertical faces using Equations Equation 2-5 to Equation 2-9. To find the value of h for a horizontal area facing upwards, we can apply Equation 2-10 to Equation 2-13. We then have:

Equation 2-10

$$h = \frac{k}{L_c} Nu$$

Note that this formula is very similar to Equation 2-5. The only difference is that L (length of surface) is Lc, which is the ratio between the surface area and the perimeter of the area. Its formula can be found in Equation 2-13.

The Nusselt number for this position of the surface also changes. However, here we need only the Ra number, as in the following equation:

Equation 2-11

$$Nu = 0.54 Ra_{L_c}^{1/4}$$

The formula for Ra is:

Equation 2-12

$$Ra_L = \frac{g\beta(T_s - T_\infty)L_c^3}{v^2} Pr$$

Note that L is now Lc, and the last variable is:

Equation 2-13

$$L_c = \frac{A_s}{p}$$

where, if we are referring to a square surface,

- As = Surface area = L^2
- P= perimeter of area= 4L

Finally, for a horizontal surface with the hot face down, we can use Equation 2-10. Here, the value of Nu will be:

Equation 2-14

$$Nu = 0.27 Ra_{L_c}^{1/4}$$

Note that the value of Nu for the hot plate facing upwards is almost twice the value of Nu with the hot plate facing downwards, corresponding to a higher convection heat transfer rate. This is because, if the hot surface is facing down, the hot air will be trapped under the hot object.

Therefore, the amount of energy and the resultant temperature of the solid body are determined by the type of material, the temperature and kind of fluid among the object, the shape or area which is in contact with the fluid, and the difference in temperature between the solid and the fluid.

Appendix B shows a table with the value of h if a hot surface were a square of 1 by 1 at 1 atmosphere of pressure for different film temperatures. These calculated values will be used for the finite element analysis explained in section 2.3 of this thesis.

2.2 Arc Welding

The major difference between Arc Welding (AW) and conventional welding is the way in which heat is generated. AW is powered by electricity while conventional welding uses a flame. In this thesis, only two forms of AW are explained (TIG and MIG), as the developed robotic system uses Tungsten Arc Welding and the experiments are done with an MIG robot. Explaining more forms of AW would therefore be irrelevant. The experiment chapter provides details of the MIG experiment.

The basic concept for any kind of arc welding is the generation of heat when an electric current is not permitted to freely continue its way. Figure 2-5 presents a simple arc welding circuit. In this picture, the power source is a battery, which means there is a direct current, and the electrons go from negative to positive. The current then goes from the torch to the base metal. However, the torch and the base metal are not connected with anything but air or inert gas, which are very good resistors. In fact, they can even be insulators if the positive and negative sides are distant enough. For instance, the distance between the two poles could range from 2 to 5mm, and the speed as well as the pressure of the current could boost electrons to pass from the torch to the welded metal. At the same time, the high resistance produces sufficient heat to reach the melting point of the metal being welded. The heat produced is so high that it reaches visible waves and it is possible to see a light arc. Now we know why it is called Arc Welding. Also, from the above explanation, we can assert that the amount of heat the arc produces will depend on the current, voltage, surrounding gas and distance between the torch and the welded metal.

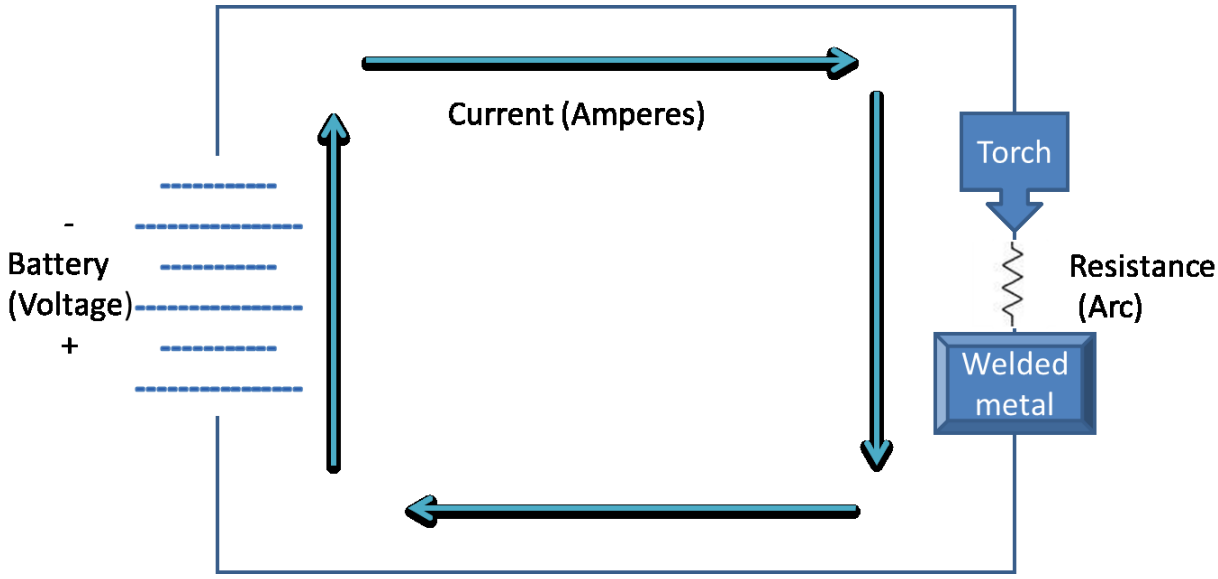

Figure 2-5: Basic welding circuit

Direct current is much powerful than alternating current, which is why the first welding machine used batteries and a dynamo to produce an electric current. This machine was invented by N. Benardos and S. Olszewski in Great Britain[i].

2.2.1 Gas Tungsten Arc Welding (TIG)

At the time of its demise, Tool-Tec Inc. was working on a robot that uses TIG welding, which is a type of arc welding process. The following section will explain the process of TIG welding and describe the equipment used in this method.

2.2.1.1 Process

In Gas Tungsten Arc Welding, the arc is located between a non-consumable tungsten electrode and the part to be welded. While this arc is working, an inert gas produces a shell which covers the arc, the heat affected zone, and the part of the metal that is being welded. This gas protects the weld from the surrounding air, as an inert gas does not react with other gases. Another advantage about this type of gas is that it does not have an odour and is transparent, which provides good visibility of the arc.

There are three kinds of currents in TIG welding: direct current electrode negative (DCEN), direct current electrode positive (DCEP), and alternating current. The DCEN is the most commonly used current and works for all metals. With DCEN, 70% of the heat goes into the work piece, allowing a high penetration. During the DCEP mode, the electrode contains the majority of the heat generated, which is why the electrode most be sufficiently large to avoid electrode melting. However, as the penetration is not that good, it can be a bad choice, but this sort of polarity is nevertheless very useful for aluminum or magnesium.

For an AC current, it is necessary to make a rectification of the current before the process starts, as the current is not accurate enough for welding purposes. The rectification can have more positive time, more negative time, or equal times for negative and positive. Each option can get the best of each part. For example, if there is more negative than positive, the result is good penetration, less need for shield gas, and less current need. On the other hand, if the current is more positive, the result is a maximum cleaning.

2.2.1.2 Equipment

- ✓ Torch. Because most of the heat is concentrated close to the torch, it needs to be cooled down, either with water or air. Water is recommended for long periods of welding. The torch has

everything connected: the coolant, the electrode, gas tubes, energy cable and the cup that protects the torch.

- ✓ Shielding gas helps to reduce porosity in the weld bead. Argon and Helium are most commonly used for TIG welding, but Hydrogen and Nitrogen can also be used. To be effective, these gases must be 99.995% pure. As Argon is denser than air, it goes directly to the bottom of the arc while Helium tends to go up. That is why, to obtain the best results, it is recommended to mix gases. The ionization point (i.e., the voltage required to electrically charge the gas to conduct electricity) is very important to select an inert gas because that will determine the minimum amount of volts during the welding process. For example, the ionization point for Argon is 15.7 volts.
- ✓ The power source is the engine of the process; without the electricity, there is no arc welding. Some machines can be AC or DC and they can even be used for MIG or TIG. The machine chosen will depend on the process to be covered.
- ✓ Electrode. The main characteristic of a TIG electrode is that it is not consumable and is made of Tungsten. There are specifications and standards for these electrodes regulated by the American Welding Society as well as the American Society for Testing and Materials. .
- ✓ Table III contains the classification of the electrodes. In the first column, we can see the names of the electrodes starting with the letters "EW", which stands for Electrode Tungsten (W is the chemical symbol for Tungsten). These letters are followed by, for instance, a P, which stands for pure or Ce (Cerium), La (Lanthanum), Th (Thorium), Zr (Zirconium) or G (other). Finally, the number means the percentage of the alloy which is used in the electrode. In the case of G, the manufacturer has to write the name of the alloy instead of the letter d. The second column has the numbering system of metals and alloys. The third column specifies the minimum percentage of Tungsten. The 4th, 5th, 6th and 7th columns contain the ranges of the alloy in the electrode, while the last column shows the weight percentage of Oxides and other elements that can have EW.

Table III: Tungsten electrode requirements[3]

[3] This table was taken from Edwards i book, p. 32.

Chemical Composition Requirements for Electrodes[a]

AWS Classification	UNS Number[b]	Weight Percent					
		W Min. (difference)[c]	CeO_2	La_2O_3	ThO_2	ZrO_2	Other Oxides or Elements Total
EWP	R07900	99.5	—	—	—	—	0.5
EWCe-2	R07932	97.3	1.8 – 2.2	—	—	—	0.5
EWLa-1	R07941	98.3	—	0.8 – 1.2	—	—	0.5
EWLa-1.5	R97942	97.8	—	1.3 – 1.7	—	—	0.5
EWLa-2	R07943	97.3	—	1.8 – 2.2	—	—	0.5
EWTh-1	R07911	98.3	—	—	0.8 – 1.2	—	0.5
EWTh-2	R07912	97.3	—	—	1.7 – 2.2	—	0.5
EWZr-1	R07920	99.1	—	—	—	0.15 – 0.40	0.5
EWG[d]	—	94.5	———	NOT SPECIFIED		———	0.5

Notes:

a. The electrode shall be analyzed for the specific oxides for which values are shown in this table. If the presence of other elements or oxides is indicated, in the course of the work, the amount of those elements or oxides shall be determined to ensure that their total does not exceed the limit specified for "Other Oxides or Elements, Total" in the last column of the table.

b. **SAE/ASTM** Unified Numbering System for Metals and Alloys.

c. Tungsten content shall be determined by subtracting the total of all specified oxides and other oxides and elements from 100%.

d. Classification EWG must contain some compound or element additive and the manufacturer must identify the type and minimal content of the additive on the packaging.

- ✓ Filler. There are several kinds of fillers. These are selected based on the material of the work piece to be welded.
- ✓ Protection. In the case of automatic welding, the whole cell in the automatic system must be covered with a filter to reduce the lightness of the arc. Cylinders need to be checked for safety reasons and everything must be free of lick due to high voltage work.

Figure 2-6: shows the basic equipment for a TIG process. Notice that there is no need for a filler.

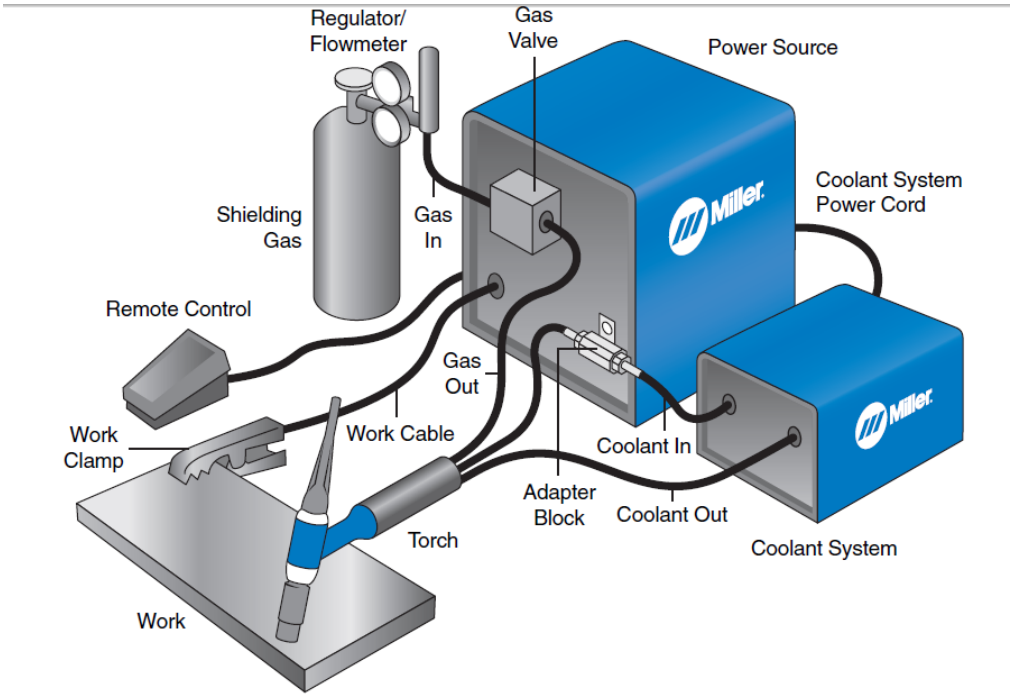

Figure 2-6: Essential Equipment for the TIG process, taken from i

2.2.2 Metal Inert Gas (MIG) Welding

2.2.2.1 Process

This process is also called Gas Metal Arc Welding (GMAW) because it not only uses inert gases but also active gases for shielding purposes. It was first commercially available in 1948. The main characteristic of this process is the automatic feeding of a consumable electrode. This process was made to be faster than the TIG welding; in fact, by itself, it is a semi-automatic process which only needs travel speed, guidance and position from the operator. It is important to note that the arc is situated between the work piece and the consumable electrode.

There are five types of transfer modes:

a) Axial Spray works with at least 3.2mm of material thickness. Figure 2-7 a) shows this process, in which the sizes of the droplets are no bigger than the size of the electrode. To achieve this effect, it is necessary to have at least 80% of Argon for the shielding gas, resulting in high current levels.

b) In addition to Axial Spray, Globular works with a minimum of 3.2mm of material thickness. The globular transfer uses CO_2 or Helium to reduce spatter. As you can see in Figure 2-7 b), the resultant bead is more random than other types of MIG welding. However, there is greater penetration depth.

c) In Short Circuit, the transfer occurs only when the electrode is in contact with the molten puddle. In Figure 2-7 c), we can see that in F, G and H states, there is no current. This transfer is very useful for thin work pieces since the penetration as well as the energy used is low.

d) Pulse spray is made for material thicker than 3.2mm. This kind of transfer has the advantage of Axial Spray and short circuit. It can work at high energy and has current control. Figure 2-7 d) displays the variation of current that goes from peak levels to background levels at a frequency of 40 kHz. This results in a stable arc and greater control of metal transfer.

e) Surface Tension Transfer also works with a small thickness. In Figure 2-7 e), we can see how current and Voltage are stopped between T1 and T2 in order to minimize spatter. STT controls the current in a logical way, making it more efficient than short circuit transfer.

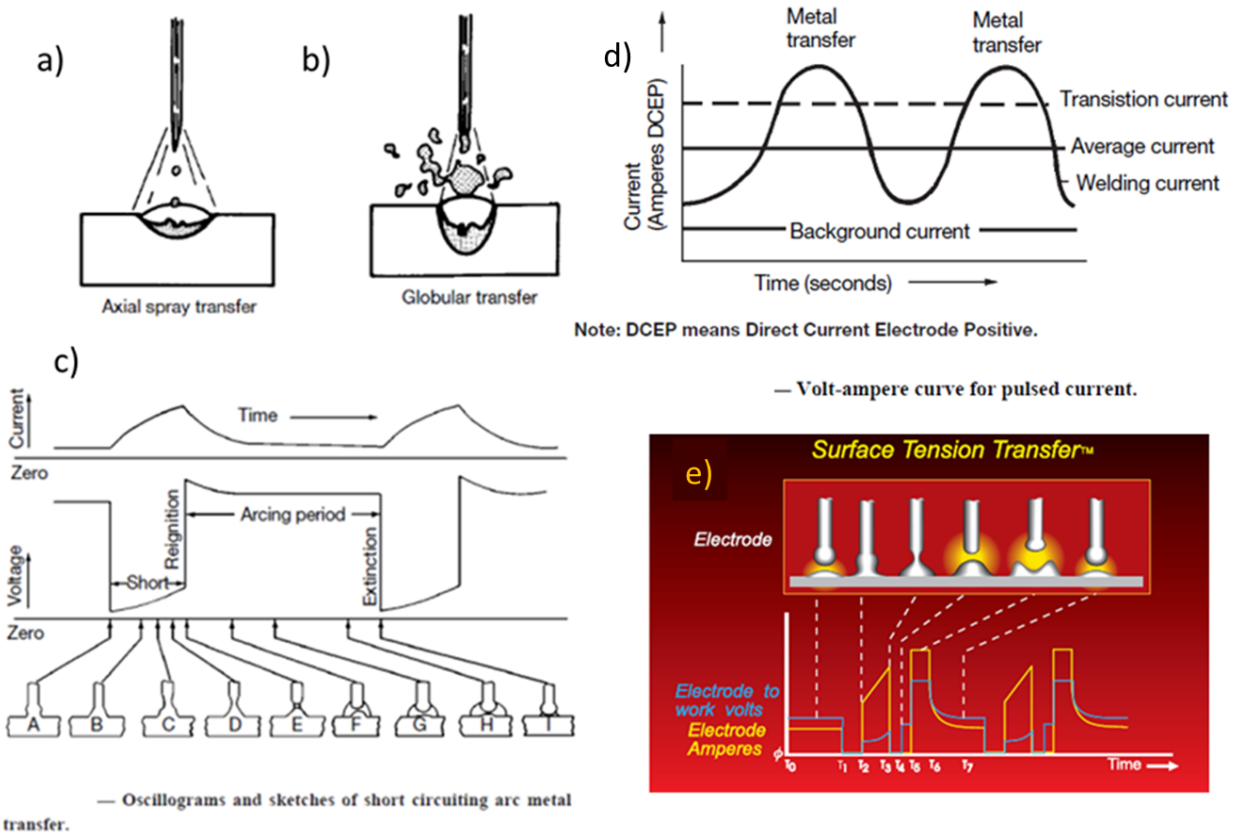

Figure 2-7: Five types of MIG welding: a) Axial Spray; b) Globular transfer; c) short circuit; d) Pulse current; and e) Surface Tension Transfer[4]

2.2.2.2 Equipment

- ✓ The welding gun and cable assembly contains the shield gas tube, the consumable electrode and the electrical power.
- ✓ Shielding gases. Appendix B has two tables[ii]: Table XIII and Table XIV. The first table presents the typical application for the different gases that can be used in TIG welding. As can be seen, Argon, Helium and Nitrogen can be mixed with themselves or with other gases such as oxygen from CO_2. The second table contains examples of metals and combinations of gases that can be used for those specific metals, in addition to listing some advantages that occur when those arrangements are chosen. For instance, shielding gases can affect cleaning action, arc characteristics, penetration, and speed of welding.

[4] This picture is taken from the Pennsylvania State University ii book.

- ✓ The power source for GMAW welding is direct current with a positive polarity, and they can have transformer-rectifier and inverters as well.
- ✓ An electrode can also be a filler metal for the MIG process. The wired feed motor is thus essential to control the speed and amount of the metal to be deposited on the work piece. In Figure 2-8, a wire ready to be used is illustrated.

Figure 2-8: MIG wired feeder

2.2.3 Comparison between TIG and MIG

Table IV compares TIG and MIG welding. One of the major differences between these processes is the heat generated by the arc. MIG requires less energy than TIG, but it travels with more noise and spatter at high speeds. Moreover, TIG generates more light than MIG when used for longer periods. As it is possible to generate and control a current in a variety of ways, TIG controls the current while MIG controls Voltage. Both kinds of arc welding are used in the industry for different reasons. In order to choose the most suitable method, a welder must know the type of material to be worked on and the amount of money involved in terms of energy, working hours and quality needed.

Table IV: Comparison between TIG and MIG processes

Characteristic	TIG	MIG
Generated temperature	19,426C	4,150C
Type of electrode	No consumable	Consumable
Crack noisiness	Low	High
Spatter	Low	High

Characteristic	TIG	MIG
Travel Speed	3-9 mm/s	25-63 mm/s
Rays	High amount of UV rays	Less UV rays
Voltage	5-10 Volts	20-40 Volts
Current	100 Amperes	100-400 A
Type of energy	Control current, DC/AC	Control Voltage DC

2.3 Finite Element Analysis (FEA) Modeling

2.3.1 Finite Element Analysis (FEA)

Numerical methods transform differential equations into algebraic equations. This is commonly done by converting derivatives into differences, thereby making the infinite finite. However, to have a good approach, it is necessary to use a large amount of differences, and it is only worthwhile if:

- ✓ We have complex geometries.
- ✓ We need to change parameters in order to study different possibilities, which is expensive to do in real life.
- ✓ The analytical results are complex.
- ✓ We have a high-speed computer and appropriate software.

2.3.1.1 Taylor series expansion

If we have a function f that depends on x, the first derivative of f(x) is equal to the limit of Δx when it tends to be 0. Then we have:

Equation 2-15

$$\frac{df(x)}{dx} = \lim_{\Delta x \to 0} \frac{\Delta f}{\Delta x} = \lim_{\Delta x \to 0} \frac{f(x + \Delta x) - f(x)}{\Delta x}$$

This means that:

Equation 2-16

$$\frac{df(x)}{dx} \cong \frac{f(x + \Delta x) + f(x)}{\Delta x}$$

This equation makes an approximation of the first derivative using differences. It can be also written as the Taylor series expansion:

Equation 2-17

$$f(x + \Delta x) = f(x) + \Delta x \frac{df(x)}{dx} + \frac{1}{2}\Delta x^2 \frac{d^2 f(x)}{dx^2} + \cdots$$

We should keep in mind that this is an approximation only, which is arrived at by defining Δx greater than 0 and not tending to 0 (which means – the smaller the gradient, the smaller the error).

2.3.1.2 One-dimensional steady heat conduction

If we want to know the temperature of the surfaces of a wall using a numerical equation, we have to divide the wall into several equal-sized parts. The intersections between the parts are called nodes and are at a distance of Δx=L/M, where L is equal to the thickness of the wall and M is the number of nodes along the wall. We then have M-1 number of nodes. At that point, we can calculate the temperature of each node with the following formula:

Equation 2-18

$$\begin{pmatrix} Rate\ of\ heat \\ conduction \\ at\ the \\ lefthand\ side \\ of\ the\ element \end{pmatrix} + \begin{pmatrix} Rate\ of\ heat \\ conduction \\ at\ the \\ right\ hand\ side \\ of\ element \end{pmatrix} + \begin{pmatrix} Rate\ of\ heat \\ generation \\ inside\ the\ element \end{pmatrix} = \begin{pmatrix} Rate\ of\ change \\ of\ the\ energy \\ content\ into \\ the\ element \end{pmatrix}$$

$$\dot{Q}_{left} + \dot{Q}_{right} + \dot{E}_{element} = 0$$

where Q is the heat conduction, E is the energy generation, and the change into the element is equal to zero due to the fact that we are talking about a steady state condition where there is no change in time. The equations for Q and E are:

Equation 2-19

$$Q \doteq kA\frac{\Delta T}{L}$$

Equation 2-20

$$\dot{E} = e_m \dot{A} \Delta x$$

where k is the coefficient of the heat conduction of the wall, A is the area in which the conduction took place, ΔT is the temperature change across the wall, and e is the rate of heat generation per unit volume in W/m2. At this point, we can write the steady heat conduction formula as:

Equation 2-21

$$kA\frac{T_{m-1}-T_m}{\Delta x}+kA\frac{T_{m+1}-T_m}{\Delta x}+e_m\dot{A}\Delta x=0$$

where m is the number of the node in which we want to know the temperature. Thus, m-1 is the node on the left-hand side and m+1 is the node on the right-hand side. Simplifying, we get:

Equation 2-22

$$\frac{T_{m-1}-2T_m+T_{m+1}}{\Delta x^2}+\frac{\dot{e}_m}{k}=0$$

with the differential equation:

Equation 2-23

$$\frac{d^2T}{dx^2}+\frac{\dot{e}}{k}=0$$

Both equations above are graphically explained in Figure 2-9, where we can see the thickness of the wall, and the surface of the wall is in a plane perpendicular to the paper.

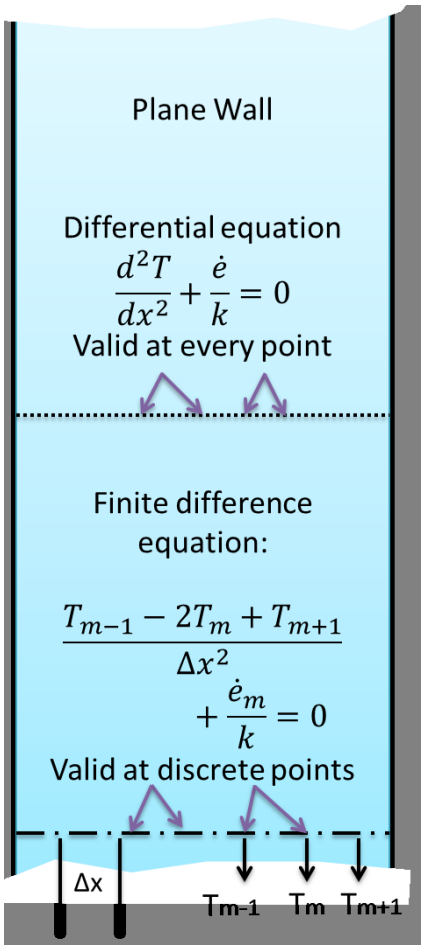

Figure 2-9: Plane wall with differential equation valid at all points in the upper side, and Finite different Equation valid only for nodes in the down level

However, not all nodes are among the wall. Instead, some of them are in contact with air or are insulated and it is therefore necessary to add convection, radiation and/or insulation. All these variations as well as geometric variations such as triangular fins are explained by Çengel[iii].

2.3.1.3 Two-dimensional steady heat conduction

The concept for the two-dimensional steady state heat conduction is the same as for dimensional analysis. However, the object to be analysed has a temperature change not only across the horizontal plane but also in the vertical plane. We can then divide the object into squares, though they can also be triangles to fit into the shape of the body. Assuming that a node is among other conduction nodes, we have:

Equation 2-24

$$\begin{pmatrix} Rate\ of\ heat \\ conduction \\ at\ the \\ left, top, right\ and \\ bottom\ surfaces \\ of\ the\ element \end{pmatrix} + \begin{pmatrix} Rate\ of\ heat \\ generation \\ inside\ the\ element \end{pmatrix} = \begin{pmatrix} Rate\ of\ change \\ of\ the\ energy \\ content\ into \\ the\ element \end{pmatrix}$$

$$\dot{Q}_{left} + Q_{left} + \dot{Q}_{left} + \dot{Q}_{right} + \quad \dot{E}_{element} \quad = \quad 0$$

Following the same method, it is possible to extend the formula three-dimensionally. Also, squares and bricks are not the only shape a segment can take. Figure 2-10 shows some common finite elements.

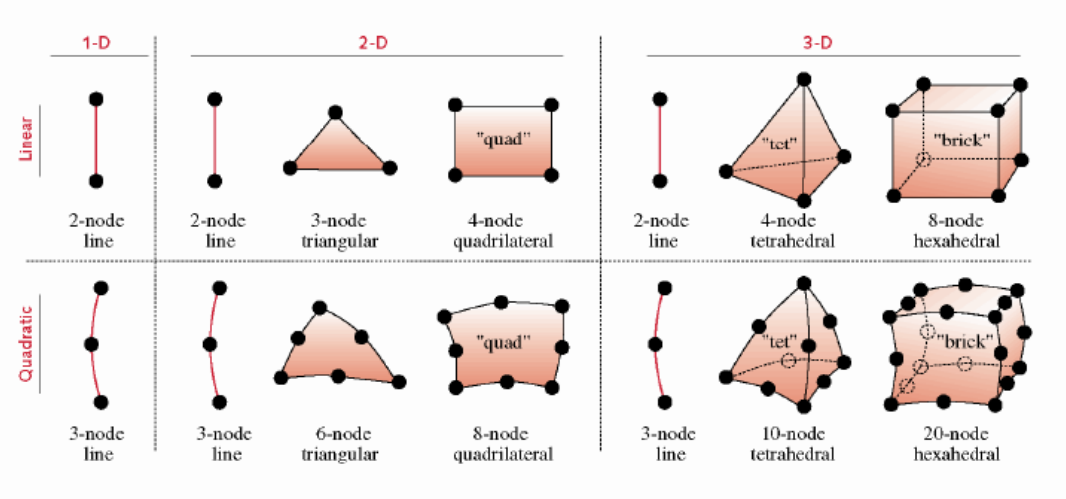

Figure 2-10[iv]: Most common finite elements

2.3.1.4 Transient heat conduction

In a transient study, we not only know the temperature of all discrete points in an object but also the change in temperature during and after a certain time. Hence, we can divide that time into small intervals and make an iteration for each one. This means that the change of energy content into the element is no longer zero but ΔE of the element. Note that:

Equation 2-25

$$\Delta E = mc_p\Delta T = \rho V c_p \Delta T$$

where ρ is the density, V is the volume of the element, c_p is the specific heat, ΔT is the change in temperature, and m is the mass of the temperature. Finally, we have:

Equation 2-26

$$\begin{pmatrix} Heat\ transferred\ into \\ the\ volume\ element \\ from\ all\ of\ its\ surfaces \\ during\ \Delta t \end{pmatrix} + \begin{pmatrix} Heat\ generated \\ within\ the \\ volume\ element \\ during\ \Delta t \end{pmatrix} = \begin{pmatrix} The\ \ change\ in\ the \\ energy\ contnet\ or \\ the\ volume\ element \\ during\ \Delta t \end{pmatrix}$$

$$\sum \dot{Q} \quad + \quad \dot{E}_{element} \quad = \quad \rho V c_p \frac{T_m^{i+1} - T_m^i}{\Delta t}$$

where ΣQ is the sum of the heat transfer from all elements around the element, T^i_m is the temperature of node m at times ti=iΔt, and t^{i+1}_m is the temperature of node m at times ti+1=(i+1)Δt. Note that Δt is equal to the total time to examine divided by the number of steps to reach the total time.

2.3.2 ANSYS 12.1 Workbench

ANSYS workbench is software that uses FEA to make simulations. This interface is arranged in two areas:

- Toolbox, which presents the kind of data to be selected depending on the project. The next figure contains options to choose from. Once the type of project most suitable to the desired analysis has been determined, the next step is to add information to that system.

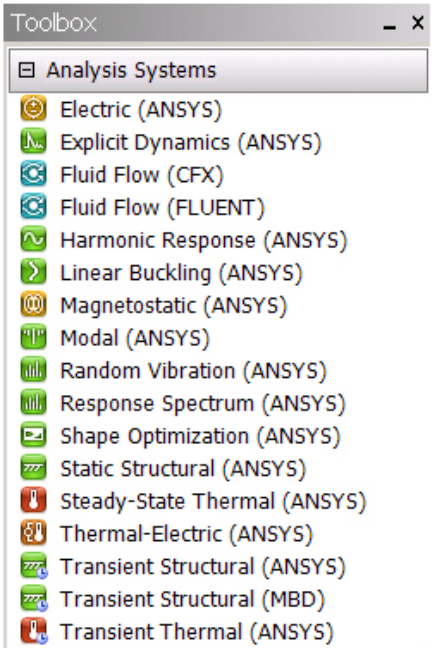

Figure 2-11: ANSYS 12.1 Workbench Toolbox

- Project schematic gives a visual representation of the project being worked on. As can be seen in Figure 2-12, two or more different simulations can be done to the same geometry. Also, it is possible to take the solution from one and use it as a setup for the next simulation. This is very useful, as sometimes one project can have several different analyses. For example, the analysis of a mould's preheat thermal expansion is a steady-state system, while the welding process of the mould is a transient thermal process that can be done after the steady state practise.

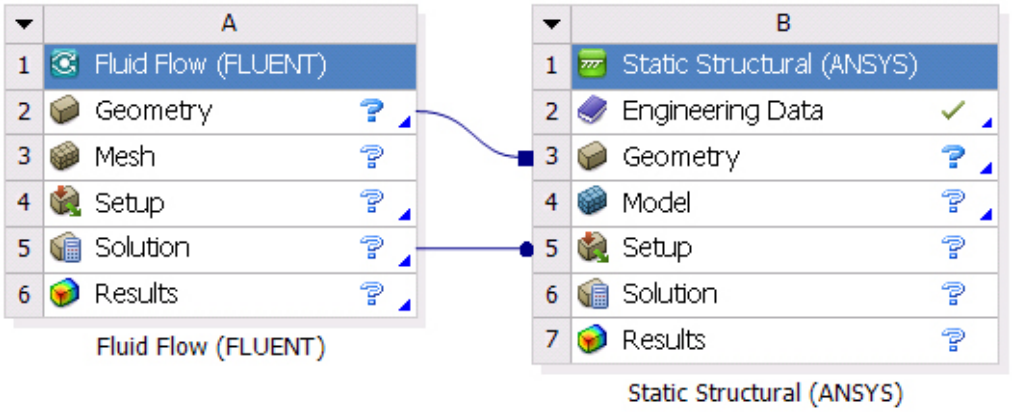

Figure 2-12: ANSYS 12.1 Workbench Project Schematic

As can be seen in the project schematic figure, it is necessary to enter data to get results in a single analysis. The data required is:

1. *Type of Analysis*. Before starting any project, it is necessary to know both the problem to be analyzed and the type of analysis necessary for that specific problem.
2. *Engineering Data*. For some kinds of analyses, the material to be used and its properties are very important, as changes in any property will change the results.
3. *Geometry*. It is possible to import the geometry from a GPS file, which is the universal file for engineering drawing. It is also possible to use another format or draw a model using ANSYS.
4. *Mesh.* Mesh can be custom-designed or a default. However, it is always a good idea to check the mesh because it can also change the results. An ANSYS mesh is shown in Figure 2-13.
5. *Setup.* Incomes for simulation (such as force, heat, or fixed part) are called setup in ANSYS.
6. *Solution.* The solution is the final number after the numerical analysis.
7. *Results.* Results can be presented in video format or on a graph to see what would happen if the project setup were real. For a thermal simulation, one could theoretically obtain graphic results of thermal expansion or even a final temperature.

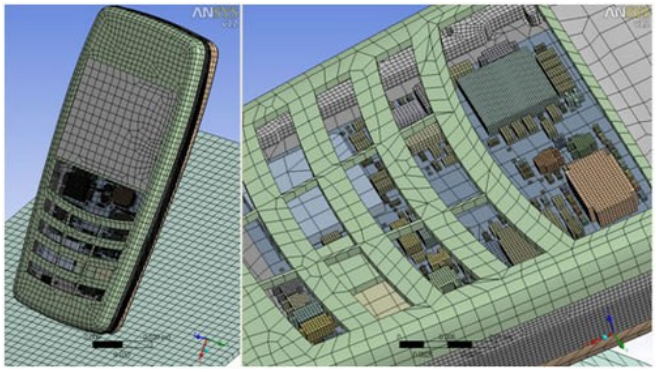

Figure 2-13: ANSYS mesh

2.3.3 . Numerical Proposed Model

To find a relationship between mass and temperature, moulds with different shapes but the same mass are designed. The figures are blocks and pyramids in a variety of sizes. In addition, the weld area is placed at the centre in a corner. Some of the virtual parts are presented in Figure 2-14.

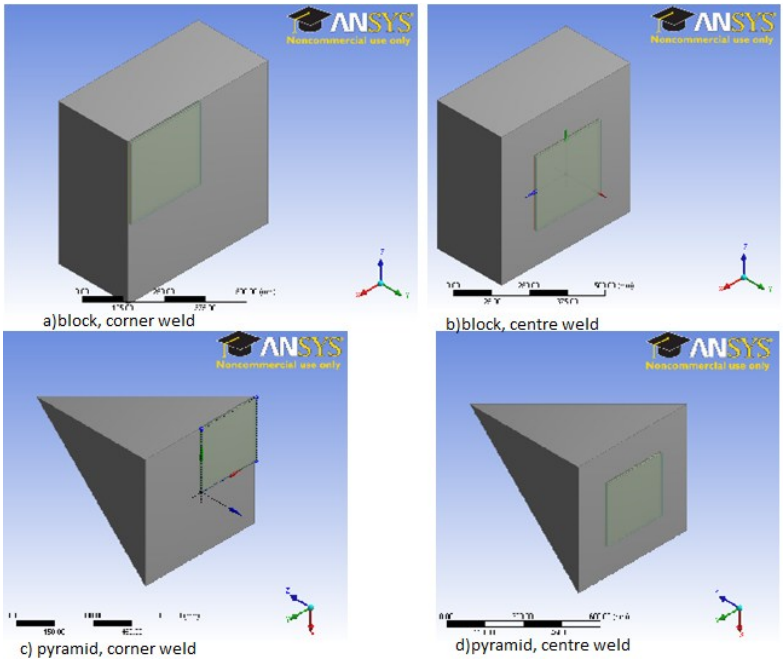

Figure 2-14: Mould used in simulation

The volumes and welding areas that were used for the simulation are in the following table:

Table V: Weight and size of designed moulds

Shape	Size	Volume	Weld Area	% Area	Weld V/layer	% Volume	t per layer
	x,y,z [mm]	mm^3	mm^2		mm^3		Seg.
BLOCK	60,30,60	$1.08x10^5$	$9x10^2$		5400	0.05	60
	120,60,120	$8.64x10^5$	$3.6x10^3$		21600	0.03	240
	240,120,240	$6.91x10^6$	$1.44x10^4$		86400	0.01	960
	600,300,600	$1.08x10^8$	$9x10^4$	$6.25x10^{-2}$	$5.4x10^5$	$5x10^{-3}$	6000
	1000,500,1000	$5x10^8$	$2.5x10^5$		$1.5x10^6$	$3x10^{-3}$	16700
PYRAMID	60,60,90	$1.08x10^5$	$9x10^2$		5400	0.05	60
	120,120,180	$8.64x10^5$	$3.6x10^3$		21600	0.03	240
	240,240,360	$6.91x10^6$	$1.44x10^4$		86400	0.01	960
	600,600,900	$1.08x10^8$	$9x10^4$	$6.01x10^{-2}$	$5.4x10^5$	$5x10^{-3}$	6000
	1000,1000,1500	$5x10^8$	$2.5x10^5$		$1.5x10^6$	$3x10^{-3}$	16700

As can be seen from the above table, the weld volume is the same for both the block and the pyramid, as is the total volume. Also, the area covered by the weld layers is the same for each size of pyramids and blocks. These calculations were made to find a relationship between the volume of the mould and the welded volume, irrespective of the mould's shape.

In order to recreate the model in a dynamic way, the steps followed to find the final temperature of the mould after each layer in the ANSYS simulation are:

1. Set up the initial temperature of the mould.

2. Determine the first layer at 3mm depth, 3mm height and 5mm wide with a melting temperature of $1.43e^3$C.

3. Run the ANSYS program with the following loads:

   a. 20 degrees C of ambient temperature.

   b. Convective heat transfer only. To find a more accurate heat transfer, the values for vertical and horizontal surfaces are placed in the ANSYS formulas. These values are calculated with formulas from section 2.1.3.2 and presented in Appendix B.

   c. The duration of the process is the same as the time per layer, as that is the time the welding robot torch takes to weld that area at a speed of 5m/s.

4. Extract the resulting temperatures of the mould and the layer to do a new simulation with the last data.

5. Repeat step 3.

6. Then, repeat step 4 until reaching four layers of weld material.

The next figure contains the resultant temperatures of different moulds after four layers of welding when the initial temperature for each mould is 300 degrees C. The temperature after each layer is shown behind the line, which corresponds to each mould modeled. At the end of every line, the size of the part appears (the format of the dimension is XxYxZ and is in mm), followed by a comma and its last temperature in Celsius degrees. The letter C is next to the size that means that the welding work is in the centre of the face of the part; if not, the welding job is at the corner of the object. Thus, for instance, if you want to know the temperature of the pyramid after the third layer (whose size is 60x60x90 mm) and the welding is at the center, you will find that the temperature is 471.63 degrees C in the ANSYS model.

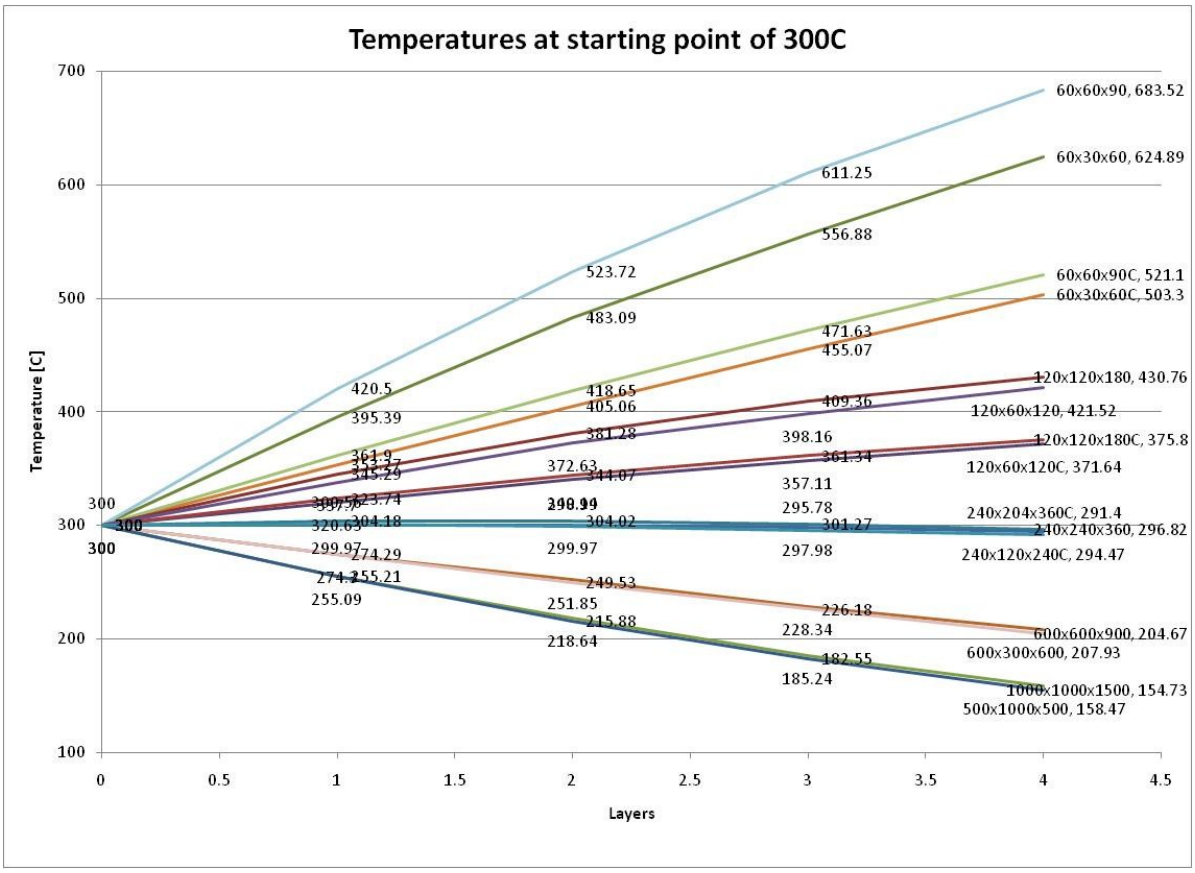

Figure 2-15: Temperature of moulds while welding. At the end of each line, you will see the size of the mould, followed by its final temperature in Celsius.

The temperature grows linearly in small moulds and decreases linearly in large moulds because the heat gain is less than the heat loss. Furthermore, the difference in shape affects larger moulds less than smaller ones. It is important to note here that the part with a volume of 6.91×10^6 mm^3 remains almost constant throughout the whole process, indicating equilibrium between energy loss and energy gain, which is precisely what this research is looking for.

During the welding process, there is an addition of mass and energy at the same time. Thus, to have everything in terms of internal energy, the resultant temperature in the previous section is converted into m-Joules.

To convert temperature into energy, the following formula is used:

Equation 2-27

$$\rho * V * Cp * T = H$$

where:

ρ=density [kg/mm^3]

V= volume [mm^3]

Cp = specific heat [mJ/Kg.C]

T = Temperature [C]

H= thermal energy [mJ]

and the specific heat for P-20 steel is taken as 4.8x10^5 mJ/Kg.C. Using this formula, it is possible to convert the mould's temperature into thermal energy.

After the conversion of the temperature into energy inside the mould using the heat capacity of the P-20 steel, a chart of three axes was made to determine these findings. If different shapes are taken into consideration, the difference in heat will not be as significant as with changes where different volumes are considered. This can be seen in the charts below.

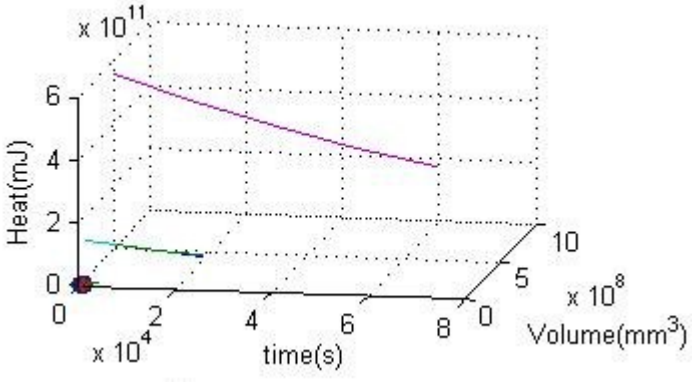

Figure 2-16: Heat in different volumes

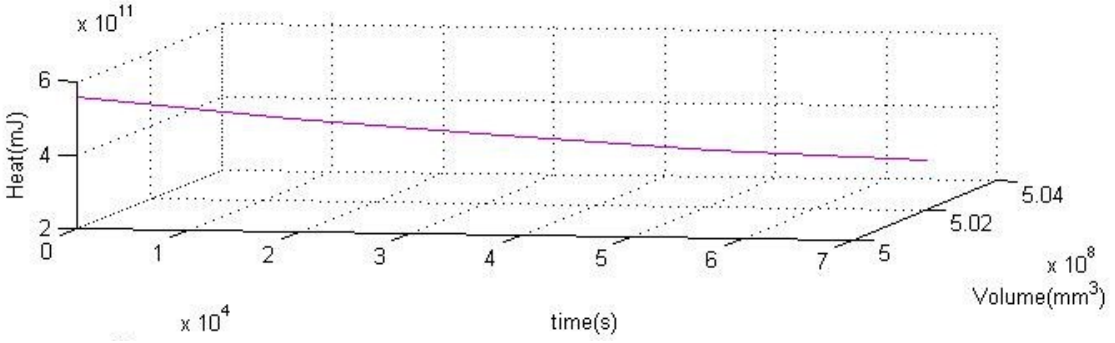

Figure 2-17: Heat in 5x10^{8}mm^3 mould

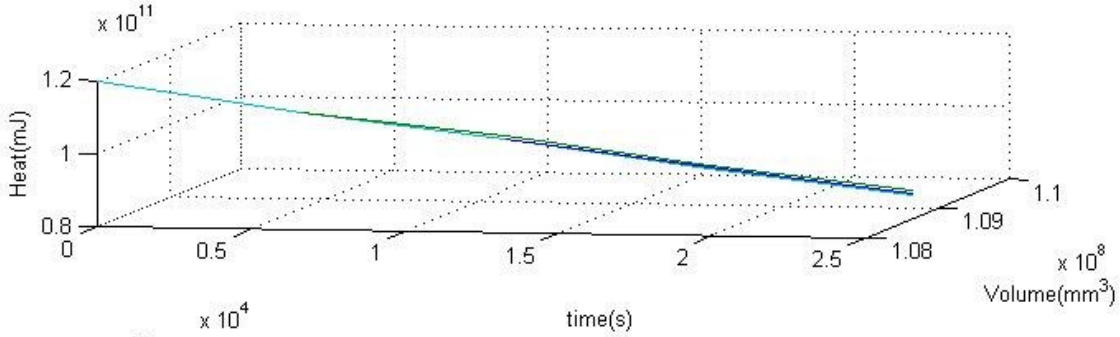

Figure 2-18: Heat in 1x10^8 mm^3 moulds

In the Figure 2-19, we can see there is a point at which the mould loses more heat than it gains, perhaps due to the mass already gained.

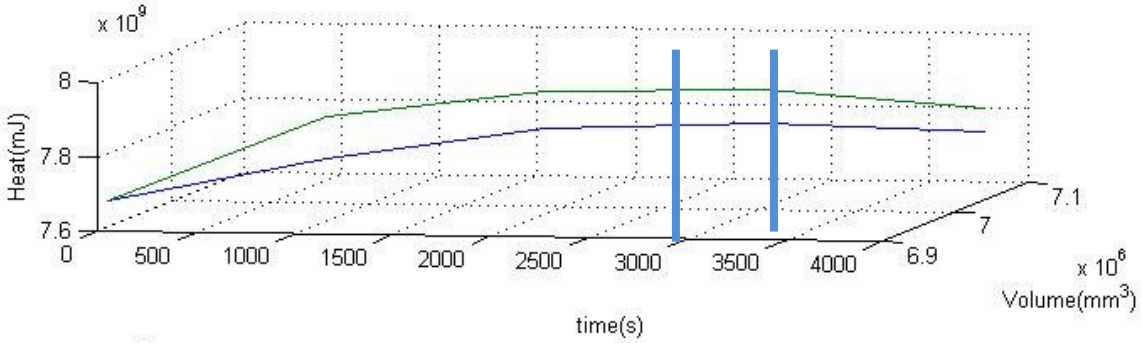

Figure 2-19: Heat in 7x10^{6}mm^3 mould

For small moulds, there is an increase in internal heat, as shown below:

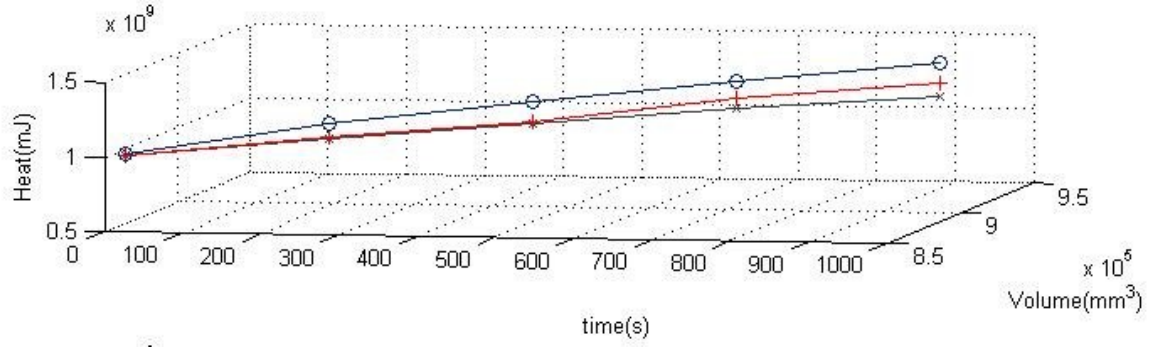

Figure 2-20: Heat in 8.5x10^{5}mm^3 mould

In this simulation, the rate of energy and mass per unit time added to each mould is the same. For this reason, the volume and energy are divided by time. The resulting chart is presented below. Parallel lines are found as a relationship between heat and volume.

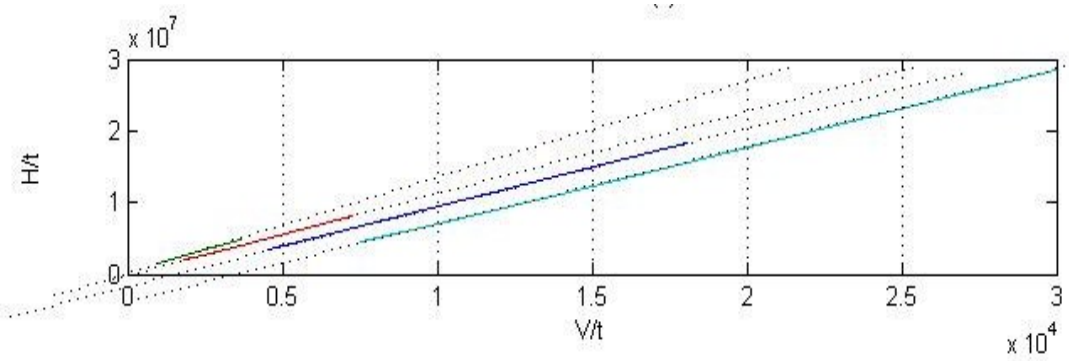

Figure 2-21: Heat and volume divided by time

From this information, a process was created, as presented in Figure 2-23. This process has six steps:

1. Find the maximum expansion.
2. Find the temperature limit.
3. Find the energy in the mould.
4. Add heat and mass during the welding process.
5. Verify temperature.
6. Calculate addition of heat or waiting time.

The first two steps can be used in both the fuzzy logic and numerical methods, while the rest of the

steps are operations that are made instead of the fuzzy rules and fuzzy operations. The following sections will explain each step of the method. Note that this process is formulated in such a way that a programmer can easily define all variables before the formula appearances, since this model was given to Feng Guan, the Software Engineer of Tool-Tec Welding Inc., to create a code and add it to the Tool-Tec system.

2.3.3.1 Determine longest size after preheat process

1. *Longest Edge (LE)*. In this step, it is necessary to enter the size of the longest edge of the mould, as it is the size that will change first due to thermal expansion. Mould size should be given in millimetres.
2. *The initial temperature will be 20 degrees C using CAD draws (Ti)*. It is assumed that the CAD information is given for room temperature, which is 20 degrees C, and that is the value of Ti.
3. *Decide the final temperature (the temperature which the mould will have during welding (Tp))*. The next variable is Tp, which is the preheat temperature of the mould. Every mould has to be preheated to avoid crashes in the Heat Affected Zone. This temperature depends on the size of the mould as well as the kind of work to be performed on the mould. For this reason, the client decides the preheat temperature. However, typically, smaller moulds need a preheat temperature of 300 degrees C and larger ones 400 degrees C.
4. *Select coefficient of expansion value (e)*. Due to the fact that the coefficient of expansion varies depending on the final temperature, Table VI shows three different coefficients of expansion for P-20 steel. If the preheat temperature is 300 degrees C, then the value of e will be $1.27e^{-5}$ C^{-1}.

Table VI: Coefficient of expansion for proposed model using a P-20 steel mould

Coefficient of Thermal Expansion [C^-1]	Tp [C]
$1.27e^{-5}$	200-399
$1.36e^{-5}$	400-539
$1.37e^{-5}$	540-1,427

Ti [C]	
20	

5. *Total expansion*. To obtain the total expansion that the mould will experience, the formula is:

Equation 2-28

$$TE = LE * e * (Tp - Ti)$$

where TE is the Total expansion, LE is the Longest Edge (given in mm), e is the coefficient of expansion (given in mm/mm C), Tf is the final temperature in C, and Ti is the initial temperature in C. All variables are already explained above.

6. *Final Length*. The maximum expansion of the mould occurs in the largest edge. The formula to determine the final size of the longest edge after the preheat process is:

Equation 2-29

$$Lf = LE + TE$$

where Lf is the final size of the largest edge after the preheat process (in mm), LE is the longest edge (in mm) and TE is the Total expansion (in mm). All variables are already explained above.

2.3.3.2 Find the temperature limits

The main purpose of this model is to maintain the preheat expansion size and avoid changes larger than ±0.5mm caused by the thermal expansion effect. This step is divided into two parts. The first part is to find the maximum temperature limit, and the second is to find the minimum temperature limit.

1. *Maximum temperature to avoid more than 0.5mm of expansion*. To find the maximum temperature, the formula is:

Equation 2-30

$$Tmax = \frac{0.5}{Fs * e} + Tp$$

where Tmax is the maximum temperature in C, 0.5 corresponds to the maximum expansion allow to maintain the quality of the mould and it is given in mm; Fs is the final size, which is given in mm, e is the coefficient of expansion, and the Tf is the final temperature which is the preheat temperature in C.

2. *Minimum temperature to avoid more than 0.5mm contraction*. To find the minimum temperature and avoid a contraction larger than 0.5 mm, the formula is:

Equation 2-31

$$Tmin = -\frac{0.5}{Fs * e} + Tp$$

where Tmin is the minimum temperature in C (with the minus sign corresponding to the 0.5 mm of contraction, which is in the opposite way of expansion), Fs is the final size (given in mm), e is the coefficient of expansion and the Tf is the final temperature, which is the preheat temperature in C.

2.3.3.3 Find the energy in the mould

This step is the last step that defines the initial state of the mould before the welding process begins. It is divided into two parts: the first part gives the formula, and the second part gives specific values for the new variables that are introduced in the process.

1. *Thermal energy inside the mould.* The formula intends to find the specific heat of the mould or, in other words, the amount of energy inside the mould after the preheat process. The formula is:

Equation 2-32

$$H = Tp * Cp * V * \rho$$

where Tp comes from step 1 point 3 and is given in C, Cp is the specific heat in J/Kg.C, V is volume in mm^3, ρ is the density in Kg/mm^3 and H is heat in mille-Jules. Note that three variables are introduced at this point and that the values of Cp and ρ are unknown.

The values for P-20 steel are Cp= $4.8e^5$ mJ/Kg.C; for the density, Table VII shows the values for at 20, 200 and 400 degrees Celsius. Because the preheat temperature of the mould will not be less than 200 degrees C and not more than 400 degrees C, the density will be $7.75e\text{-}^6$ Kg/mm^3. Thus:

Equation 2-33

$$H = Tp * 4.8e^5 * V * 7.75e^{-6}$$

Table VII: Density of P-20 steel

Density [kg mm^3]	Temperature [C]
7.80E-06	20
7.75E-06	200
7.70E-06	400

2.3.3.4 Heat and mass added during the welding process

This step starts with a dynamic analysis of the process. The heat and mass added to the mould by the welding torch is calculated for a specific period of time.

1. *Calculation of Volume added during a period of time*. The approximated amount of material that is added during a specific time period can be calculated if the size of the welding bead and the welding speed are known. Thus, we have:

Equation 2-34

$$Vad = tw * WS * Bh * Bw = WT * 5 * 3 * 6$$

where Vad is the added Volume in mm, tw is the welding time in seconds, Ws is the welding speed in mm/s, Bh= high of bead in mm and Bw= bead wide in mm.

2. *New volume*. Here, we have to know the total volume after the welding process.

Equation 2-35

$$Vn = V + Vad$$

where Vn is the new volume in, V is the original volume, and Vad is the added Volume, all in mm^3.

3. *Heat added*. Now we continue with the calculation of heat in the same way we do for the calculation of volume. As we have quantified the added volume, we can assume that the pool behind the bead and the bead have the same size. As well, we can assume that the highest temperature of the welding bead will be the melting point, which is necessary to reach in any welding process. Thus, we can say that:

Equation 2-36

$$Hadd = Cp * \rho * 2Vad * 1.43e^3C$$

where Cp is the specific heat of the material, ρ is the density of the material, Vad is the volume added, and 1,427 C is the melting point of the P-20 steel.

4. *New heat*. We already have H from Equation 2-32 and Hadd from Equation 2-36. These values are needed to obtain the new value of heat (Hn). which is:

Equation 2-37

$$\boldsymbol{Hn = H + Hadd}$$

5. *Calculate the ratio of H/t after convection*. If we take Figure 2-21: Heat and volume divided by time) and extend each line, the resultant graph will be the one in Figure 2-22. This graph presents the relationship between the new volume of a mould divided by the duration of the welding process versus the amount of heat inside the mould at the same time divided by the time of the welding process, calculated using the information of the ANSYS simulation. There are five lines in the chart that correspond to five different initial volumes of the moulds. To determine the initial volume of the mould with the purple line, look at the name of the line that states 6.91E+6, which means that the initial volume of the mould was $6.91e^{6}$ mm^{3}.

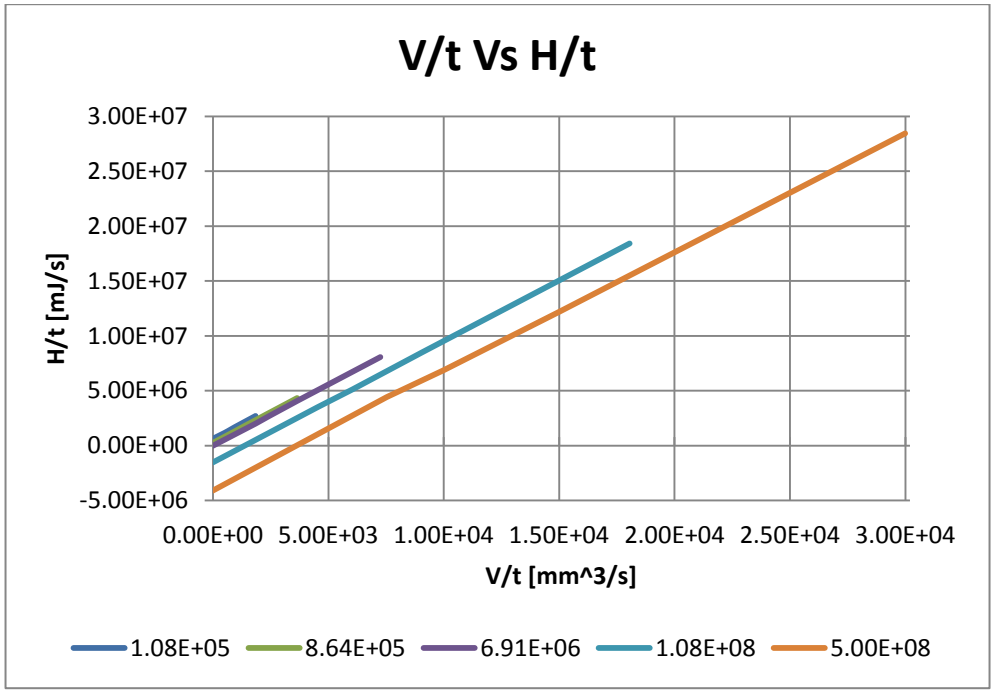

Figure 2-22: V/t Vs H/t

Here, all lines have the form of $y = xb + a$, and the values of a and b for each initial volume can be found in Table VIII. As the values of b are very similar to each other, the value of b for all lines equal to the average value was taken.

Table VIII: Values of a and b for different initial volumes

V [mm³]	a	b
1.08E+05	6.33E+05	1.13E+03
8.64E+05	2.71E+05	1.12E+03
6.91E+06	-7.61E+02	1.12E+03
1.08E+08	-1.52E+06	1.10E+03
5.00E+08	-4.08E+06	1.08E+03
average		**1.11E+03**

We can now determine the ratio of H and t, taking into account the convection heat transfer during the welding process. The formula is:

Equation 2-38

$$\frac{Hac}{t} = 1.11e^3 * \frac{Vn}{t} + a$$

where H/tac is the ratio of heat and time at the end of the process, Vn/t is the ratio of the new volume and the time, and a can be taken from Table VIII. If the volume of the mould is not equal to the any of the values in the table, a can be interpolated. Furthermore, 1.11e3 corresponds to the average value taken from Table VIII.

6. *Heat after convection*. Now that we know H/tac, we can easily multiply that value by the duration of the process in seconds to know the actual heat inside the mould at the end of the welding process (Hac). So, we now have:

Equation 2-39

$$Hac = \frac{H}{tac} * t$$

2.3.3.5 Verify temperature

1. *New temperature of the mould*. The new temperature (Tn) of the mould can thus be calculated using the actual heat inside the mould in order to determine if it is outside the limits. Here, we should keep in mind that this temperature will be the temperature of the mould if nothing is done to maintain it at the preheat temperature.

Equation 2-40

$$Tn = \frac{Hac}{Vn * Cp * \rho}$$

2.3.3.6 Addition of heat or waiting time

The objective of this model is to prevent temperature changes during the welding process in order to achieve the highest quality welding job. This final step determines if it is necessary to wait for the heat to dissipate or if it is necessary to add heat. Heat can be added placing the mould on a table with burners and turning them on if necessary.

1. *Desired ratio*. First of all, we have to know what we want, which is to maintain the same initial ratio of heat and volume along the welding process. The desired ratio is:

Equation 2-41

$$Rd = \frac{H/V}{t}$$

2. *Required time*. To maintain the temperature of the mould, it is necessary to keep the value of Rd the same at all times. In the dynamic analysis, the new value of H is Hac and the new value of V is Vn. To maintain the value of Rd, it is necessary to calculate the new value of t, which is tr. Then,.

Equation 2-42

$$tr = \frac{Hac/Vn}{Rd}$$

3. ***Waiting time.*** The difference between tr and t will be the wait time required to maintain the temperature of the mould at the preheat temperature. Note that this number will not always be positive. It can be equal to zero, which means that no wait time is needed, or it can be negative, which means that we have to add heat instead of wait time. Thus:

Equation 2-43

$$Waiting\ time = tr - t$$

4. Required heat. In a similar way to what we do with tr, we will find the required heat (Hr) not the actual heat of the process. The result of this is:

Equation 2-44

$$Hr = Rd * Vn * t$$

5. ***Adding heat.*** Now we find the difference between Hr and Hac and, if the result is positive, we need to add some heat to the mould. If not, the value of tr will be positive. Remember that the values of Hr and Hac are in mJ.

Equation 2-45

$$Adding\ heat = Hr - Hac$$

2.3.3.7 Summary of model

To summarize the proposed model made with the analysis of the simulation results, Figure 2-23 presents the five steps with their corresponding formulas. Table IX shows the meaning of each variable in chronological order. The value of a in step 4 is in Table VIII, and you can use interpolation to obtain the value for any volume. Also, a detailed explanation of each step is provided in subsections **Error! Reference source not found.** to 2.3.3.6

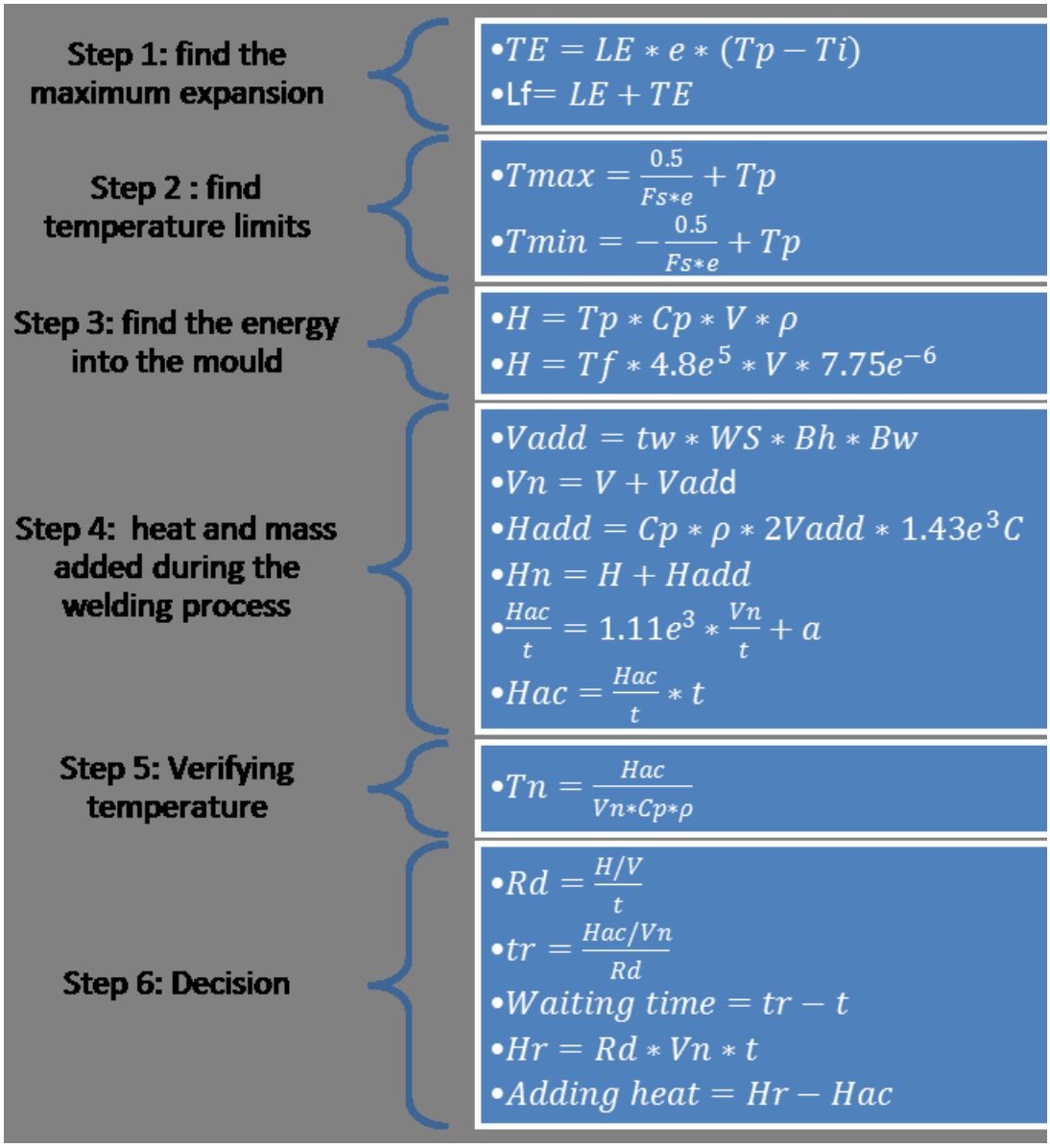

Figure 2-23: Summary of proposed model

Table IX: Variables of proposed model

Nomenclature	Meaning	Units
TE	total expansion	mm
LE	longest edge	mm
e	coefficient of thermal expansion	1/C

Nomenclature	Meaning	Units
Tp	preheat temperature	C
Ti	initial temperature	C
Lf	final length	mm
Tmax	maximum temperature limit	C
Tmin	minimum temperature limit	C
H	thermal energy	mJ
Cp	specific heat of material	mJ/kg.C
V	volume of mould	mm^3
ρ	density of mould	kg/mm^3
Vadd	volume added	mm^3
tw	welding time	S
WS	welding speed	mm/s
Bh	bead high	mm
Bw	bead wide	mm
Vn	new volume	mm^3
Hadd	added heat	mJ
Hn	new heat	mJ
Hac	Actual heat	mJ
a	variable for linear relation	mJ/s
Tn	new temperature	C
Rd	desired ratio	$mJ/mm^3.s$
tr	required time	s
Hr	required heat	mJ

Chapter 3
Fuzzy Modeling and Heated Moulds

In Chapter 2, the construction of a model based on physics knowledge and FEA analysis was described in detail. The intent of the project was to calculate and determine how a piece being worked on could remain at an average temperature at all times. In this chapter, another model is presented that is based on the expert knowledge and experience of the Tool-Tec welders, who used arc welding on a daily basis and were therefore intimately acquainted with its abilities and limitations. The fuzzy logic method will be applied here as a tool, as fuzzy logic is widely used to automate processes utilizing human knowledge and expertise.

This chapter explains the fuzzy logic method, describes the basic fuzzy logic operators, introduces concepts like fuzzification and de-fuzzification, and provides a simplistic example of how to apply fuzzy logic. Section 3.3 illustrates in detail an actual model to be used to determine the correct amount of heat or time to be added to the process to avoid changes in the average temperature on the work piece during the automatic welding process. The chapter ends with a comparison between the results of the model generated using FEA analysis and the model using the fuzzy logic method.

3.1 Literature Review

In the past, researchers have used numerical and fuzzy logic techniques to solve temperature and welding problems. For example, Gao Xiangdong[v] designed a fuzzy logic controller for an arc welding robot using a vision sensor. However, the six-axis robot for this project did not use vision sensors. Zafer[vi] used fuzzy logic to control the torch position during arc welding, but the position of the torch is not an issue in this project. Akira[vii] considered the pool phenomena, and Hartman[viii] also worked with pool geometry by regulating heat input during the welding process. Li Di[ix] regulated the weld geometry by using neural networks, thereby eliminating the need for consultants and Austin[x] showed that the very complex process of welding can benefit significantly form the use of fuzzy logic controls. From the above research, it is reasonable to assume that fuzzy logic systems and neural networks have been successfully used in past welding processes.

3.2 Fundamentals of Fuzzy logic

3.2.1 Fuzzy Logic Operators

✓ **NOT** is the complement or negation of a fuzzy set. This equation is represented as follows:

Equation 3-1

$$\mu_{A'}(x) = 1 - \mu_A(x) \; for \; all \; x \epsilon X$$

where A is a fuzzy set in the universe X and its complement is A'. We can have a graphic representation at the bottom of Figure 3-1, where cool is the fuzzy set A and not cool is its complement.

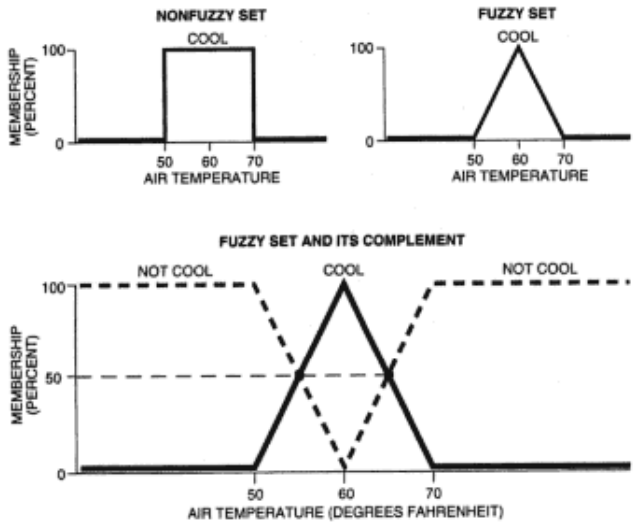

Figure 3-1: Differences between crisp logic and fuzzy logic (upper diagram) and complement of a fuzzy set (lower diagram).

✓ **OR** is the union or disjunction of two fuzzy sets. Its function is given by:

Equation 3-2

$$\mu_{A \cup B}(x) = \max[\mu_A(x), \mu_B(x)] \;\; \forall x \epsilon X$$

where A and B are fuzzy sets in the same universe X and the operation is denoted by ∪. The operator uses the term "max" because the element x belongs to one of the sets, which means that the larger membership grade will be the outcome. Figure 3-2 (right-hand side) shows graphically the union of two fuzzy sets.

- ✓ **AND** is the intersection or conjunction of two fuzzy sets and contains all elements that are common to both sets. It is characterized by

Equation 3-3

$$\mu_{A\cap B}(x) = \min[\mu_A(x), \mu_B(x)] \ \forall x \epsilon X$$

where A and B are two fuzzy sets in the same universe X. The operator is denoted by ∩. Here, the operator is represented by "min" because, this time, the result will be the minimum value between both sets A and B. Figure 3-2 presents this idea in a chart.

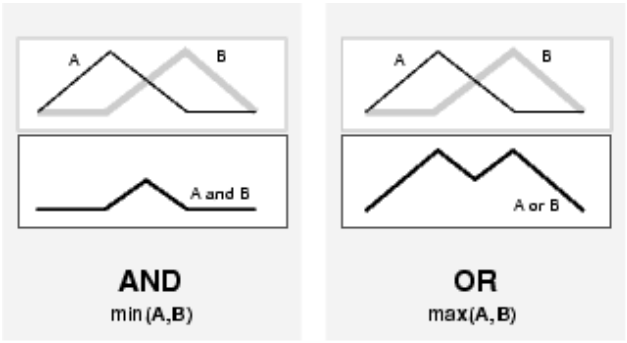

Figure 3-2: Graphic representation of a union and an intersection between two fuzzy sets

3.2.2 Fuzzification

With the operators above, we can go back to the set of rules. The operator between states is an intersection and the operator between rules is the union operator. This is the typical way that states and rules are related.

The consequence of each rule is then unified with the others to reach a final decision. It is important to note here that, prior to starting the operations, the rules have to be fuzzified and, after the fuzzy logic process, the results must be de-fuzzified.

Fuzzification is a procedure by which data is obtained. If we consider the general problem of approximate reasoning, where knowledge base D is represented in an approximate form, we have: FD=FP(D). For example, the bottom graph of Figure 2 shows that 60 degrees Fahrenheit is a cool temperature and that the number 1 represents this temperature in a fuzzy logic system. However, cool has its own representative function to allot grades to any value different than 60. In this way, every value can have a fuzzy representation, which can assume forms such as Triangular, Gaussian or Trapezoidal.

3.2.3 De-Fuzzification

De-fuzzification is the transformation of the fuzzy result (i.e., a resultant function) into a crisp value. There are many ways of performing this conversion (see [xi] for a description of these methods). However, this thesis will explain only the centroid method. This technique will be used because it takes the center of gravity of the union of the resultant actions during the fuzzy logic process and thus represents the overall result. The function of the centroid is expressed as:

Equation 3-4

$$\hat{C} = \frac{\int_{C \in S} C \mu_c(c) dc}{\int_{C \in S} \mu_c(c) dc}$$

where $\hat{C}$ is the de-fuzzified control action which is the centroid inference (assuming that the membership function of a control inference is $\mu_c(c)$, a part of which is $S = \{C | \mu_c(c) > 0\}$). For example, if the function is

$$M_C(C) = 44 \qquad For\ 0 \leq C \leq 55$$

(i.e., if it is a horizontal line with a value of 44 from 0 to 55), then using Equation 3-4, the centroid will be:

$$\hat{C} = \frac{\int_0^{55} 44 C dc}{\int_0^{55} 44 dc} = \frac{\left[\frac{44}{2} C^2\right]_0^{55}}{[44C]_0^{55}} = \frac{66{,}550}{2420} = 27.5$$

3.2.4 Fuzzy Logic Example

We can see an example of a set of rules which are interconnected by the operator OR in Figure 3-3**.** This example is a problem taken from Fakhreddine[xii]'s book regarding a metallurgical process in which

the rate of fuel supply depends on the temperature of the material (T), the mass of the material (M) and the process termination time (P). T can be low (LW) or high (HG); M can be small (SM) or large (LG); P can be far (FR) or near (IN); and F can be reduced (RD), maintained (MN) or increased (IN). Inevitability, each fuzzy state has its own membership function and each rule has to be applied at every instance to determine the final resolution. Figure 3-4 shows the fuzzy result and its crisp value for a given instant, which is the singleton in red found via the centroid process.

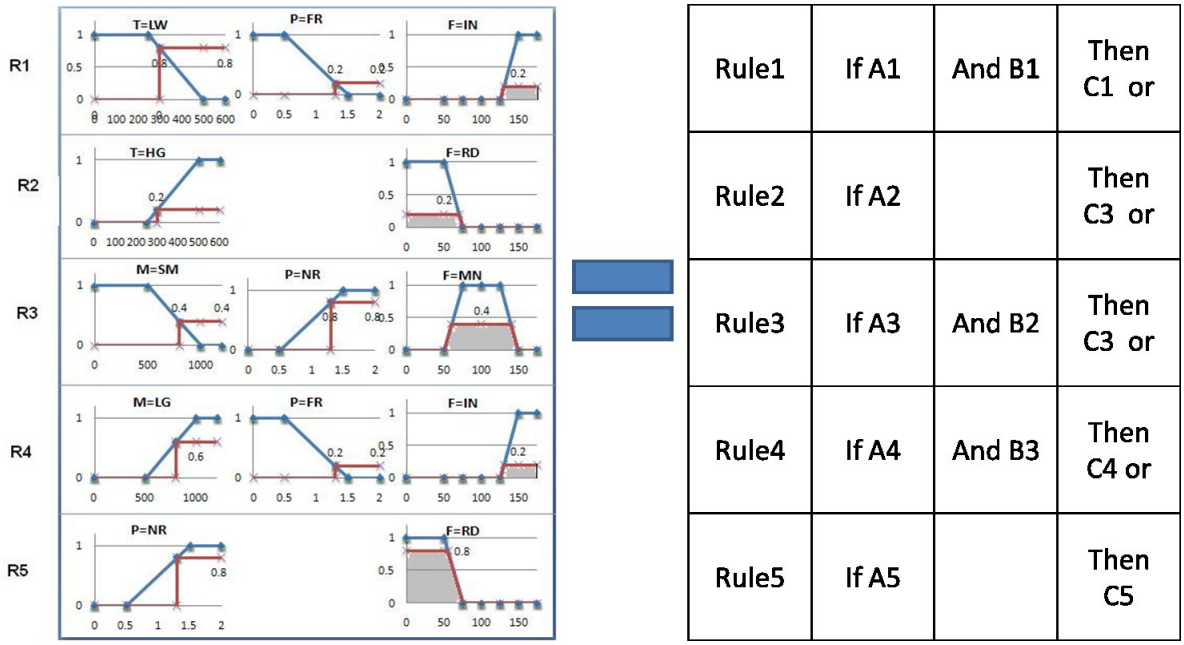

Rule1	If A1	And B1	Then C1 or
Rule2	If A2		Then C3 or
Rule3	If A3	And B2	Then C3 or
Rule4	If A4	And B3	Then C4 or
Rule5	If A5		Then C5

Figure 3-3: Graphic representation of fuzzy logic process where R1, R2, R3, R4 and R5 are the fuzzy logic rules, T (temperature), M (mass) and P (pressure) are states, and F (fuel) is the decision made.

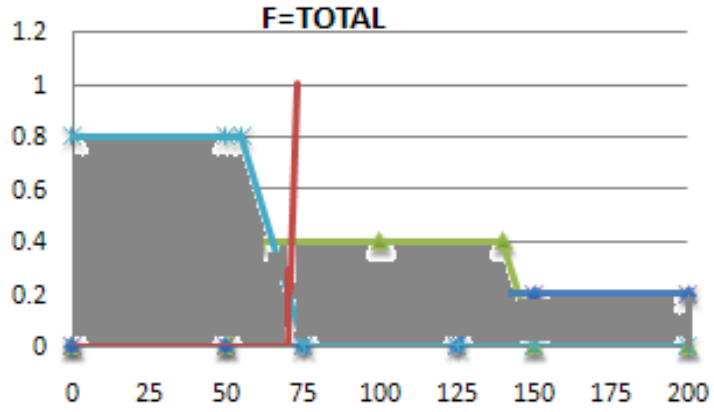

Figure 3-4: The gray area is the union of each F result and the red line is the centroid de-fuzzification.

3.3 Fuzzy Logic Proposed Model

After eight months of observation in Tool-Tec it was possible to say that if the mould is *big*, the burners are at the bottom of the mould must be at 100% of their capacity. Also, if the mould is *small* and the amount of heat is *large* the mould will need *some* time to dissipate the heat. Besides, an expert from Tool-Tec Inc. said that, if the mould has a regular size there will be time for the heat to dissipate but won't be enough time to reduce the temperature. This means that it is not necessary to add heat or wait time for *some moulds*.

Analysing the paragraph above and following the fuzzy logic method, it is possible to extract useful rules and convert them into numbers. At this point, we have two variables: size and amount of heat added to the mould. The decision that has to be made is whether to add heat, impose a waiting time, or just continue welding. Hence, the resultant rules are:

R1. If the mould is *large,* then *add 100% of heat*.

R2. If the mould is *small* and the heat from the torch is *large,* then *wait an appropriate amount of time*.

R3. If the mould is *medium-sized,* then *continue* welding without changes.

The next step is to find numbers for large, small and medium-sized moulds.

At Tool-Tec, the larger moulds were bumpers. These kinds of moulds had volumes with a range between $2.5x10^8$ mm^3 and $3.12x10^{10}$ mm^3 and lengths from 1,300 mm to 2800 mm. Size ranges such as these are typical of large moulds. Conversely, a small mould would typically be 8.8 kg with a volume of $1.13x10^6$ mm^3, and a medium-sized mould would have a volume of $7x10^6$ mm^3. Having given all fuzzy descriptors a crisp value, it is therefore possible to create a formula to describe them. Figure 3-5contains these formulations.

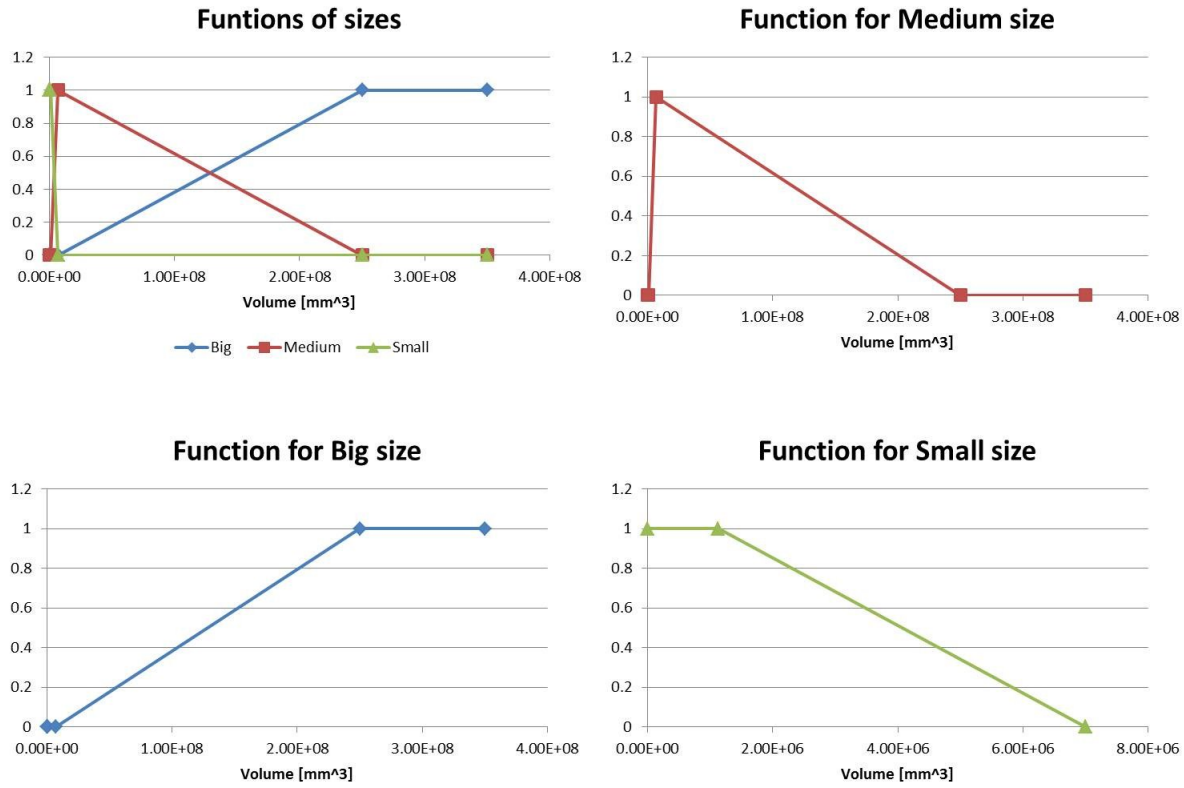

Figure 3-5: Graphic presentation of size functions

Based on this, the initial function for each fuzzy descriptor will be:

Equation 3-5

$$\mu_B(V) = 0 \qquad For\ 0 \le V \le 7e^6$$
$$= 4e^{-9}V - 0.0288 \qquad For\ 7e^6 \le V \le 2.5e^8$$
$$= 1 \qquad For\ 2.5e^8 \le V$$

where B is large size and V is Volume [mm^3]. This function is shown in Figure 3-5 c) above.

Equation 3-6

$$\mu_M(V) = 0 \qquad For\ 0 \le V \le 1.13e^6$$
$$= 2e^{-7}V - 0.1925 \qquad For\ 1.13e^6 \le V \le 7e^6$$
$$= -4e^{-9}V - 1.0288 \qquad For\ 7e^6 \le V \le 2.5e^8$$

$$= 0 \qquad For\ 2.5e^8 \leq V$$

where M is medium size and V is Volume [mm^3], as seen in Figure 3-5 b).

Equation 3-7

$$\mu_S(V) = 1 \qquad For\ 0 \leq V \leq 1.13e^6$$

$$= -2e^{-7}V - 1.1925 \qquad For\ 1.13e^6 \leq V \leq 7e^6$$

$$= 0 \qquad For\ 7e^6 \leq V$$

where S is small size and V is Volume [mm^3]. The graphic expression is shown in Figure 3-5 d).

Regarding consequences, when the bumpers are fully opened, they produce 293kW or 1,000,000 BTU/hr. Nevertheless, not all heat is injected directly to the mould; an efficiency of 60% (which corresponds to 175.8KW) results in a fuzzy number of 100. Consequently, the decision membership function will be:

Equation 3-8

$$\mu_H(F) = 0.01F \qquad For\ 0 \leq F \leq 100$$

$$= 1 \qquad For\ 100 \leq F$$

where F is the fuzzy number and H refers to the heat to be added. For the second rule, the heat that comes from the torch will be:

Equation 3-9

$$\mu_R(J) = 2e^{-5}J \qquad For\ 0 \leq J \leq 5.74e^4$$

$$= 1 \qquad For\ 5.74e^4 \leq J$$

where J means Joules per minute which are added by the welding torch and R is the fuzzy set of the rate of heat. Figure 3-6 presents this rule in a graph.

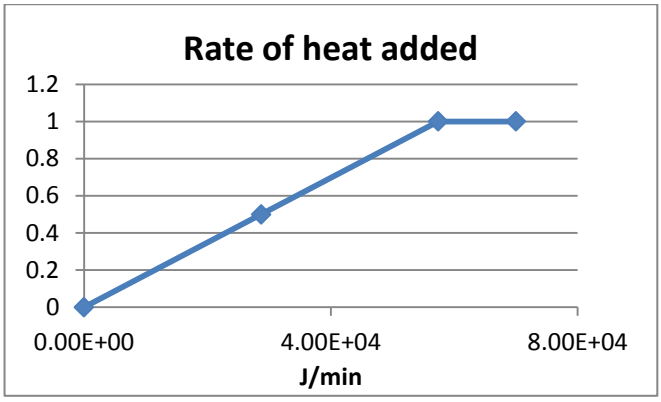

Figure 3-6: Second condition of R2

The decision of this rule has the following membership function:

Equation 3-10

$$\mu_t(F) = 1 \qquad For\ F \leq -100$$
$$= -0.01 \qquad For -100 \leq F \leq 0$$

where t is the time to be waited and F is the fuzzy number. In this case, -100 correspond to 27 seconds that the robot has to wait after every 60 seconds of welding. In the same manner, the fuzzy number 0 would be equal to 0 waiting time. Finally, for the third rule, the decision function is:

Equation 3-11

$$\mu_M(F) = 0 \qquad For\ F \leq -100$$
$$= 0.01F + 1 \qquad For -100 \leq F \leq 0$$
$$= -0.01F + 1 \qquad For\ 0 \leq F \leq 100$$
$$= 0 \qquad For\ 100 \leq F$$

where F is the fuzzy number already explained. Negative numbers denote additions of time, whereas positive numbers indicate additions of heat. It is worthwhile to mention here that this function is the complement of the other two decision functions, as the intent is to find moulds which do not require an accumulation of time or energy. The graphic representation of the three decision functions is shown in Figure 3-7.

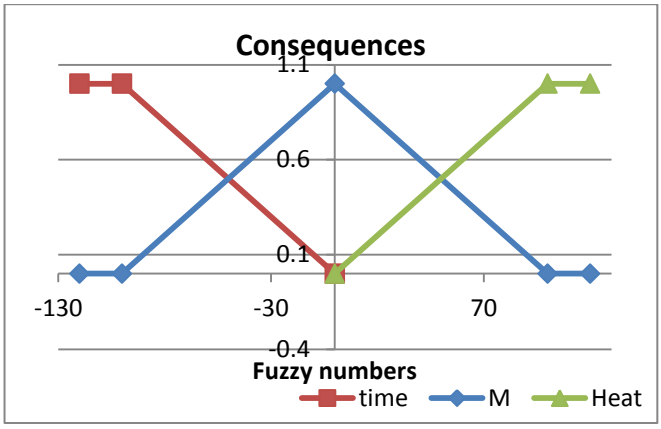

Figure 3-7: Consequences of R1, R2 and R3

The fuzzy formulas described above were automatically changed into Bell and Gaussian functions in Mat lab in order to provide better results; however, the same parameters and logic used in linear functions were maintained.

3.4 Comparison between Fuzzy Logic and Analysis of FEA Modeling Results

Thus far, there are two proposed models: the first one is explained in section 2.3.3 and the second one in section 3.3. Table X below contains the results of the fuzzy system as well as the results after the six-step process. In the table, s means the number of seconds that have to be waited for every two minutes of welding, and kW stands for kilo Watts that have to be added by burners.

Table X: Results for different methods

Volume [mm^3]	Fuzzy logic with Bell and Gaussian functions	Fuzzy logic with linear functions	Numerical method
$1.08e^4$	19.84 s	9.52 s	150.85 s
$1.08e^5$	19.78 s	15.4 s	18.12 s

Volume [mm³]	Fuzzy logic with Bell and Gaussian functions	Fuzzy logic with linear functions	Numerical method
8.64e⁵	18.82 s	15.4 s	14.75 s
6.91e⁶	0.00254 s	0.0728 s	42.42W
1.08e⁸	128.861 kW	30.24 kW	4.18 kW
5e⁸	142.92 kW	140.11 kW	4.25 kW

The first column shows various volumes that a mould could have. In reviewing the table, it is useful to remember that a mould can take any form and can be solid, holey, pocked or full of cavities. The two proposed models presented in this chapter generalize the process, such that there is no need to know the shape of the mould; the volume and the largest edge are the only data required. An example of a mould is given in Figure 3-8. The mould is irregularly shaped but, using CAD data, we can determine that it has a volume of $1.13e^6$ mm^3 and that the largest size is 178.7 mm (which corresponds to the X direction or the blue arrow, if we see the ANSYS orientation). This is considered a small mould since its size can be placed between the 2nd and the 3rd volume on the table above. Smaller values were adopted for possible volumes in order to have a wider range of volumes and to keep the idea that the two proposed models are universal.

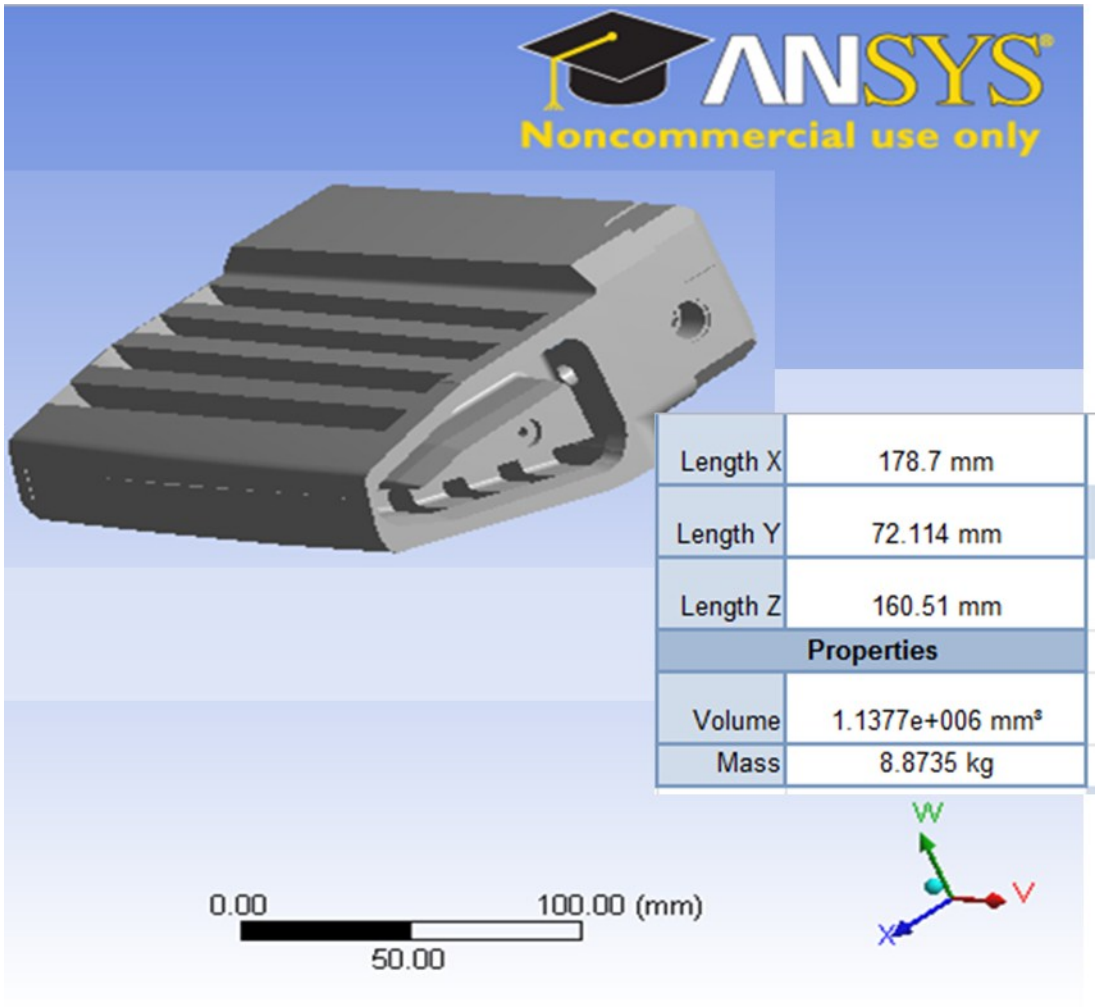

Figure 3-8: Example of mould using CAD information

The second column of Table X provides results for the fuzzy logic method that uses Gaussian and Bell functions. The 3rd column shows results for the fuzzy logic method that uses Linear Functions, and the last column shows results for the proposed numerical method. The column of the numerical solution is linear, since the base of this method is a linear function that was found in the analysis of the results after several simulations using ANSYS Workbench. This linear function is Equation 2-38 (see subsection 7.3.4 of this thesis). Here, the fuzzy logic methods are conservative in nature and generally closer to the highest value, which is why the results of these methods are very different. Nevertheless, we can see that when the size of a mould is close to a medium, the values of all methods are close to 0, and thus the medium-sized mould is nearly the same for all methods.

Chapter 4
Experimental Testing

As explicated in Chapters 1, 2 and 3 of this thesis, two models to maintain the preheat temperature of P-20 steel moulds during the welding process have thus far been created and described. One of the models had its genesis in the expertise and hands-on experience of the welders at Tool-Tec Welding Inc., and the other was made using established theories of heat transfer and thermodynamics. However, problems arose when it came time to validate those models. Unfortunately, and as mentioned previously, Tool-Tec Inc. closed down before the theories could be put to the test. The University of Waterloo does have an arc welding robot for experimental purposes and an IR camera which can be used to take the overall temperature in one single shot, but there is only one mould that can be used for experiments and the robot uses MIG welding instead of TIG welding. (For differences between MIG and TIG welding, see section 2.2.3.)

Nevertheless, the above-mentioned circumstances were not sufficient to cancel the research experiments of this study, as heat transfer properties for most steels are almost the same. Moreover, these models work for any size and shape of piece to be worked on, and the differences between MIG and TIG welding can be compensated from a thermal point of view. Specifically, the highest temperature of the welding bead will always be the melting point, and the final shape, for quality purposes, will be the same for both MIG and TIG welding.

To make the requisite temperature measurements, an infrared (IR) camera was used. An IR camera makes heat radiation visible by capturing IR waves and transforming them into images. To better explain the technology, the first section of this chapter focuses on thermography and presents a literature review of how IR cameras have been used in the past for welding and other IR applications. This first section also explains what thermal radiation is and how an IR camera works.

Following the thermography section, details about the experiment and its setup will be explained, including the parameters of the welding robot and the IR camera arrangement.

During the experiment, measurements were taken with an FLIR Thermacam SC500 and the data stored in 521 frames. These frames were arranged to extract the necessary information to be able to study the results. How a mat lab program was created to do that job is described in the first section of this chapter,

while the second part analyses and discusses the results given by the mat lab program and the experiment overall.

4.1 Thermography

4.1.1 Literature Review

Despite the limitations of an IR camera in terms of resolution and noise, it can be more accurate than other methods used nowadays. For example, Thomas E. Salem, Dimeji Ibitayo, and Bruce R. Geil[xiii] validated the FLIR Systems Thermacam SC500 (IR) camera system, showing that it has better results than two different spray coatings to create a uniform surface emissivity. And a lot of research has been done to determine temperature by using infrared thermography such as Y. Kiwamoto,a) H. Abe, Y. Tatematsu, T. Saito, M. Kurata, K. Kajiwara, Y. Kikuchi, T. Takahashi, and T. Tamano[xiv] who determine the temperature of gray objects in exotic environments and not in laboratories or T. C. Cetas[xv] who try to tackle the difficulties that presented IR cameras in 1977. And companies like Hathmore Thecnologies[xvi] make External/Internal Infrared Thermography Inspection for Air Leakage Detection using infrared cameras. IR cameras are very powerful when the target object is difficult to reach, for example, John A. Stevenson and Nick Varley[xvii] monitored the temperature of fumaroles of the Vocan of Colima at a distance of 6 km with an IR camera. However, all this work has been done in a level of Thermography and not in a Computer Vision level.

On the other hand, intelligent algorithms have been appeared to detect the temperature of the target object automatically. For example, Shuaiyin Wang, Yajuan Wang and Yongtao Zhang[xviii] used a combination of Genetic Algorithm and Back Propagation Neural Network to determine the temperature of a target object. Though, they still have some problems due to the large number of parameters to be adjusted since they are using two different techniques.

4.1.1.1 Welding applications

Welding is an operation which needs a lot of human effort not only in working time but also in terms of knowledge. In fact it is almost an artistic work and most of times it has to be a perfect work for safety reasons. That is why researchers had study the process in order to able to automate it. One of the issues during the welding process is the temperature which plays an important part to get a perfect bead. Many

people like S. Nagarajan, W. H. Chen, and B. A. Chin[xix], P. W. Ramsey[xx] or J. P. Boillot[xxi] have used IR cameras to control the bead's temperature.

Talking about arc welding Sundaram Nagarajan, Probal Banerjee, WeiHua Chen, and Bryan A. Chin[xxii] controlled bead width, penetration depth and torch position at the same time using the B. A, Chin's technique about sensing only long wavelengths capture only the temperature of the welding part and not the arc temperature. A really good paper which writes about automation of arc welding was done by D. V. Nishar, J.L. Schiano, W. R. Perkins and R. A. Weber[xxiii] in 1994 in which one of the goals is reduce cost to install an optical system for measuring weld temperature and the controller algorithm.

However, all those works only take care of the temperature of the material near to the torch and don't look at the overall temperature of the part that is been welding. And the temperature of the welding part matters when the welding process could take several hours and the welding part cools down or warms up so much that the welding part change size.

4.1.1.2 Almost IR applications

It is worth it to mention that a CCD camera can detect invisible waves for our eyes which are part of the thermal radiation and it can be used for industrial inspections avoiding high commercial value of IR cameras as J. Chen, P. Osbom, A. Paton and P. Wall[xxiv] did. It even can be used for pedagogic porpoises as Zden.ek Bochn L.cek[xxv] described very well in his paper.

4.1.2 Radiation

All bodies with a temperature greater than 0K (absolute zero) emit thermal radiation. Radiation heat transfer occurs between two bodies separated by a medium colder than both, while thermal radiation is part of electromagnetic radiation, which are waves that travel at the speed of light in a vacuum (c=2.9979 x 10^8 m/s). Electromagnetic waves have a frequency (v) which is the number of oscillations per second and a wavelength which is the length of the wave in μm (λ).

Depending on the wavelength, there are several types of radiation. Nevertheless, the one that concerns us here is thermal radiation emitted as a result of energy transitions of molecules, atoms or electrons. Temperature is a measurement of the strength of these activities. The wavelength of this radiation goes from 0.1 to 100 μm, and this range also covers infrared (IR), visible (light, 0.4 – 0.76 μm) and a portion of UV radiation.

If an amount of thermal radiation or heat flux (Φ) touches the surface of a body, not all the heat will be absorbed (Φ_A). Some will be reflected (Φ_R) or transmitted. (Φ_T Figure 4-1 shows the effect graphically.)

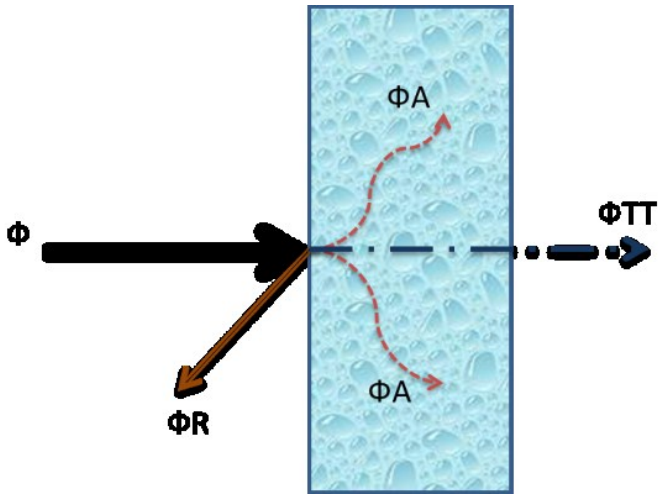

Figure 4-1: Incident radiation on a body

There may also be some coefficient of the body, as in:

Equation 4-1

$$A = \frac{\Phi_A}{\Phi}, R = \frac{\Phi_R}{\Phi} \; and \; TT = \frac{\Phi_{TT}}{\Phi}$$

where A is the absorbance coefficient, R is the reflectance coefficient, and TT is the transmission coefficient. The quantity of radiation emitted by the surface of a body depends on several factors, including the material of the body, the condition of its surface, and its temperature. Different substances with different characteristics emit different amounts of radiation, even when they are at the same temperature. Knowing this, the introduction of an ideal body which can emit the maximum amount of radiation becomes very useful. This ideal body, called a 'blackbody', also absorbs all incident radiation, such that for a blackbody A=1, R=0 and TT=0.

It is worth mentioning that no body can emit more energy than a blackbody. The emissivity (ε) of a surface is 'the ratio of the radiation emitted by the surface at a given temperature to the radiation emitted by a blackbody at the same temperature'. Thus, the emissivity of a surface goes from 0-1.

4.1.3 Components of an IR Camera

The most important parts of an infrared (IR) camera are:

- **Optical System**. The optical system will capture some wavelengths of the object to be visualized. In this case, special filters must be used to see infrared wavelengths. Furthermore, the set of filters used in the IR camera depends on the range of wavelength that the camera must detect. For example, if the IR camera is sensible to a band that goes from 8 to 14 μm, it can require Silicon, Germanium or Zinc. However, if the band is 3 to 5 μm, the material may be Sapphire or KRS5. Mirrors, coatings and protective films for coatings are also used in optical systems. Some coatings for mirrors can be MgF_2, SiO or SiO_2, but if the coating is made of Al or Ag, it will need a protective film. Finally, for special applications such as those required for industry or specific purposes, the use of an IR window that is placed between the thermal imager and the IR camera would be very useful to protect the camera or to give lightness to the target object.
- **Detector.** The detector converts radiation into electrical signals. There are two types of detectors: thermal detectors and photon detectors. Thermal detectors sense radiation using micro-electrical systems that consist of several micro-sensors that together form the thermal image. Photon detectors change their energy state when interacting with photons. The energy of the photon is given by hc/λ , where h is Planck's constant, c is the velocity of light, and λ is the wavelength of the photon. The cut-off wavelength is then given by $\lambda_0 = {}^{hc}/_{E_g}$, where Eg is the energy gap corresponding to the quantum level change. The signal response depends on the number of photons that touch the detector. Generally, these kinds of detectors need to be cooled and have a combination of chemicals, for example: Cadmium mercury telluride, Indium antimonite, or Platinum silicide.
- **Scanning mechanism**. As its name implies, a scanning mechanism scans the thermal image and moves it towards the detector. Some cameras do not require this mechanism because their detector is big enough to cover the file view of the imager. The scanning system can be one-dimensional (1D), two-dimensional (2D), or even in a polygonal mirror arrangement, depending on the number of mirrors the system contains. However, if the system is 1D, there are three kinds of possible arrangements: object space scanner, image space scanner and afocal scanner. Figure 1 a) presents the object space scanner. In this type of mechanism, the scanner goes first in order to catch only the aimed-for object. Figure 1 b) shows the image space scanner where the position of

the lens can cause quality problems because lenses tend to modify the thermal image. On the other hand, an afocal telescope (Figure 1 c)) has the advantages of a space scanner arrangement and can also vary the spatial resolution by modifying the afocal front end. Lastly, to increase the resolution of the imager, the scanner can make half pixel movements to the right, left, up and down and capture objects that can be smaller than a pixel.

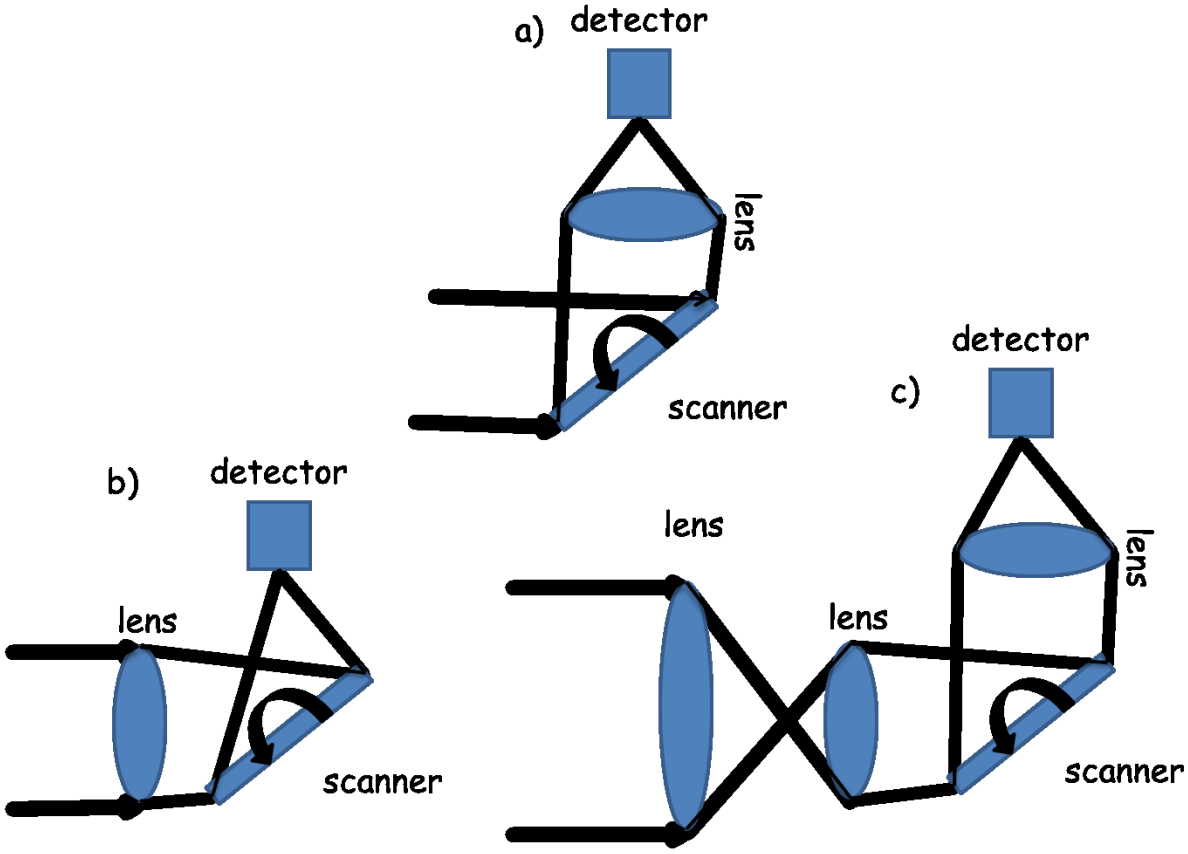

Figure 4-2: 1D scanning systems

- **Electronic processor**. After the detection of the energy or photons, it is important to correctly interpret the signals and take a reference temperature in order to proportionally calculate the rest of the temperatures.
- **Display unit.** Some cameras have the display unit integrated into the rest of the camera, while some have a computer with special software that is able to display and generate some other features, such as graphs and parameters.

Figure 4-3 illustrates the process.

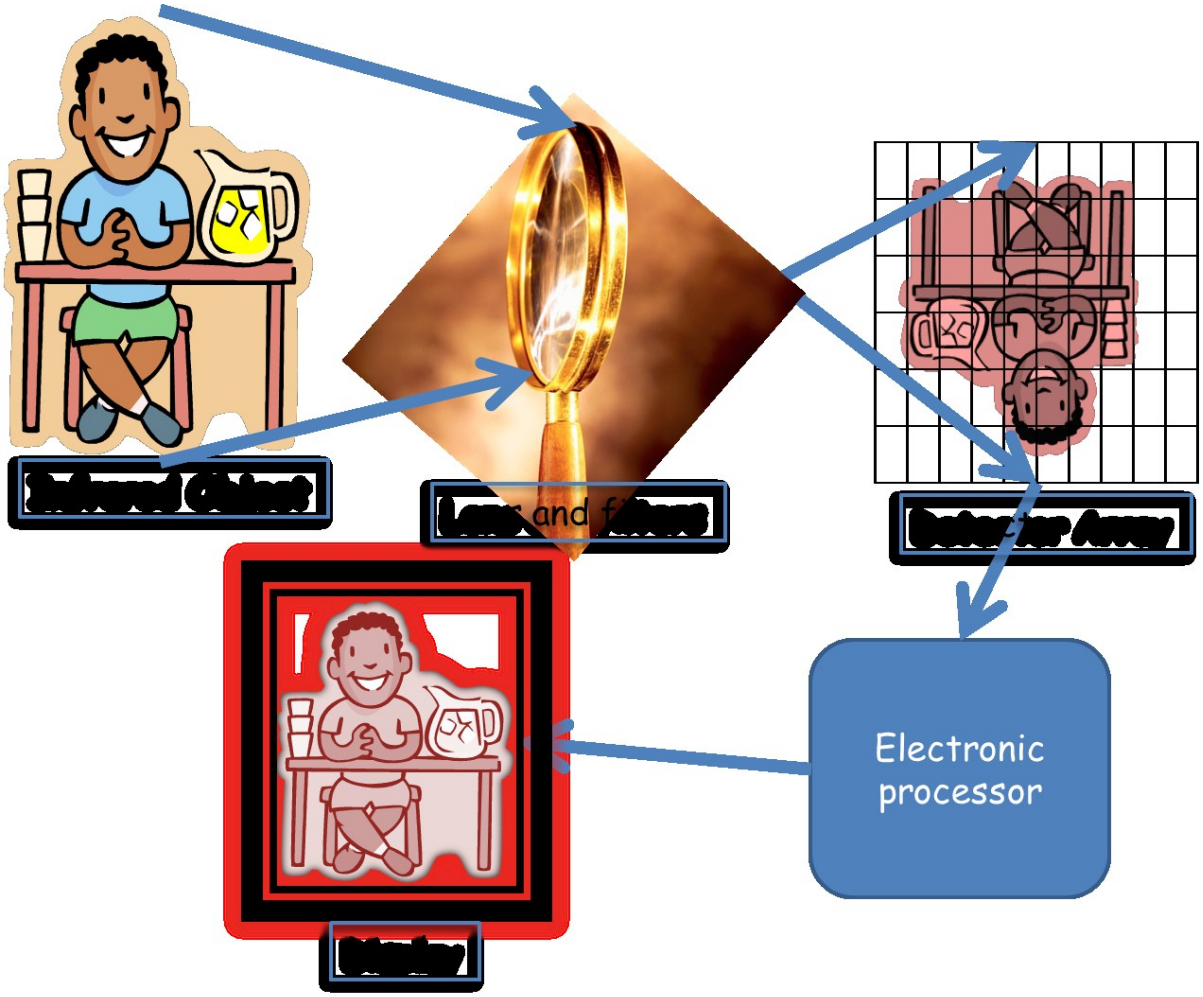

Figure 4-3: Process of display unit on a camera

4.1.4 Measurements

The first thing that needs to be known about a body to be measured is its emissivity, and this number can be obtained through experimentation. While there are several possible ways to perform these experiments, two options are chosen here. The first is to compare the object with another whose emissivity is already known by putting both objects at the same temperature and adjusting the emissivity until the IR camera detects the real temperature of the unknown emissivity object. The second way is to use a contact thermometer and move the parameters of the IR camera (e.g., ambient temperature, humidity, distance from the object to the camera and emissivity) until the same reading appears on the thermometer and on the IR camera.

Once the emissivity of the object is known, it is important to find out the noise equivalent temperature difference, the field of view, and the instantaneous field of view of the camera that will be used to take temperature measurements. These indicators need to be known in order to set up the camera and the hot object in such a way that the camera can take the best measurements. All these concepts mentioned above will be explained in the following paragraphs.

Noise Equivalent Temperature Difference (NETD). Mikina's (2009) definition of NETD is "the difference between the temperature of an observed object and the ambient temperature that generates a signal level equal to the noise level." It is given by:

Equation 4-2

$$NETD = \frac{U_n}{\frac{\Delta U_n}{T_{ob} - T_o}}, [K]$$

where U_n is the smallest noise voltage, ΔU_n is the increment of the detector signal, T_{ob} is the object temperature and T_o is the ambient temperature. There is not only one formula to find this parameter, but this one gives a better understanding of what NETD means.

- **Field of view (FOV)** is the area that can be detected by an IR camera. Manufacturing companies specify this in grades. To find the resolution at different distances, we use the following formulas: H=d.sinH˚ and V=d.sinV˚, where H is the horizontal resolution of the area, V is the vertical resolution of the area, d is the distance between the IR camera and the object, H˚ is the horizontal angle given by the manufacturer, and V˚ is the vertical angle given by the camera's manufacturer. For example, the FLIR Thermacam SC500 has a FOV of 25˚ x 19˚. With this information, we can say that, to capture an object with a length of 2m and a height of 1.5 m, the minimum distance d must be:

Equation 4-3

$$d_H = \frac{H}{\sin H°} = \frac{2m}{\sin 25°} = 4.7\ m\ and\ d_V = \frac{V}{\sin V°} = \frac{1.5m}{\sin 19°} = 4.6\ m$$

This means that the minimum distance d for the IR camera to sense the entire object is 4.7m.

- **Instantaneous Field of View (IFOV)** is the resolution of a pixel. In the specification of an IR Camera, it is given in milli-radians and is based on the following formulas:

Equation 4-4

$$\alpha_{radH} = \frac{H°\pi}{180N_H}, H_{min} = d.\sin\alpha_{radH} \ , \ \alpha_{radV} = \frac{V°\pi}{180N_V} \ and \ V_{min} = d.\sin\alpha_{radV}$$

where α is the angle of flare in radians, N is the number of detectors in a horizontal or vertical arrangement, H_{min} is the minimum detected length in the horizontal plane, and V_{min} is the minimum detected length in the vertical plane. In the example of the Thermacam SC500, the special resolution is 2.7 mrad. Using the above formula, we can say that N_H is almost 162 and N_V is almost 123, while the IFOV for a d equal to 4.7m would be 0.0127 m or 1.27 cm. Although is appears that, if an object has a size of 1.27 cm2, it will be detected by the camera, the truth is that the object must be a square and has to be allied with one of the camera's detectors for that to happen.

4.2 Experiment Setup

The process of the experiment is very simple. There are three steps, as follows:

1. Preheat the mould at 350 degrees Celsius using a blowtorch.

2. Weld two rectangular layers using 20 beads, 10 in the first layer and 10 in the upper layer. This block is 406 mm in length, 204 mm wide, and has a height of 100 mm. The block after welding is presented in Figure 4-4.

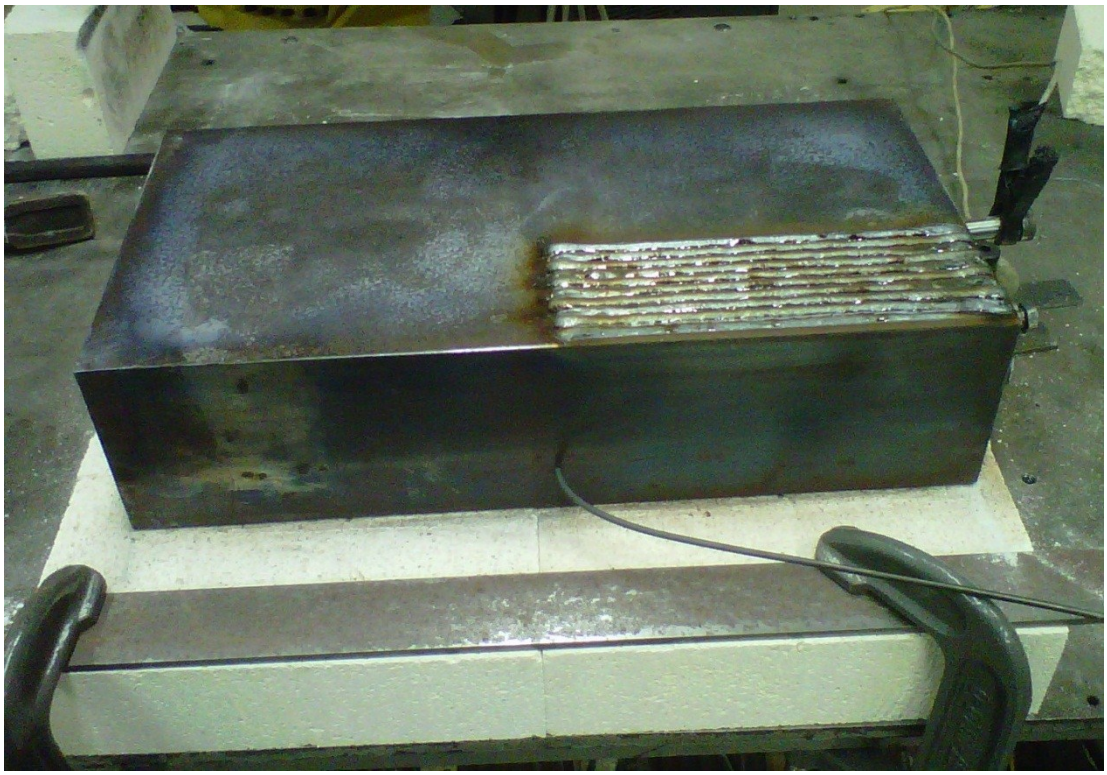

Figure 4-4: Steel block with two layers of welding

3. Take temperature measurements with an IR camera. Figure 4-5 presents the IR camera used in the experiment.

Figure 4-5: FLIR Thermacam SC500

4.2.1 AB Welding Robot

The robot used in the experiment is Fanuc Arc Mate 120. It is a six-axis robot with a mass of 370 kg, and was specially made for MIG and TIG applications. The parameters used during the experiment are shown in Table XI. The shielding gas is MIG Mix Gold, which is a mixture of more than 90% Argon with less than 10% Carbon Dioxide; this mixture is expressly done for MIG welding and stain-steel by the Praxair Company.

Table XI: Parameters used in experiment

Wire Feed Speed	148.16 mm/s
Volts	29
Travel Speed	19.05 mm/s

Table XII presents the important differences between ideal and the experimental process. As we can see in the first column, the width of the bead is larger using MIG and results in fewer layers compared to the TIG process. The experiment consists of two layers of 10 lines (beads) per layer. From information given

in the table below, we know that if we run the experiment without pause, the welding time would be 1,469 seconds faster than the ideal experiment.

Table XII: Differences between ideal and experimental processes

	TIG Robot (ideal)	MIG Robot (experimental)
Bead width	5mm	6.5mm
Bead height	3mm	3mm
Bead length	195 mm	195 mm
Number of lines for one layer	13	10
Seconds per line	65.17	10.26
Travel speed	5mm/s	19 mm/s
One-layer time	836.03 s	101.2 s
Two-layer time	1672.06 s	202.4 s

Using the method presented in section 2.3 of this thesis, the results suggest that we either have to provide a heat flux of 0.03 kW during the entire process or eliminate eight seconds from it. The second option – eliminating eight seconds – would not make any sense in a normal situation. Nonetheless, here it is the better alternative, since the experimental process is using a faster robot than the ideal one. So, instead of running the process for 1,469 seconds, it would be run for only 1,461 seconds, with a pause of 73.04 seconds between each line to maintain preheat temperature.

Applying the fuzzy logic method to the process, the fuzzy number is 0.19 for the linear functions and 2.81e-15 for the bell functions. Both numbers are very close to zero, especially the bell fuzzy number. Also, both values are positive, which means that little additional heat is needed. These suggestions agree with the FEA model. Furthermore, upon de-fuzzifying the results, the linear functions model gives a heat flux of 0.33 kW that the mould needs during the welding process and the bell model gives a heat flux 0.00 kW. However, these results do not provide a time decrease, as the FEA number does. For this reason, the FEA suggestion was used during the experimental testing.

4.2.2 Infrared Camera

The ambient temperature and general conditions of the laboratory in which the experiment was done were very similar to the conditions where the robot was. The lab was an inner room, heated to 22 degrees C, with no strong air currents or other extreme conditions.

The target object is a block of steel 406mm in length, 204mm wide, and 100mm high, with a volume of 8.28x106mm^3. This block is placed on fire-proof bricks on a steel table.

The field of view (FOV)[xxvi] is the area that can be detected by an IR camera. The FLIR Thermacam SC500 has a FOV of 25˚ x 19˚. Using Equation 4-3, it is possible to find the minimum distance from the IR camera to the hot object for the camera to detect the whole object.

Where H is the horizontal resolution of the area, V is the vertical resolution of the area, d is the distance between the IR camera and the object, H˚ is the horizontal angle given by the manufacturer, and V˚ is the vertical angle given by the manufacturer. With this information we can say that to capture an object with a length of 0.406m and a height of 0.1 m, the minimum distance d must be:

$$d_H = \frac{H}{\sin H^\circ} = \frac{0.406\text{m}}{\sin 25^\circ} = 0.96 \text{ m and } d_V = \frac{V}{\sin V^\circ} = \frac{0.1\text{m}}{\sin 19^\circ} = 0.307 \text{ m}$$

This means that the minimum distance d for the IR camera to sense the entire object is 0.96m. The camera is then placed at about 1.2 m from the target object in order to have a better vision of the process. Figure 4-6 demonstrates the position of the camera relative to the steel block.

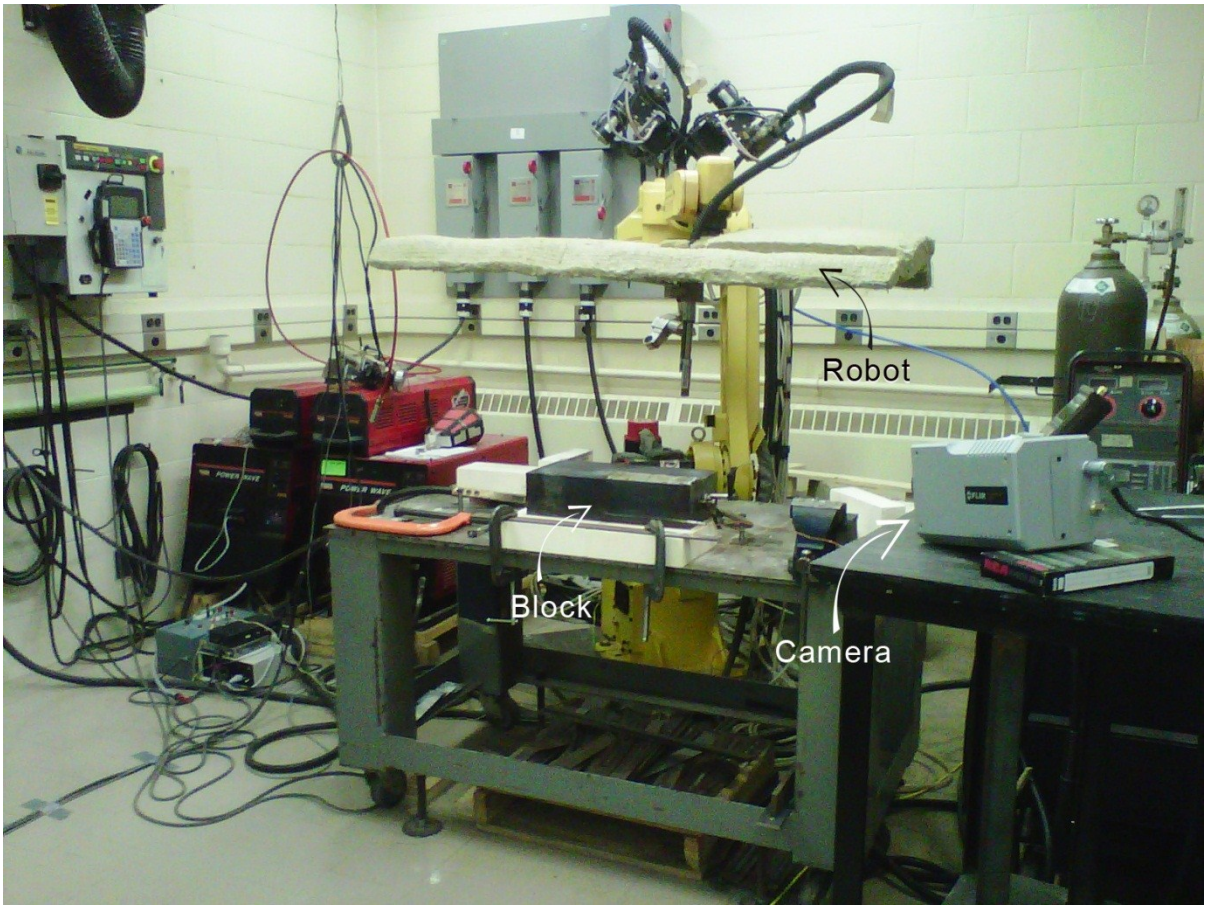

Figure 4-6: Robot, camera and block ready for experiment

The IR camera starts taking images when the block is heated to a temperature of 350 degrees C and continues to take images until the welding process finishes and the block cools down. The interval of time between each frame is approximately 9.99±0.055s, at a rate of five or six captures per minute. The start time was 11 hours, 53 minutes, 1 second and 54 milliseconds, and the last frame was recorded at 14 hours, 35 minutes, 0 seconds and 999 milliseconds. However, there were five pauses during the experiment. As a result, there are 521 pictures to be analyzed.

Each picture can be saved in Mat lab format. The FLIR program creates a structure for each recorded frame that has five matrices. The first matrix takes the name of the Mat lab file and contains the absolute temperature value of each pixel of the image in 8-byte double precision float numbers; the size of the matrix is 240x320. The other four matrices give data about the stored images. The camera's user

manual[xxvii] provides an example with the image XXXX (see Appendix C) as well as an example from the first image of the actual experiment.

In this way, all the necessary information stored in each picture is easily obtainable. With the information given by the user as well as the scaling that the user sets, the program can calculate the temperature for each pixel. Therefore, the more accurate the initial values are, the more accurate the measured temperature will be.

By choosing one of the frames randomly and normalizing it into a gray scale image, it is possible to draw the perimeter of the target object manually and transform the original image into one black and white object. The Mat lab code used to transform the image is:

```
clear
I = imread('A1.jpg');
J = rgb2gray(I);
figure(1), imshow(J);
BW = im2bw(J,0.8);
figure(4), imshow(BW)
bw1 = imfill(BW,'holes');
figure(5), imshow(bw1)
s1=sum(bw1)
s2=sum(s1)
```

in which the ‘A1.jpg’ file is the image that has been manually recognized in Paint. The figure below shows visually the conversion of the image.

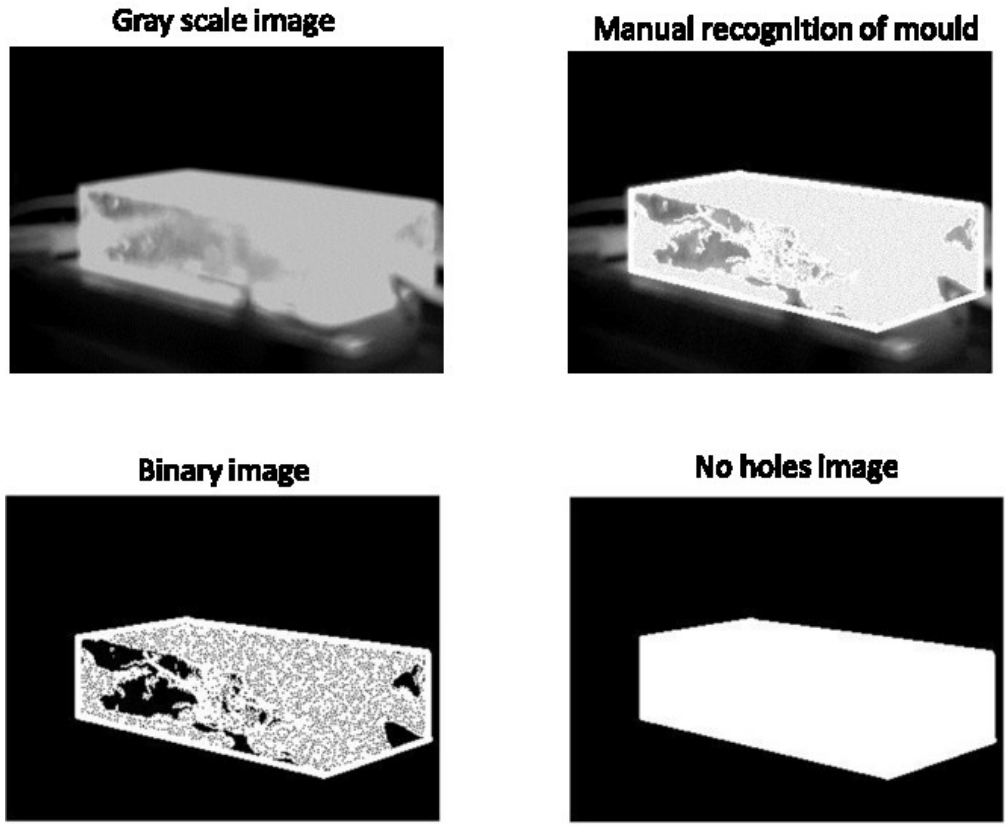

Figure 4-7: Manual recognition of the mould

In this case, s2 is equal to the white pixel. Its value is 23,520 pixels, which is 30.625% of the entire image.

4.3 Experimental Results and Discussion

4.3.1 Automatic Recognition Program to Get Results

The main purpose of the recognition program is to select the useful images from the 521 pictures taken during the experiment and give the average temperature of the mould in the image. To do this, the following the steps were taken:

1. Organize the data. Convert the 521 Mat lab files with five matrices into five files with 521 matrices, one matrix per image.
2. Convert the temperature values into gray scale values to work with the picture.

3. Select the useful images. During the experiments, some problems occurred (e.g., people blocked the camera view). It is also important to remember that this program selects only the pictures where the target object is hot enough to be welded.
4. Automatic recognition of the mould.
5. Get the average temperature of the mould.
6. Show the main temperature of the mould at the time the picture was recorded.

4.3.1.1 Organize the data.

The idea in this step was to organize the data by type – the absolute temperature values for each image in one structure, the date and time information in another structure, and so on. After that, the temperature and time structures were converted into multi-dimensional arrays. Thus, the dimension of the temperature array was 240x320x521, and the dimension for the date and time array was 1x7x521. However, as the date and time array was not suitable (as only the time when the picture was recorded was needed), the hour was converted to minutes and the seconds into hours. The total of the results created a more suitable array of 1x521, which worked as the x axis value for the final plot.

4.3.1.2 Converting temperature values into gray scale values

The absolute temperature values of the matrices needed to be converted into values that could be read by Mat lab as image values; for this reason, values from 0 to 1 were given to each temperature, with the lowest number being equal to 0 and the highest equal to 1. However, the absolute data gave too much information of the background, as can be seen in the resultant image in Figure 4-8 a). However, it was possible to increase the contrast by changing the absolute values to Celsius values before normalizing it to gray scale, as shown in Figure 4-8 b). Nevertheless, the concentration of one value of the pixels was higher in 4-8 c), where a further 100 degrees were removed from the Celsius values. Thus, to obtain the gray level value for each pixel in the figure below, section a), the formula is:

Equation 4-5

$$g(i,j) = \frac{f(i,j) \times 0.5}{\frac{\max\{F(m \times n) - \min\{F(m \times n)\}}{2}}$$

where g is the gray level value of the pixel, f is the absolute temperature value of the pixel, and F is the matrix of the image.

In the same way, the formula to obtain the gray level value for the next figure, b) is:

Equation 4-6

$$g(i,j) = \frac{(f(i,j) - 194.15) \times 0.5}{\frac{[\max\{F_n(m \times n)\} - 194.15] - [\min\{F_n(m \times n)\} - 194.15]}{2}}$$

The difference in this formula is that the absolute temperature value is now 194.15 less, giving Celsius degrees. Also, the n in F has been used to note that

Finally, the last image in Figure 2 has the following formula:

Equation 4-7

$$g(i,j) = \frac{(f(i,j) - 294.15) \times 0.5}{\frac{[\max\{F_n(m \times n)\} - 294.15] - [\min\{F_n(m \times n)\} - 294.15]}{2}} = \frac{(f(i,j) - 294.15) \times 0.5}{M}$$

In this case, 294.15 instead of 194.15 was taken to obtain more contras in the final image. Note that the numerator is represented by the letter M.

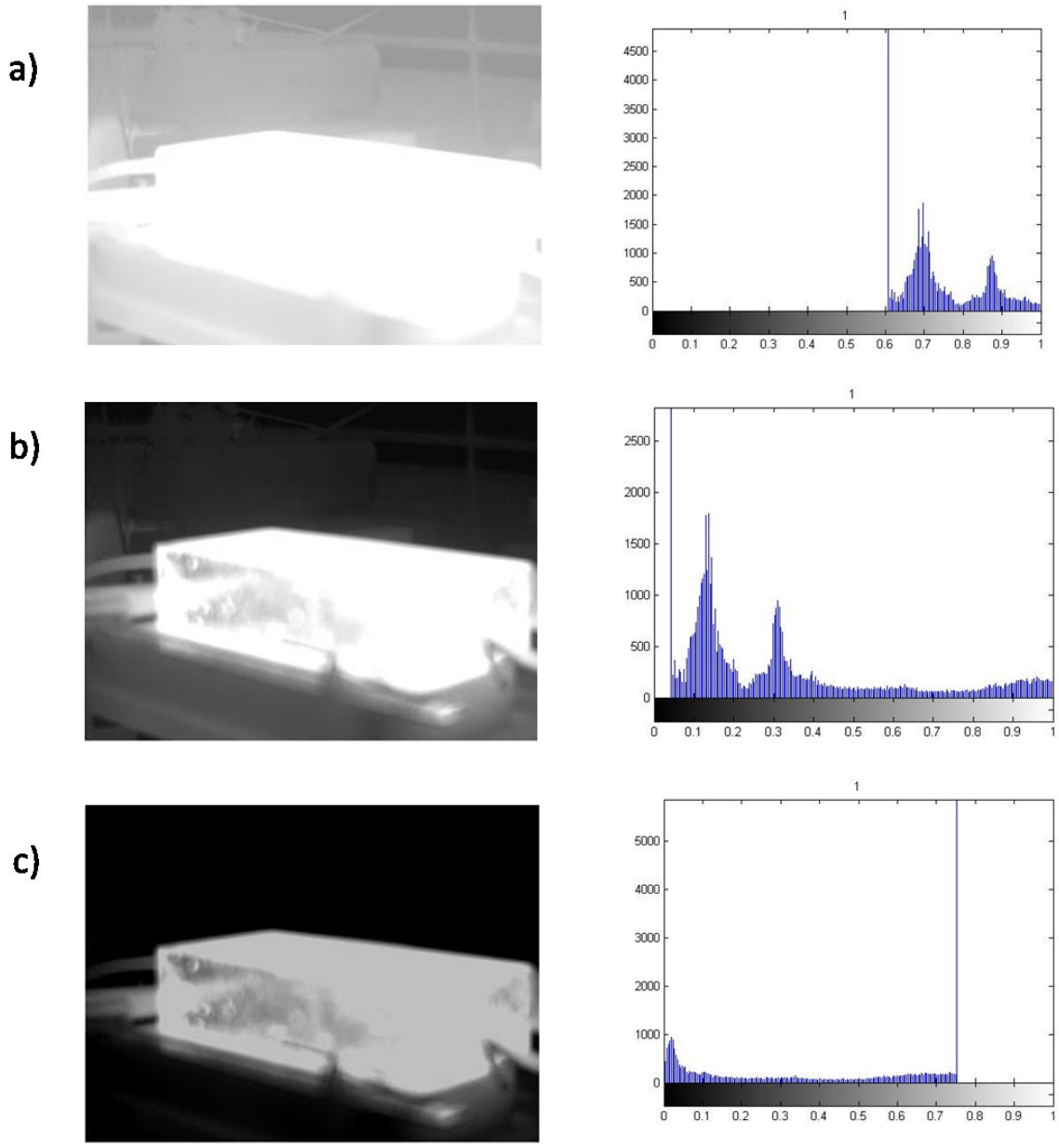

Figure 4-8: Adjusting contrast of images: a) equation 33, b) equation 34, c) equation 35

4.3.1.3 Selecting the useful images

Not all photos were as good as the one above. As mentioned previously, some did not contain the hot mould, and the camera took pictures while the block was heating up with a torch. Some examples of the frames created in the experiment can be seen in Figure 4-9. In picture a) of the next figure, the block is

almost at ambient temperature; in pictures b), c), d) and f), the block does not have a uniform temperature; in e), the block is not there; in picture g), the heat of a person prevented the block from being seen completely. Finally, picture h) is the only correct frame. Looking at the histogram, we can see that the main concentration of one gray level value is in the h) picture, with more than 5,000 pixels. This highest value corresponds to the highest temperature in the picture (which is, at the same time, the block).

From the information above, the selection process consisted of finding the average gray level value for the useful frames and taking only the value that corresponded to the images needed to be analyzed. Thus:

Equation 4-8

$$\tilde{x} = \frac{1}{m \times n} \sum_{(i,j)=(1,1)}^{(m,n)} g(i,j)$$

$$if\ 0.18 \leq \tilde{x} \leq 0.27\ then\ continue\ process$$

where $\tilde{x}$ is the average value of the gray level image and the useful images have a value between 0.18 and 0.27.

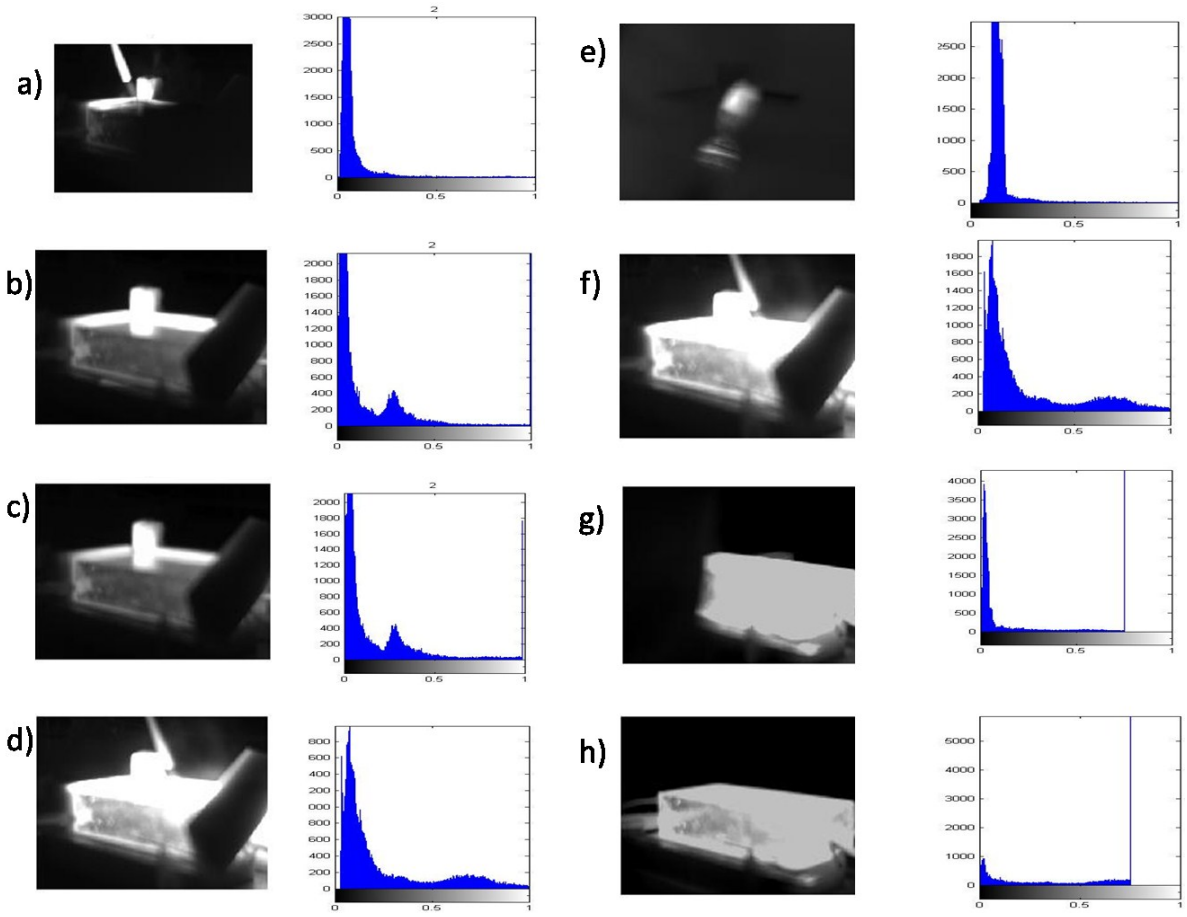

Figure 4-9: Histograms of gray scale pictures

4.3.1.4 Recognition of mould

Taking the matrix with the absolute temperature minus 294.15 and knowing that the brightest pixels correspond to the pixels of the block (as in Figure 4-9, h)), it is possible to convert the gray scale image into a binary image, giving the value of one to all pixels larger than M (the value of M is given in Equation 4-7) and zero to all pixels smaller than M.. Now, the matrix is a binary image where the block is white. The binary image in Figure 4 is an example of the result of this step. After that, to suppress small islands from the binary image, the opening of the following morphological operation was performed:

Equation 4-9

$$A \circ B = (A \ominus B) \oplus B,$$

where A is the set of the binary image, B is the structuring element that, in this case, is equal to 19,000 to ensure that the only object in the image is the block, and ⊖ and ⊕ denote erosion and dilation, respectively.

Finally, a hole was filled in the area's open image. This was done according to the image processing toolbox manual[xxviii]: "A hole is a set of background pixels that cannot be reached by filling in the background from the edge of the image." The resultant image is the "no holes" picture in the figure below.

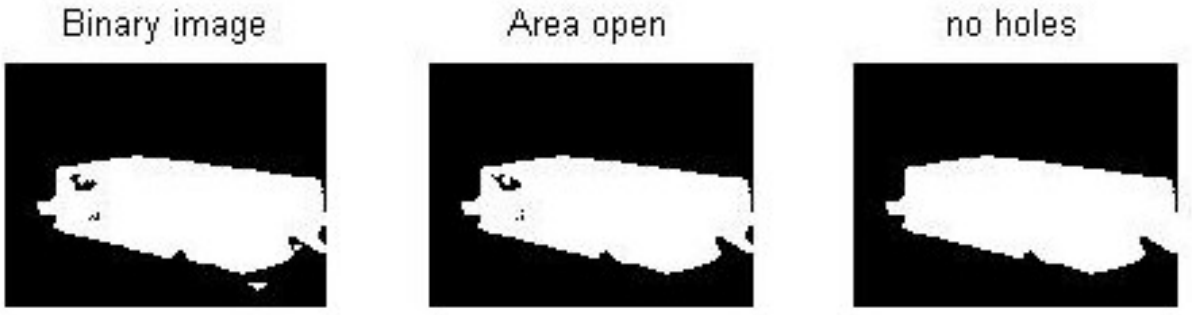

Figure 4-10: Binary image of frame 500

4.3.1.5 Average temperature of mould

The tot product of the original matrix and the "no holes" matrix left only the values of the original image that corresponded to the absolute temperature of the block. From these, an average of those values was obtained.

4.3.1.6 Plot Temperature versus Time

To achieve the objective of this program, a graph was made that shows the behavior of the mould while it was being welded and some minutes after the process was finished (without the noisy elements).

4.3.1.7 Resultant graph

The resultant graph of the program is presented in Figure 5. As can be seen, the x axis shows the hour of the day in which the frame was taken and the y axis has two meaning values. The red line indicates the average temperature of the block in degrees Celsius, and the blue line indicates the average gray level of the entire picture multiplied by 100.

The selection part of the program successfully worked, with 0% error in the experiment. However, the condition section of Equation 4-8 should be adjusted, depending on the area that the mould covers in the image.

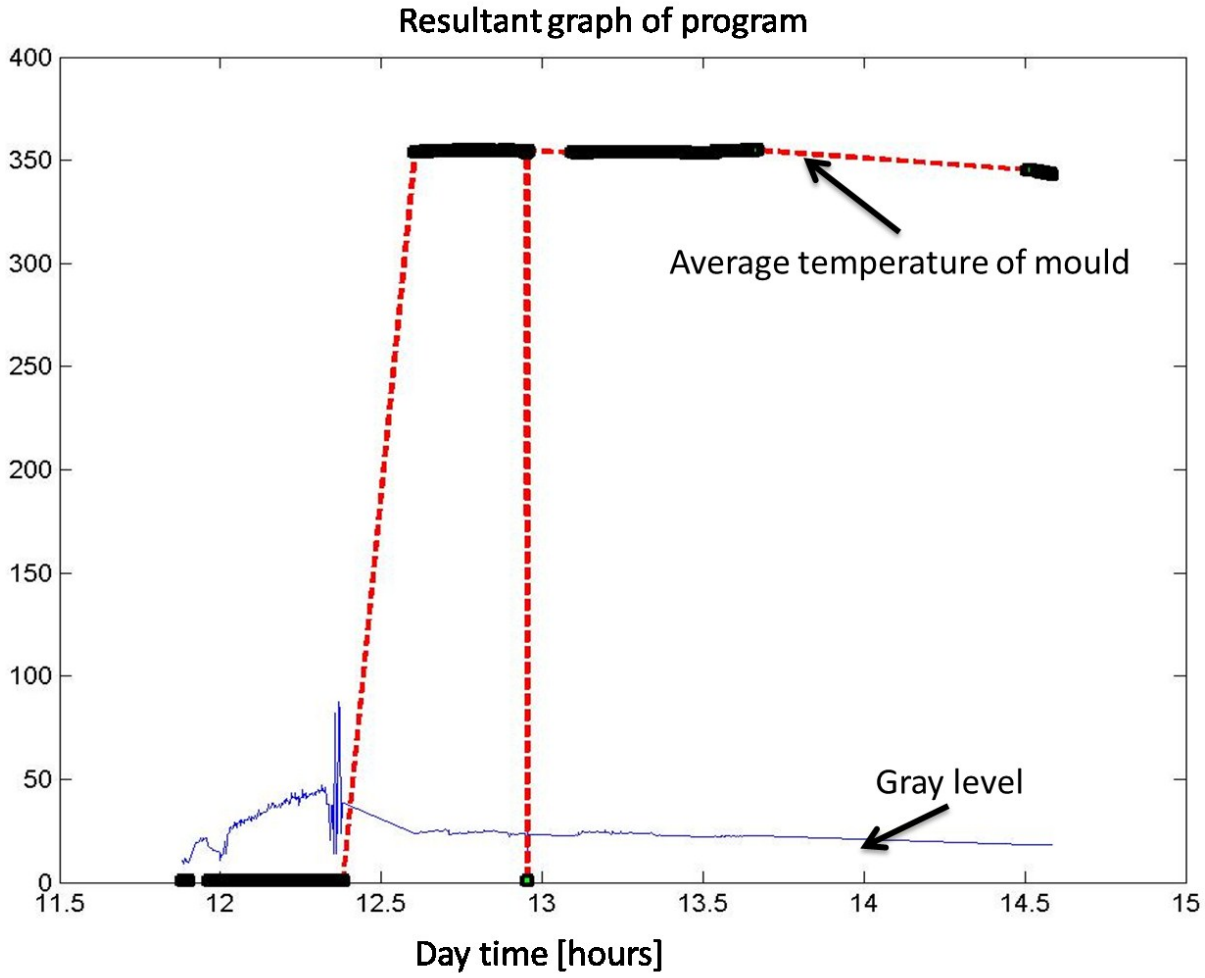

Figure 4-11: Temperature and gray level average

With reference to the accuracy of the object selected, a comparison was done with the manual segmentation. The standard deviation for the area of each image was calculated, the average value indicating that the average deviation was 2,320.14 pixels. This means that the average error of the calculated area was 9.86% or the accuracy was 90.13%. Thus, it can be assumed that when the block is at the highest temperature, the object area of the image is larger because the items among the block are as hot as the target piece.

4.3.2 Analysis and Discussion of Results

Figure 4-12 contains a chart with the values taken from the results of the Mat Lab program in blue; the red line is the highest temperature that the steel block can have to avoid thermal expansion larger than 0.5mm. The green mark is the lowest temperature it can have to avoid a contraction larger than 0.5mm. Further, as all of the blue points are within the delimited range, we can say that the mould did not experience a significant change in shape.

The maximum and minimum temperature limits appear to be wide-ranging. In fact, the difference between them is 193.15 degrees C, as the high limit is 446.58 degrees C and the low limit is 253.42 degrees C. However, if we look at Figure 2-2: Thermal expansion for different initial lengths), section 2.1.1.1, we will see that, if the mould has a length of about 400 mm, it can have a difference in temperature of 200 degrees C before it changes more than one millimetre. As the length of the experimental mould was 406 mm, the temperature limits to prevent size changes should not be surprising.

At this juncture in the discussion, one might suggest that if the limits are so large, there is little point in making an effort to keep the mould at a single temperature. However, for small moulds, this method can be used to prevent cracks in the heat-affected zone as well as over the heat of the mould, because the mould has to be cooled down at the end of the welding process.

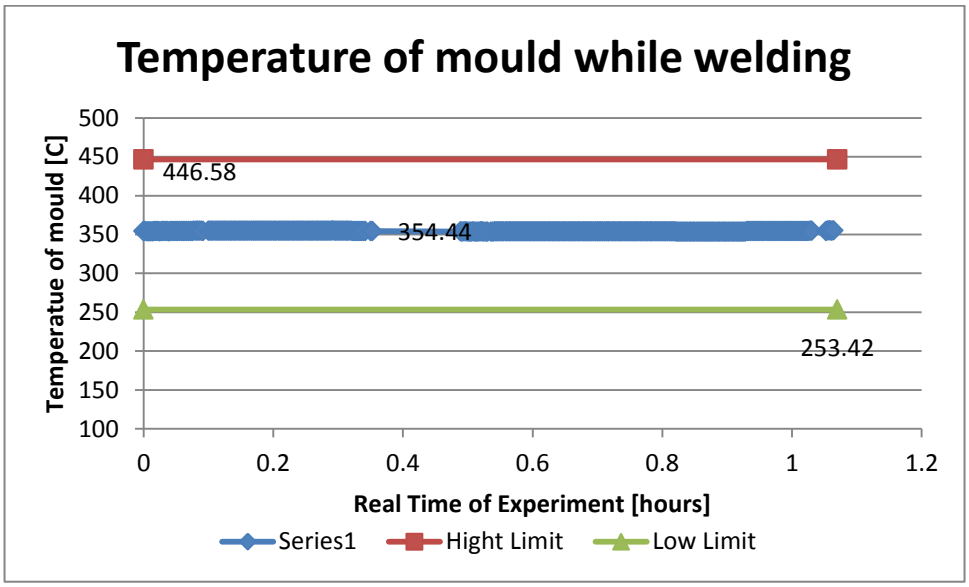

Figure 4-12: Temperature limits to avoid excessive thermal expansion

Figure 4-13 shows a closer view of the mould temperature. The point marked with a red circle does not follow the temperature trend. That picture was taken 0.344 hours after the experiment started, and Figure 4-14 shows that picture together with another three pictures, for comparison purposes. The second picture (from left to right) is the picture at issue; we can see that someone is obstructing the file view of the camera and so we cannot see the entire hot block of steel during the experiment. That picture is thus eliminated from the data base manually. The picture taken 0.35 hours after the experiment started was already eliminated with the Mat lab program, as explained in section 4.3.1. Finally, the other two images are good photographs and can be included in the data base.

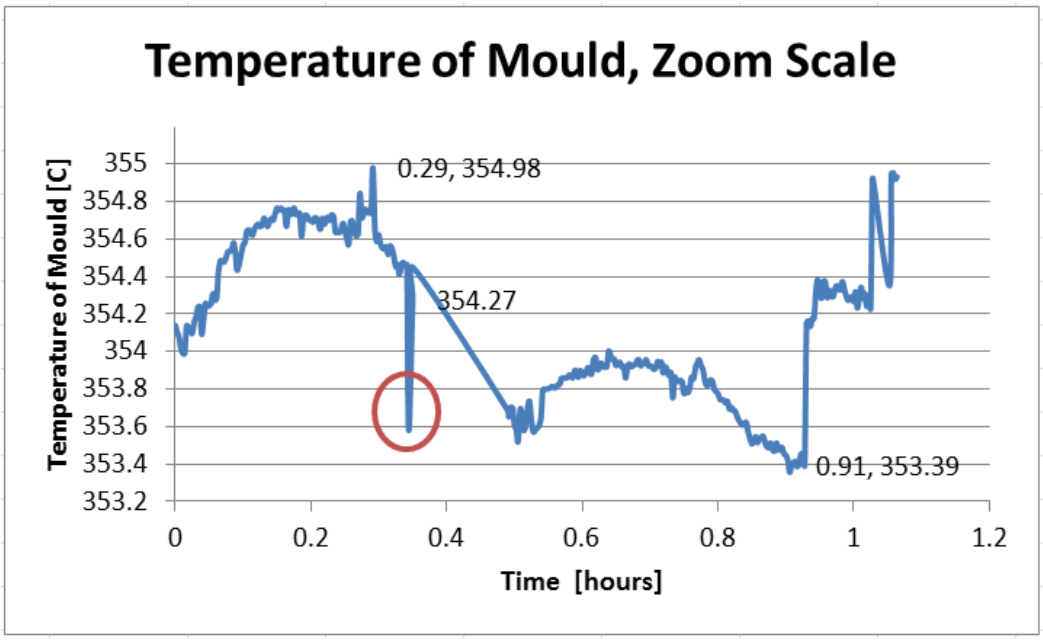

Figure 4-13: Temperature of mould, closer view

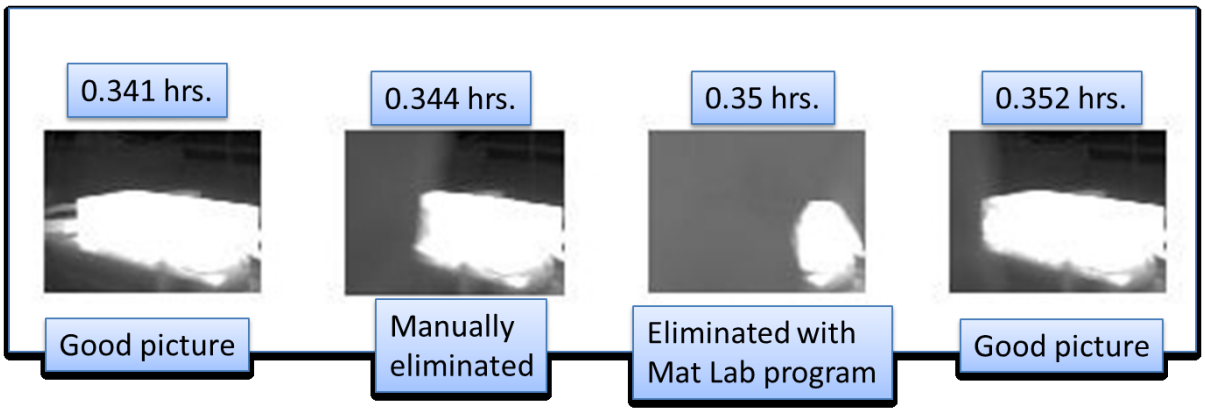

Figure 4-14: Pictures taken with infrared camera at 0.341, 0.344, 0.35 and 0.352 hours

After the manual elimination of the useless frame, Figure 4-15presents the temperature of the block during the welding process. We can see from Figure 4-13 that the process took less than an hour and a half, which is why the decision was made to change the time scale into minutes. Three lines were also added; the red and green lines indicate that the electrode had to be changed during the experiment, and that this change created a pause of approximately twelve minutes. The red line marks the beginning of the pause and the green line represents the end of the pause or the point at which the robot continued welding. The purple line corresponds to the endpoint of the welding process and the start of the cooling down process. From this, we know that the duration of the process was approximately 44 minutes, with the peak temperature occurring at 17.48 minutes and measuring 354.89 degrees C, and the lowest temperature occurring at 30.32 minutes and measuring 353.52 degrees C.

Section 4.2.1 of this thesis suggests waiting approximately 73 seconds before starting to weld a new line, in order to maintain the preheat temperature. However, the electrode of the welding robot had to be changed during the experiment. This occurred from minute 17 to 29 of the experiment, resulting in a waiting time of about 12 minutes, during which the temperature decreased from 354.74 to 353.65 degrees C. If we view the entire process, we will find that the torch has to add approximately 1,597.7 kJ in 1,663 seconds, which means a continuous average rate of 960.6 Jules per second. When 12 minutes (720 seconds) are added to the process, the heat rate reduces to 670.45 J/s. Hence, the average temperature of the mould would be less that the initial temperature until the required heat would be compensated. For this reason, the waiting time at the end of the experiment was eliminated even though the temperature of the mould did not substantially increase.

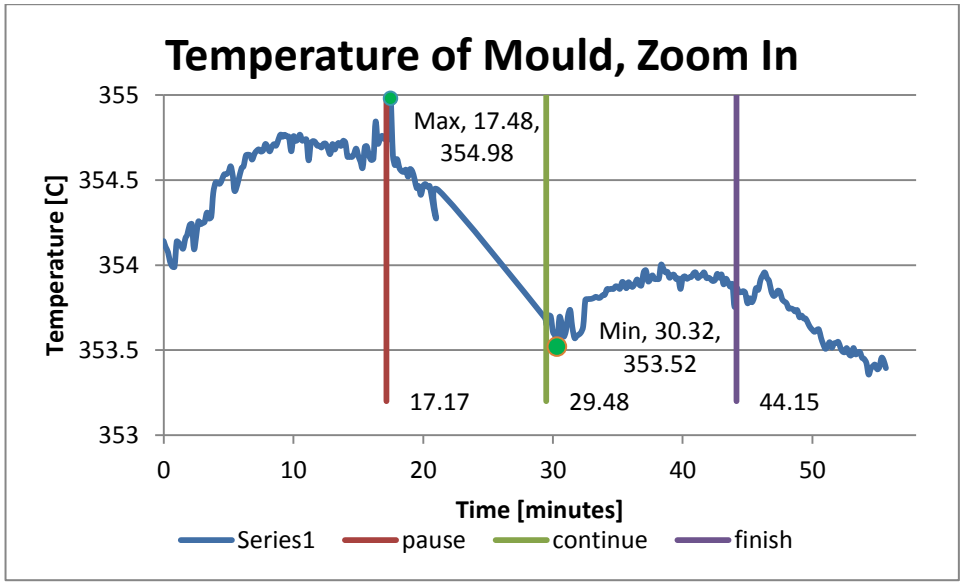

Figure 4-15: Temperature of mould, zoom in

After the completion of the welding process (see Figure 4-16), the temperature of the mould decreased, but twelve minutes later the temperature rose again. After that, there was a gap of 50 minutes (from minute 64 to minute 114) and the process moved faster than at the beginning. To fill the gap, a trend line was added to determine what could have happened during that time. The trend line suggests that the temperature could not go higher than 356 degrees C before going down.

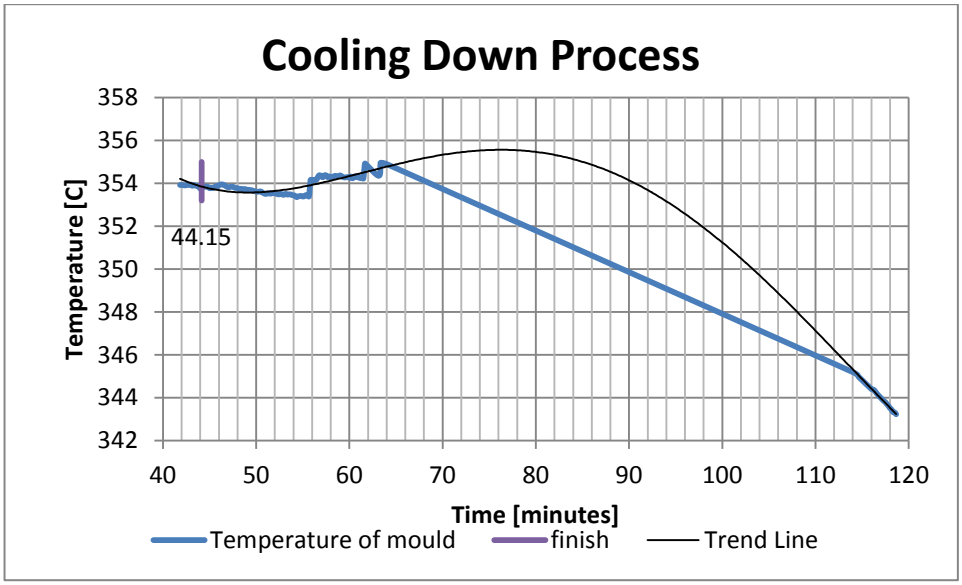

Figure 4-16: Cooling-down process

The question remains: why does temperature rise if heat is added? The answer is: thermal conductivity. The average temperature of the mould at the end of the welding process was 353.86 degrees C. However, the temperature of the recent welding was higher than that. Some of the heat was quickly dissipated via convection, while some was absorbed by the rest of the mould via conductivity. Moreover, convection was faster at the beginning, as the temperature of the welded portion of the block was very high. Nonetheless, there was a point at which conductivity was faster and the average temperature of a block rose, but once all parts of the block achieved the same temperature, a faster cooling-down process was begun.

Chapter 5
Conclusion and Future Work

In this final chapter of the thesis, some conclusions are drawn and recommendations made regarding current and future investigations into automatic systems used for building up multiple layers with TIG welding technology.

5.1 Conclusions

The general hypothesis in this research study was that it is possible to maintain the temperature of a mould if the volume of the work piece is known. As most types of steel have similar thermal properties, the project was based on experiments made with P-20 steel; however, the validation testing used stainless steel instead of P-20 steel and it still maintained the preheat temperature inside the required limits simply by knowing the volume of the mould.

Due to the fact that it is not necessary to conserve one precise temperature but is instead more useful to maintain the mould within a certain temperature range, automation of the process without the use of expensive sensors is possible.

Furthermore, as small moulds have a large range of temperature limits and will tend to gain temperature, we can maintain the temperature of these moulds in order to achieve a stable process. On the other hand, large moulds will have a smaller range of temperature limits, and so it is necessary in cases involving large moulds to maintain their temperature by using burners. Medium-sized moulds generally require little addition of heat over time; however, if the volume added by welding is sufficiently large over a long duration, it may convert the medium-sized mould into a large one at a certain point in the process. For this reason, a dynamic calculation is necessary. In other words, if the welding process takes three hours, the calculations can be done in a simulation every 30 minutes to ensure that the changing conditions (such as time, volume and heat) are taken into account.

During the experimental testing, the torch was found to be a good power source, but a technical stop could cause heat loss. It is thus recommended that the user be prepared to turn on burners or cover the working piece with thermal cloths in case of unplanned pauses during the welding process.

Finally, the fuzzy logic models and the FEA model suggest similar solutions to the problem. The temperature of the mould was maintained at the preheat temperature, which means that the objective of this thesis was successfully achieved.

5.2 Future Work

Every fuzzy logic model has to be tuned, mainly because people who work with the automatic system discover more rules and better parameters as they gain more experience with it. After installation of the fuzzy method, it will be necessary to make slight changes and refinements until the best fuzzy logic model of the process is reached.

The major difference between the fuzzy and FEA methods is that the efficiency of the burners is assumed to be 60% with the burners fully opened. However, it is possible that the efficiency is less than that. To test this theory, further experiments using an MIG welding robot would be recommended as future work in order to adjust and validate the two methods presented in this thesis.

Appendices

Appendix A

Shielding gases tables

Table XIII: Shielding gases for MIG

Shielding gas	Chemical behavior	Typical application
Argon	Inert	Virtually all metals except steels.
Helium	Inert	Aluminum, magnesium, and copper alloys for greater heat input and to minimize porosity.
Ar + 20-80% He	Inert	Aluminum, magnesium, and copper alloys for greater heat input and to minimize porosity (better arc action than 100% helium).
Nitrogen		Greater heat input on copper (Europe).
Ar + 25-30% N_2		Greater heat input on copper (Europe); better arc action than 100 percent nitrogen.
Ar + 1-2% O_2	Slightly oxidizing	Stainless and alloy steels; some deoxidized copper alloys.
Ar + 3-5% O_2	Oxidizing	Carbon and some low alloy steels.
CO_2	Oxidizing	Carbon and some low alloy steels.
Ar + 20-50% CO_2	Oxidizing	Various steels, chiefly short circuiting mode.
Ar + 10% CO_2 + 5% O_2	Oxidizing	Various steels (Europe).
CO_2 + 20% O_2	Oxidizing	Various steels (Japan).
90% He + 7.5% Ar + 2.5% CO_2	Slightly oxidizing	Stainless steels for good corrosion resistance, short circuiting mode.
60% to 70% He + 25 to 35% Ar + 4 to 5% CO_2	Oxidizing	Low alloy steels for toughness, short circuiting mode.

Table XIV: Typical applications for common shielding gases for MIG welding

Shielding gas	Chemical behavior	Typical application
Argon	Inert	Virtually all metals except steels.
Helium	Inert	Aluminum, magnesium, and copper alloys for greater heat input and to minimize porosity.
Ar + 20-80% He	Inert	Aluminum, magnesium, and copper alloys for greater heat input and to minimize porosity (better arc action than 100% helium).
Nitrogen		Greater heat input on copper (Europe).
Ar + 25-30% N_2		Greater heat input on copper (Europe); better arc action than 100 percent nitrogen.
Ar + 1-2% O_2	Slightly oxidizing	Stainless and alloy steels; some deoxidized copper alloys.
Ar + 3-5% O_2	Oxidizing	Carbon and some low alloy steels.
CO_2	Oxidizing	Carbon and some low alloy steels.
Ar + 20-50% CO_2	Oxidizing	Various steels, chiefly short circuiting mode.
Ar + 10% CO_2 + 5% O_2	Oxidizing	Various steels (Europe).
CO_2 + 20% O_2	Oxidizing	Various steels (Japan).
90% He + 7.5% Ar + 2.5% CO_2	Slightly oxidizing	Stainless steels for good corrosion resistance, short circuiting mode.
60% to 70% He + 25 to 35% Ar + 4 to 5% CO_2	Oxidizing	Low alloy steels for toughness, short circuiting mode.

Appendix B

Coefficient of convection

Temperature [C]	k [W/m.C]	Prandtl Pr	v [m^2/s]	β= 1/Tf [1/K]	h ↑ hor[5]	h ↓hor[6]	h vert[7]
20	0.02514	0.7309	1.52E-05	0.003411	4.123739	2.06187	3.919128154
25	0.02551	0.7296	1.56E-05	0.003354	4.338539	2.169269	4.159124144
30	0.02588	0.7282	1.61E-05	0.003299	4.519349	2.259674	4.359772803
35	0.02625	0.7268	1.66E-05	0.003245	4.674515	2.337257	4.530274626
40	0.02662	0.7255	1.7E-05	0.003193	4.811611	2.405806	4.679387662
45	0.02699	0.7241	1.75E-05	0.003143	4.932927	2.466463	4.809436416
50	0.02735	0.7228	1.8E-05	0.003095	5.041207	2.520603	4.924228617
60	0.02808	0.7202	1.9E-05	0.003002	5.230523	2.615261	5.120121772
70	0.02881	0.7177	2E-05	0.002914	5.392462	2.696231	5.282495856
80	0.02953	0.7154	2.1E-05	0.002832	5.529809	2.764905	5.41524651
90	0.03024	0.7132	2.2E-05	0.002754	5.648586	2.824293	5.525682267
100	0.03095	0.7111	2.31E-05	0.00268	5.755311	2.877656	5.621398258
120	0.03235	0.7073	2.52E-05	0.002544	5.934504	2.967252	5.772325168
140	0.03374	0.7041	2.75E-05	0.00242	6.082941	3.04147	5.887269039
160	0.03511	0.7014	2.98E-05	0.002309	6.206907	3.103453	5.974669446
180	0.03646	0.6992	3.21E-05	0.002207	6.31194	3.15597	6.041563149
200	0.03779	0.6974	3.46E-05	0.002113	6.402611	3.201306	6.093544841
250	0.04104	0.6946	4.09E-05	0.001911	6.582347	3.291173	6.177470762
300	0.04418	0.6935	4.77E-05	0.001745	6.714213	3.357107	6.218149728
350	0.04721	0.6937	5.48E-05	0.001605	6.812864	3.406432	6.232174551
400	0.05015	0.6948	6.22E-05	0.001486	6.889515	3.444758	6.230840738
450	0.05298	0.6965	7E-05	0.001383	6.945577	3.472789	6.215481038
500	0.05572	0.6986	7.81E-05	0.001261	6.943583	3.471792	6.144150884
600	0.06093	0.7037	9.52E-05	0.00112	7.000135	3.500067	6.087586129
700	0.06581	0.7092	1.13E-04	0.001007	7.026126	3.513063	6.018457089
800	0.07037	0.7149	1.33E-04	0.000915	7.024343	3.512171	5.936650244
900	0.07465	0.7206	1.53E-04	0.000838	7.005877	3.502939	5.850654646
1000	0.07868	0.7260	1.74E-04	0.000773	6.976103	3.488052	5.763452174

[5] Coefficient of convection when the face is horizontal and facing up
[6] Coefficient of convection when the face is horizontal and facing down
[7] Coefficient of convection when the face is vertical

Temperature [C]	k [W/m.C]	Prandtl Pr	ν [m^2/s]	β= 1/Tf [1/K]	h ↑ hor[5]	h ↓hor[6]	h vert[7]
1500	0.09599	0.7478	2.92E-04	0.000558	6.749583	3.374791	5.350007103
2000	0.11113	0.7539	4.27E-04	0.000436	6.545174	3.272587	5.032153242

Appendix C
Example of image XXX

XXXX_DateTime(1,1): Year

XXXX_DateTime(1,2): Month

XXXX_DateTime(1,3): Day

XXXX_DateTime(1,4): Hour

XXXX_DateTime(1,5): Minute

XXXX_DateTime(1,6): Second

XXXX_DateTime(1,7): Millisecond

XXXX_ObjectParam(1,1): Emissivity

XXXX_ObjectParam(1,2): Object distance

XXXX_ObjectParam(1,3): Reflected Temperature

XXXX_ObjectParam(1,4): Atmospheric Temperature

XXXX_ObjectParam(1,5): Relative Humidity

XXXX_ObjectParam(1,6): Computed atm. transmission

XXXX_ObjectParam(1,7): Estimated atm. Transmission

XXXX_ObjectParam(1,8): Reference Temperature

XXXX_ObjectParam(1,9): External optics temperature

XXXX_ObjectParam(1,10): External optics transmission

XXXX_Scaling(1,1): Blackbody range min

XXXX_Scaling(1,2): Blackbody range max

XXXX_Scaling(1,3): Type of output

0 = temperature

2 = difference temperature

4 = object signal

5 = difference object signal

XXXX_Scaling(1,4): Camera scale min

XXXX_Scaling(1,5): Camera scale max

XXXX_Scaling(1,6): Calculated scale min

XXXX_Scaling(1,7): Calculated scale max

XXXX_Scaling(1,8): Actual scale min

XXXX_Scaling(1,9): Actual scale max

XXXX_FrameInfo(1,1): Image number

XXXX_FrameInfo(1,2): Trig count

Now the same example is shown, this time with the first image of the actual experiment:

Sample0001_DateTime(1,1): 2010

Sample0001__DateTime(1,2): 12

Sample0001__DateTime(1,3): 6

Sample0001__DateTime(1,4): 12

Sample0001__DateTime(1,5): 2

Sample0001__DateTime(1,6): 21

Sample0001__DateTime(1,7): 13

Sample0001__ObjectParam(1,1): 0.26300001144409

Sample0001__ObjectParam(1,2): 1.20000004768372

Sample0001__ObjectParam(1,3): 295.149993896484

Sample0001__ObjectParam(1,4): 293.149993896484

Sample0001__ObjectParam(1,5): 0.300000011920929

Sample0001__ObjectParam(1,6): 0.994584681311919

Sample0001__ObjectParam(1,7): 0

Sample0001__ObjectParam(1,8): 294.149993896484

Sample0001__ObjectParam(1,9): 293.100000000000

Sample0001__ObjectParam(1,10): N/A

Sample0001__Scaling(1,1): 233.149993896484

Sample0001__Scaling(1,2): 393.149993896484

Sample0001__Scaling(1,3): 0

Sample0001__Scaling(1,4): 296.850159504867

Sample0001__Scaling(1,5): 554.073382784165

Sample0001__Scaling(1,6): 300.381879627006

Sample0001__Scaling(1,7): 554.073382784165

Sample0001__Scaling(1,8): 296.850159504867

Sample0001__Scaling(1,9): 554.073382784165

Sample0001__FrameInfo(1,1): 1

Sample0001__FrameInfo(1,2): 0

Bibliography

Andres E. Rozlosnik (2005). "Infrared windows in industrial applications." I. SPIE Proceedings, **5782**:438-466

Akira Hirai, Satoshi Yamane, Masaki Miyazawa and Kenji Ohshima (1995). "Application of Multi-layered Fuzzy Inference Based on Back Propagation Method to the Robotic Welding." 1995 International IEEE/IAS Conference page 52. dio:10.1109/IACET.1995.527539

Bhalchandra V. Karlekar (1982). Heat transfer. West Pub. Co. St. Paul, Minn.

D. V. Nishar, J.L. Schiano, W. R. Perkins and R. A. Weber (1994). "Adaptive Control of Temperature in Arc Welding.'' Control Systems Magazine, IEEE **14**(4):4-12. Dio: 10.1109/37.295964

D.A. Hartman, D.R. DeLapp, G.E. Cook, R.J. Barnett (1999). "Intelligent Fusion Control Throughout Varying Thermal Regions." Industry Applications Conference, 1999. Thirty-Fourth IAS Annual Meeting. Conference Record of the 1999 IEEE **1**: 635-644. dio: 10.1109/IAS.1999.800018

Edward R. Bohnart (1995). "Gas Tungsten Arc Welding TIG handbook." Miller Electric Mfg. Co. Retrive from http://www.millerwelds.com/resources/TIGhandbook/

Fakhreddine O. Karray and Clarence de Silva (2004). Soft Computing and Intelligent System Design Theory Tools and Applications. Pearson Education Limited, England

FLIR systems (2006). User's manual ThermaCAMTM Reasercher. Profesional edition, Version 2.8 SR-3

Gao Xianglong, Motoji Yamamoto and Akira Mohri (1997). "Aplication of Fuzzy Logic Controller in the Seam Tracking of Arc-Welding Robot." Industrial Electronics, Control and Instrumentation, 1997. IECON 97. **3**:1367-1372. dio: 10.1109/IECON.1997.668515

Gerald L. Rogoff and Sanborn C. Brown (1970). "Thin Fused Quartz Window for Far Infrared Radiation." Review of Scientific Instruments **41**(10):1500 – 1503. dio: 10.1063/1.1684320

Inoue Kabunori (1997). "Neural Network based self-organized fuzzy Logic Control in arc Welding process." Fist International Conference on Knowledge-Based Intelligent Electronic Systems, 1997. KES '97. Proceedings., 1997 First **2:**684-689. dio: 10.1109/KES.1997.619453

J. Chen, P. Osbom, A. Paton and P. Wall (1993). "CCD near infrared temperature imaging in the steel industry." Instrumentation and Measurement Technology Conference, 1993. IMTC/93. Conference Record., IEEE 299-303. dio: 10.1109/IMTC.1993.382631

J. P. Boillot et al. (1985), "Adaptive welding by fiber optic thermography sensing: An analysis of thermal and instrumental considerations." Welding Journal **64**(7): 209-217

John A. Stevenson and Nick Varley (2008). "Fumarole monitoring with a handheld infrared camera: Volcán de Colima, Mexico, 2006–2007." Journal of Volcanology and Geothermal Research **177**(2008)**:**911-924. doi:10.1016/j.jvolgeores.2008.07.003

Lonnie Shanks (2009). "External/Internal Infrared Thermography Inspection for Air Leakage Detection." Tevis Architects **2**: 339-340. dio: 10.1109/ICIMW.2005.1572551

Mary A. Austin and Whitney (1996). "Real-Time Multi-Processing Fuzzy Logic Adaptive Control Gas Tungsten Arc Welding System." 4th International Workshop on Parallel and Distributed Real-Time Systems 139-142. dio: 10.1109/WPDRTS.1996.557652

P. W. Ramsey et al. (1963). "Infrared temperature sensing systems for automatic fusion welding." Welding Journal. **42**(8) 337-342

Paul A. Tipler and Gene Mosca (2008). Physics for Scientists and Engineers. Sixth Edition, Volume 1. New York, NY: Worth Publishers. pp. 586-588.

Pennsylvania State University (1995), "MIG/MAG welding guide." Lincoln Electric Co. Retrieved from http://www.lincolnelectric.com/assets/en_US/Products/literature/C4200.pdf

Robert L. Norton (2006). Machine designed: an integrated approach. Pearson Education, Inc, New Jersey

S. Nagarajan, W. H. Chen and B. A. Chin (1989). "Infrared sensing for adaptive arc welding." Welding Journal **68**(11): 462-466.

Shuaiyin Wang, Yajuan Wang and Y ongtao Zhang (2010). "The Demarcating Method of Infrared Image Measuring Temperature Based on GA-BP." 2010 International Conference on Computer and Communication Technologies in Agriculture Engineering **3**: 97-100. dio: 10.1109/CCTAE.2010.5543414

Sundaram Nagarajan, Probal Banerjee, WeiHua Chen and Bryan A. Chin (1992). "Control of Welding Process Using Infrared Sensors." IEEE Transactions on Robotics and Automation, **8** (1):86-93. dio: 10.1109/70.127242

T. C. Cetas (1977). "Practical thermometry with a thermographic camera-calibration, transmittance, and emittance measurements." Review of Scientific Instruments **49**(2): 245-254. dio: 10.1063/1.1135377

The MathWorks Inc (2008). Image Processing Toolbox™ User's Guide. Retrieved from www.mathworks.com/help/pdf_doc/images/images_tb.pdf

Thomas E. Salem, Dimeji Ibitayo and Bruce R. Geil (2007). "Validation of Infrared Camera Thermal Measurements on High-Voltage Power Electronic Components." Instrumentation and Measurement, IEEE Transactions on **56** (5): 1973-1978. Dio: 10.1109/TIM.2007.903590

Thomas L. Williams (2009). Thermal Imaging Cameras Characteristics and Performance. CRC Press

Vogt, C. (1999). "Creating Long Documents using Microsoft Word." Published on the Web at the University of Waterloo

Waldemar Minkina and Sebastian Dudzik (2009). Infrared Thermography, error and uncertainties. Wiley, USA

Y. Kiwamoto, H. Abe, Y. Tatematsu, T. Saito, M. Kurata, K. Kajiwara, Y. Kikuchi, T. Takahashi and T. Tamano (1997). "Thermographic temperature determination of gray materials with an infrared camera in different environments." Review of Scientific Instruments Japan. **68**(6): 2422 – 2427. dio: 10.1063/1.1148127

Ynus A. Gengel and Michael A. Boles (2006). Thermodynamics an Engineering Approach. McGraw-Hill Higher Education, New York

Yunus A. Cenge (2003). Heat and Mass Transfer. McGraw Hill, New York

Zafer Bingül, George E. Cook, Fellow (2000). "Application of Fuzzy Logic to Spatial Thermal Control in Fusion Welding." IEEE transaction on Industry Applications **36**(6): 1523-1530. Dio: 10.1109/28.887202

Zdenˇek Bochn´ıˇcek (2008). "An amateur video camera as a detector of infrared radiation." Physics Education **43** (1): 51-56. doi:10.1088/0031-9120/43/01/004

[i] Edward R. Bohnart .1995. "Gas Tungsten Arc Welding TIG handbook." Miller Electric Mfg. Co. Retrive from http://www.millerwelds.com/resources/TIGhandbook/.p.5

[ii] Pennsylvania State University. 1995. "MIG/MAG welding guide." Lincoln Electric Co. Retrieved from http://www.lincolnelectric.com/assets/en_US/Products/literature/C4200.pdf

[iii]Yunus A. Cenge. 2003. Heat and mass transfer. New York: McGraw Hill. p. 85-334

[iv] Robert L. Norton. 2006. Machine designed: an integrated approach. New Jersey: Pearson Education, Inc. p. 910

v Gao Xianglong, Motoji Yamamoto and Akira Mohri (1997). "Aplication of Fuzzy Logic Controller in the Seam Tracking of Arc-Welding Robot." IECON 97. **3**:1367-1372. dio: 10.1109/IECON.1997.668515

[vi] Zafer Bingül, George E. Cook, Fellow (2000). "Application of Fuzzy Logic to Spatial Thermal Control in Fusion Welding." IEEE Transaction on Industry Applications **36**(6): 1523-1530. Dio: 10.1109/28.887202

[vii] Akira Hirai, Satoshi Yamane, Masaki Miyazawa and Kenji Ohshima (1995). "Application of Multi-layered Fuzzy Inference Based on Back Propagation Method to the Robotic Welding." 1995 International IEEE/IAS Conference. p. 52. dio:10.1109/IACET.1995.527539

[viii] D.A. Hartman, D.R. DeLapp, G.E. Cook, R.J. Barnett (1999). "Intelligent Fusion Control Throughout Varying Thermal Regions." Industry Applications Conference, 1999. Thirty-Fourth IAS Annual Meeting. Conference Record of the 1999 IEEE **1**: 635-644. dio: 10.1109/IAS.1999.800018

[ix] Inoue Kabunori (1997). "Neural Network based self-organized fuzzy Logic Control in arc Welding process." First International Conference on Knowledge-Based Intelligent Electronic Systems, 1997. KES '97. Proceedings., 1997 First **2:**684-689. dio: 10.1109/KES.1997.619453

[x] Mary A. Austin and Whitney (1996). "Real-Time Multi-Processing Fuzzy Logic Adaptive Control Gas Tungsten Arc Welding System." 4th International Workshop on Parallel and Distributed Real-Time Systems 139-142. dio: 10.1109/WPDRTS.1996.557652

[xi] Fakhreddine O. Karray and Clarence de Silva. 2004. Soft Computing and Intelligent system design theory tools and applications. England: Pearson Education Limited. p.151,152

[xii] Fakhreddine O. Karray and Clarence de Silva (2004). Soft Computing and Intelligent System Design Theory Tools and Applications. England: Pearson Education Limited. p. 208

[xiii] Thomas E. Salem, Dimeji Ibitayo and Bruce R. Geil (2007). "Validation of Infrared Camera Thermal Measurements on High-Voltage Power Electronic Components." IEEE Transactions on Instrumentation and Measurement, **56** (5): 1973-1978. dio: 10.1109/TIM.2007.903590

[xiv]. Y. Kiwamoto, H. Abe, Y. Tatematsu, T. Saito, M. Kurata, K. Kajiwara, Y. Kikuchi, T. Takahashi and T. Tamano (1997). "Thermographic temperature determination of gray materials with an infrared camera in different environments." Review of Scientific Instruments Japan. **68**(6): 2422 – 2427. dio: 10.1063/1.1148127

[xv] T. C. Cetas (1977). "Practical thermometry with a thermographic camera-calibration, transmittance, and emittance measurements." Review of Scientific Instruments **49**(2): 245-254. dio: 10.1063/1.1135377

[xvi] 2009 Lonnie Shanks (2009). "External/Internal Infrared Thermography Inspection for Air Leakage Detection." Tevis Architects **2**: 339-340. dio: 10.1109/ICIMW.2005.1572551

[xvii] John A. Stevenson and Nick Varley (2008). "Fumarole monitoring with a handheld infrared camera: Volcán de Colima, Mexico, 2006–2007." J of Volcanology and Geothermal Research **177**(2008)**:**911-924. doi:10.1016/j.jvolgeores.2008.07.003

[xviii] Shuaiyin Wang, Yajuan Wang and Y ongtao Zhang (2010). "The Demarcating Method of Infrared Image Measuring Temperature Based on GA-BP." 2010 International Conference on Computer and Communication Technologies in Agriculture Engineering **3**: 97-100. dio: 10.1109/CCTAE.2010.5543414

[xix] Sundaram Nagarajan, Probal Banerjee, WeiHua Chen and Bryan A. Chin (1992). "Control of Welding Process Using Infrared Sensors." IEEE Transactions on Robotics and Automation, **8** (1):86-93. dio: 10.1109/70.127242

[xx] P. W. Ramsey et al. (1963). "Infrared temperature sensing systems for automatic fusion welding." Welding J. **42**(8) 337-342

[xxi] J. P. Boillot et al. (1985), "Adaptive welding by fiber optic thermography sensing: An analysis of thermal and instrumental considerations." Welding J **64**(7): 209-217

[xxii] Sundaram Nagarajan, Probal Banerjee, WeiHua Chen and Bryan A. Chin (1992). "Control of Welding Process Using Infrared Sensors." IEEE Transactions on Robotics and Automation, **8** (1):86-93. dio: 10.1109/70.127242

[xxiii] D. V. Nishar, J.L. Schiano, W. R. Perkins and R. A. Weber (1994). "Adaptive Control of Temperature in Arc Welding.'' Control Systems Magazine, IEEE **14**(4):4-12. Dio: 10.1109/37.295964

[xxiv] J. Chen, P. Osbom, A. Paton and P. Wall (1993). "CCD near infrared temperature imaging in the steel industry." IMTC/93. Conference Record., IEEE 299-303. dio: 10.1109/IMTC.1993.382631

[xxv] Zdenˇek Bochn´ıˇcek (2008). “An amateur video camera as a detector of infrared radiation.” Physics Edu. **43** (1): 51-56. doi:10.1088/0031-9120/43/01/004

[xxvi] Thomas L. Williams (2009). Thermal Imaging Cameras Characteristics and Performance. CRC Press

[xxvii] FLIR systems (2006). User’s manual ThermaCAMTM Reasercher. Profesional edition, Version 2.8 SR-3 p. 61

[xxviii] The MathWorks Inc. 2008. Image processing toolbox™ user’s guide. Retrieved from www.mathworks.com/help/pdf_doc/images/images_tb.pdf . p.10-15